



UNIVERSITY OF LEEDS

This is a repository copy of *Energy geostructures: A review of analysis approaches, in situ testing and model scale experiments*.

White Rose Research Online URL for this paper:
<http://eprints.whiterose.ac.uk/156324/>

Version: Accepted Version

Article:

Loveridge, F orcid.org/0000-0002-6688-6305, McCartney, JS, Narsilio, GA et al. (1 more author) (2020) Energy geostructures: A review of analysis approaches, in situ testing and model scale experiments. *Geomechanics for Energy and the Environment*, 22. 100173. ISSN 2352-3808

<https://doi.org/10.1016/j.gete.2019.100173>

© 2019 Published by Elsevier Ltd. This manuscript version is made available under the CC-BY-NC-ND 4.0 license <http://creativecommons.org/licenses/by-nc-nd/4.0/>.

Reuse

This article is distributed under the terms of the Creative Commons Attribution-NonCommercial-NoDerivs (CC BY-NC-ND) licence. This licence only allows you to download this work and share it with others as long as you credit the authors, but you can't change the article in any way or use it commercially. More information and the full terms of the licence here: <https://creativecommons.org/licenses/>

Takedown

If you consider content in White Rose Research Online to be in breach of UK law, please notify us by emailing eprints@whiterose.ac.uk including the URL of the record and the reason for the withdrawal request.



eprints@whiterose.ac.uk
<https://eprints.whiterose.ac.uk/>

December 20th, 2019

Title:

Energy geostructures: a review of analysis approaches, in situ testing and model scale experiments

AUTHORS:

Fleur Loveridge¹, John S. McCartney², Guillermo A. Narsilio³, Marcelo Sanchez⁴

AFFILIATION:

¹**Fleur Loveridge**, Ph.D., CEng MICE, FGS CGeol, University Academic Fellow. University of Leeds, UK

²**John S. McCartney**, Ph.D., P.E., F.ASCE, Professor and Chair, Department of Structural Engineering, University of California San Diego. USA.

³**Guillermo A. Narsilio** Ph.D., Associate Professor, Melbourne School of Engineering, The University of Melbourne, Australia.

⁴**Marcelo Sanchez**, Ph.D., Professor, Zachry Department of Civil Engineering, Texas A&M University, College Station, USA

Corresponding Author:

Marcelo Sanchez, Ph.D.
Professor
Zachry Department of Civil Engineering
Texas A&M University
201 Dwight Look Engineering Building
College Station, TX 77843-3136
Phone: 979-862-6604
<https://ceprofs.civil.tamu.edu/msanchez/>

31 **Abstract**

32 This position paper was developed by members of the task force on “Energy Geostructures” of the
33 International Society of Soil Mechanics and Geotechnical Engineering (ISSMGE) Technical Committee
34 TC308 on ‘Energy Geotechnics’. The article includes a summary and review of some of the most recent
35 analysis approaches, in situ testing, full scale testing and model scale experiments with a focus on
36 energy piles and other energy geostructures. The geotechnics literature in these topics has increased
37 rapidly in the last five years suggesting a surge in this emerging research area. Here complementary
38 lines of research can be distinguished, one focusing on thermal analysis and another focusing on
39 thermo-geomechanical analysis. Limitations, shortcomings and knowledge gaps are identified and
40 needs for further research and development within the geotechnical community are highlighted.

41 **Keywords:** geothermal, ground source heat pumps, ground heat exchangers, energy piles, review ,
42 state of the art

43

44

Table of Contents

46	1	Introduction	5
47	2	Analysis of Energy Geostrutures.....	6
48	2.1	Thermal Analysis.....	6
49	2.1.1	Overview	6
50	2.1.1.1	Thermal Loads.....	6
51	2.1.1.2	Temperature Limits.....	7
52	2.1.1.3	Mechanical Design.....	7
53	2.1.2	Piles.....	7
54	2.1.2.1	Classical G-functions.....	8
55	2.1.2.2	Pile Specific G-functions.....	10
56	2.1.2.3	Thermal Resistances.....	12
57	2.1.2.4	Transient Pile Models.....	13
58	2.1.2.5	Numerical Simulations.....	13
59	2.1.2.6	Hybrid Models.....	15
60	2.1.2.7	Pipe Arrangements and Pile Geometry	16
61	2.1.3	Energy Walls.....	17
62	2.1.3.1	Overview	17
63	2.1.3.2	The Excavation Space	17
64	2.1.3.3	Numerical Simulations.....	18
65	2.1.3.4	Analytical Methods.....	18
66	2.1.3.5	Pipe Arrangements.....	19
67	2.1.4	Energy Tunnels.....	20
68	2.1.4.1	Overview	20
69	2.1.4.2	The Tunnel Space.....	21
70	2.1.4.3	Numerical Simulations.....	21
71	2.1.4.4	Analytical Methods.....	22
72	2.1.4.5	Pipe Arrangements.....	22
73	2.1.5	Other Geotechnical Structures.....	23
74	2.2	Geomechanical and Structural Analysis.....	24
75	2.2.1	Overview	24
76	2.2.2	Piles.....	24
77	2.2.3	Other Energy Geostrutures	27
78	3	Field Scale Testing.....	27
79	3.1	Pile Thermal Tests.....	27
80	3.1.1	Thermal Performance Tests.....	27
81	3.1.1.1	Short Term Tests.....	28
82	3.1.1.2	Long Term Tests and Operation	30
83	3.1.2	Thermal Response Tests.....	31
84	3.1.2.1	Case Studies	32
85	3.1.2.2	Recommendations.....	34
86	3.2	Pile Geomechanical Tests.....	34
87	3.2.1	Single Piles	34
88	3.2.2	Pile Groups.....	35
89	3.3	Energy Walls	35
90	3.4	Energy Tunnels.....	39
91	3.4.1	Thermal Performance Tests.....	39
92	3.5	Other Energy Geostrutures.....	43
93	4	Model Scale Testing.....	43
94	4.1	Model Test on Piles.....	44

95	4.1.1	Laboratory Scale Tests (1-g).....	44
96	4.1.1.1	Overview	44
97	4.1.1.2	Evaluation of Heat Transfer in Laboratory-scale Tests	44
98	4.1.1.3	Evaluation of Soil-structure Interaction in Laboratory-scale Tests	45
99	4.1.2	Centrifuge Tests on Energy Piles (N-g)	47
100	4.1.2.1	Overview	47
101	4.1.2.2	Evaluation of Heat Transfer and Water Flow in Centrifuge-scale Tests	48
102	4.1.2.3	Evaluation of Soil-Structure Interaction in Centrifuge-Scale Tests.....	49
103	4.2	Model Scale Tests on Other Energy Geostructures	52
104	5	Discussion.....	52
105	6	Summary	54
106		References.....	55
107			

108 1 Introduction

109 There is an inexorable increase in global energy demand driven by world population growth and the
110 global pursuit of a higher 'quality' of life. As a result, the annual per capita energy consumption has
111 grown exponentially for a century (Glassley 2010). This growing demand may be satisfied by increasing
112 energy supply, for example by finding new ways to exploit oil and gas reservoirs that were previously
113 deemed uneconomical to exploit. However, the long term and more sustainable solution relies on
114 both reducing global energy demand and the use of fossil fuels and increasing the use of energy from
115 renewable sources. Geo-professionals can contribute to the development of a number of different
116 renewable energy sources with low greenhouse gas emissions (Arulrajah et al. 2015, McCartney et al.
117 2016, Sanchez et al. 2017).

118 Shallow geothermal energy or ground source heat pump (GSHP) technology can contribute to
119 lowering or flattening peak energy demand through efficient heating and cooling of residential,
120 commercial and industrial buildings (Brandl 2006; Olgun and McCartney 2014; Sanchez et al. 2017). A
121 GSHP system is inherently more efficient than alternative Heating Ventilation and Air Conditioning
122 (HVAC) systems as it exchanges heat with a more stable source/sink: the ground temperature in the
123 upper tens of meters is typically close to the mean atmospheric temperature for a given location year-
124 round. Energy geostructures are foundations or other buried geotechnical structures which have been
125 equipped with heat transfer pipes so that they may act as the ground heat exchanger (GHE) part of a
126 GSHP system. Therefore, energy geostructures remove the need for construction of special purpose
127 GHEs, offering opportunities to reduce capital costs for shallow geothermal energy (CIBSE, 2013; Park
128 et al. 2015; Lu and Narsilio 2019; Akrouch et al. 2018).

129 Piles are the most common type of energy geostructure, having been first constructed in northern
130 Europe in the 1980's (Brandl 2006). Their application has expanded in the subsequent decades (e.g.
131 Amis & Loveridge, 2014), but their numbers are still minor compared to the total GSHP installations
132 worldwide. Demonstration projects using slabs, walls and tunnels as ground heat exchangers soon
133 followed the first pile installations (Adam & Markiewicz 2009). However, these types of energy
134 geostructures are rarer, for several reasons. First, piles clearly have the potential to offer reduced
135 capital costs compared to traditional vertical GHEs (CIBSE, 2013) such as boreholes. Second, as piles
136 have a superficial resemblance to boreholes, there are available thermal design methods which can
137 be adapted for use with piles (e.g., Eskilson 1987; Pahud 2007). There remain limitations of such
138 approaches (Loveridge & Powrie 2013a), but they are readily available. Additional approaches for the
139 geotechnical design of piles subject to thermal changes are under development (e.g. Mimouni & Laloui
140 2015; Rotta Loria & Laloui 2016a). By contrast, for other structures there are no standard design and
141 analysis approaches and every project must proceed very much on a case by case basis. The
142 development of infrastructure schemes for shallow geothermal utilisation also comes with additional
143 challenges regarding users for the stored thermal energy. While piled foundations are typically
144 constructed to support a building which is then well placed to use the renewable heating/cooling
145 provided, for retaining walls and tunnels the user of the thermal energy may be a third party which
146 places additional logistical and bureaucratic barriers in place for adoption of the technology.

147 The application of energy geostructures has been summarised in Laloui & Di Donna (2013) and Soga
148 & Rui (2016). However, research in this area has both intensified and broadened in recent years. Work
149 has focused on two main areas. First, the geomechanical implications of using bearing structures also
150 for heat exchange and storage (e.g., Bourne-Webb et al. 2009, Stewart & McCartney 2012). Second,

151 the development of thermal analysis approaches to assess energy performance and understand how
152 to maximise energy efficiency (e.g. Loveridge & Powrie 2013b, Bidarmaghz et al. 2016a, 2016b,
153 Mikhaylova et al. 2016a). Both these areas have the aim of minimising uncertainty and risk in design,
154 facilitating reduction in capital costs and hence an increase in technology uptake.

155 This paper reviews recent research on energy geostructures in both these areas, covering analysis
156 approaches and the field and model scale testing that have been used to inform those approaches.
157 The topic of material parameters for energy geostructures is excluded since this is well reviewed by
158 Vieira et al. (2017). This paper will be naturally biased towards piles since these are the most common
159 installation and the area which has seen most research in recent years. However, energy walls in
160 particular have seen a recent increase in interest, and this is reflected in our review. The text is
161 arranged into three main sections covering analysis and design methods (Section 2), full-scale field
162 testing (Section 3) and model scale testing (Section 4). These will be followed by a discussion
163 pertaining to knowledge gaps and a summary of the current state of the practice. The scope of the
164 paper will focus mainly on the in-ground elements, where there is novelty and hence uncertainty due
165 to the more recent adoption of energy geostructures. However, the importance of the mechanical
166 engineering elements must not be underestimated, and some brief comments are made on these
167 aspects in Section 2.1.

168 **2 Analysis of Energy Geostructures**

169 **2.1 Thermal Analysis**

170 2.1.1 Overview

171 The thermal design of energy geostructures involves the use of analyses to estimate the amount of
172 energy that can be readily exchanged with or stored within the ground to fully or partially satisfy the
173 thermal energy loads of buildings. This includes consideration of the best arrangement of heat transfer
174 pipes for energy efficiency, determining the relationship between energy exchanged and temperature
175 changes, and selecting the heat pump and appropriately linking the source side of the energy system
176 (the ground) to the delivery system in the building. This review focuses on the first two elements, but
177 brief consideration of the building and mechanical engineering aspects is given below.

178 *2.1.1.1 Thermal Loads*

179 The nature of the thermal loads applied to a ground source heat pump system has a large impact on
180 its performance (CIBSE, 2013). For example, a system which is dominated by one-way heat transfer
181 due to heat extraction will show decreasing performance over time as the ground (source side)
182 temperature is reduced by that heat extraction. A system that is balanced between heat injection and
183 heat extraction, on the other hand, will act as an inter-seasonal store of heat and will always operate
184 at greater efficiency. Additionally, thermal loads that are “peaky”, displaying rapid changes in
185 magnitude, may be most efficiently covered with a combination of a GSHP for the base thermal load
186 and an auxiliary system for the balance.

187 Ground heat exchanger (GHE) and energy geostructure design is therefore dependent on provision of
188 these thermal loads from the mechanical engineering team. The level of detail provided can be
189 important and requirements will depend on the size and complexity of the heat pump scheme (GSHPA,
190 2012). Unfortunately, reliable prediction of the heating and cooling demands of buildings is extremely

191 difficult and current approaches often lead to an underestimate of demand, leaving a so called “energy
192 gap” (e.g. Menezes et al. 2012). To mitigate against this effect, designers can assess the risk of
193 underestimation of thermal loads and either include a factor of safety approach to thermal loads or
194 alternatively adopt installation and use of back up auxiliary heating and cooling systems (Garber et al.
195 2013b; Mikhaylova et al. 2016b).

196 2.1.1.2 Temperature Limits

197 It is important to ensure that the GSHP and the energy geostructures operate within acceptable
198 temperature limits. This serves to both, protect the structure from extreme temperature changes
199 which could impact on the geotechnical performance, and ensure that the heat pump is operating
200 within an optimal efficiency range. While the upper bound temperature depends on the particular
201 GSHP specifications (typically 30-40°C) and designer’s choice, the lower bound temperature is
202 generally taken as 0°C to 2°C to avoid ground freezing (GSHPA 2002), although lower fluid
203 temperatures can potentially be tolerated (Loveridge et al. 2012).

204 2.1.1.3 Mechanical Design

205 The mechanical design aspects of a GSHP scheme are of equal importance to the GHE design.
206 Optimisation of the heat pump and minimisation of the temperature lift are essential factors, as is the
207 pipework and pumping design. GSHP systems are complex, extending from the ground to the heating
208 and cooling delivery systems, via the ground heat exchangers, headers and manifolds, circulation
209 pumps and heat pumps. All aspects need to be properly designed and executed for a system to
210 perform well. Detailed discussion of these elements can be found in, for example, Oschner (2008).

211 Some integrated building simulation software packages allow analyses of all components of a GSHP
212 system from the in-ground components to the delivery of heating and cooling, e.g. EnergyPlus (Fisher
213 et al. 2006) or TRNSYS (2018). These and other applications are reviewed in Do & Haberl (2010) and
214 are typically aimed at borehole heat exchanger design, but a standalone implementation in TRNSYS
215 for application to energy piles is available (Pahud 2007).

216 2.1.2 Piles

217 Typically, analytical solutions are used to determine the fluid temperature changes for a given thermal
218 demand. This allows the available energy within certain temperature limits to be determined.
219 Analytical solutions are preferable to numerical solutions since fast run times are required to process
220 decade’s worth of thermal load input data which may vary on an hourly basis. However, closed form
221 solutions are sometimes associated with assumptions that limit their range of application.
222 Furthermore, some numerical tools have been implemented with sufficient computational efficiency
223 that provide reasonable alternatives (e.g. see Section 2.1.2.6).

224 To simplify the thermal problem most analysis approaches separate the temperature change into a
225 number of zones for which different solutions are applied, with the results then combined by
226 superposition. Thus, the change in circulating fluid temperature, T_f , can be given by:

$$227 \Delta T_f = \Delta T_{ground} + \Delta T_{pile} + \Delta T_{pipe} \quad (1)$$

228 When analytical techniques are adopted the ground temperature change is often calculated using a
229 transient temperature response function (G-function or G_g) evaluated at a radial coordinate $r=r_b$,
230 where r_b is the pile radius.

231
$$\Delta T_{ground} = \frac{q}{2\pi\lambda_g} G_g(t, r) \quad (2)$$

232 where λ_g is the thermal conductivity of the ground in W/(mK), q is the applied thermal power in W/m
 233 and t is the elapsed time in seconds. The G-function can take a number of different forms (Section
 234 2.1.2.1) as summarised in Table 1.

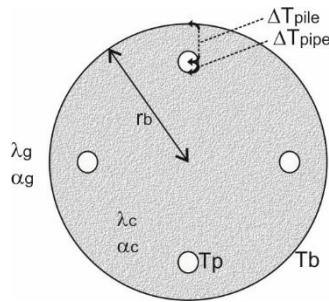
235 Traditionally ΔT_{pile} and ΔT_{pipe} are calculated using thermal resistances and assuming a thermal
 236 steady state:

237
$$\Delta T_{pile} = T_p - T_b = qR_c \quad (3)$$

238
$$\Delta T_{pipe} = T_f - T_p = qR_p \quad (4)$$

239 where R is a lumped thermal resistance (Section 2.1.2.3) in mK/W and T_b and T_p are the average
 240 temperatures at the pile edge and pipe edge respectively (see Figure 1). R_c is the resistance associated
 241 with the temperature changes within the pile concrete and R_p is that associated with the pipes and
 242 the fluid flowing within them. The latter may be further split into the conductive resistance associated
 243 with the pipe itself and the convective resistance associated with the fluid, R_{p-cond} and R_{p-conv}
 244 respectively. Together the individual resistances make up the total resistance, R_b :

245
$$R_b = R_c + R_{p-cond} + R_{p-conv} \quad (5)$$



246

247

Figure 1 Typical arrangement of an energy pile

248

249 **2.1.2.1 Classical G-functions**

250 The term G-function was originally used to describe the temperature response functions developed
 251 for borehole heat exchangers by Eskilson (1987) using the Superposition Borehole Model (SBM), see
 252 also Section 2.1.2.5. However, it has since been adopted more generally to describe any function
 253 which relates the temperature change in the ground around a vertical GHE to the applied thermal
 254 load, q . Hence the general approach is equally applicable to piles. Most typically G-functions are
 255 expressed as a dimensionless form of Equation 2:

256
$$\Phi = G_g(Fo, r^*) \quad (6)$$

257 where Φ is the dimensional temperature response, $\Phi = \frac{2\pi\lambda_g}{q} \Delta T$, Fo is the Fourier number or

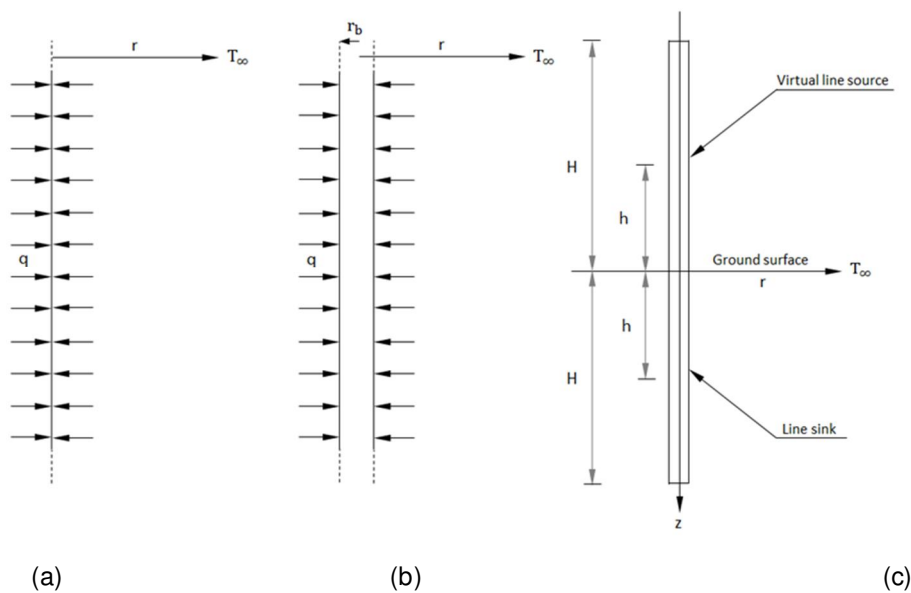
258 dimensionless time defined as $Fo = \frac{\alpha_g t}{r_b^2}$, α_g is the ground thermal diffusivity, and r_b the pile radius,

259 and r^* is a dimensionless geometry factor, often expressed as radial coordinate divided by heat

260 exchanger length (see Figure 1). Sometimes other non-dimensional parameter sets are used, but the
 261 concept is the same. The classic analytical solutions of the G-functions are based on the infinite line
 262 source (ILS), the infinite (hollow) cylindrical source, and the finite line source (FLS). These geometric
 263 configurations used in the analytical solutions are schematically presented in Figure 2, with a summary
 264 of these and other solutions listed in Table 1 and illustrated in Figures 3 and 4. Full details of these
 265 solutions are not given here since they are readily available in the literature (e.g. Bourne-Webb et al.
 266 2016a, Fadejev et al. 2017).

267 In the development of the analytical solutions, it is assumed that the ground is homogeneous and
 268 isotropic, with no initial temperature gradient nor groundwater flow and fully saturated ground
 269 conditions. Such factors are known to affect the temperature changes around vertical GHEs (e.g.
 270 Signorelli et al. 2007; Bidarmaghz et al. 2016a) but are more difficult to account for by analytical
 271 means.

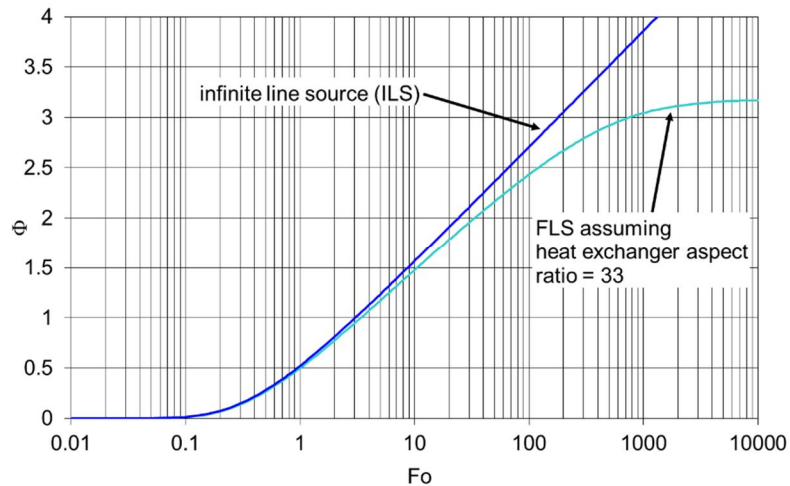
272 G-functions are normally plotted for a constant q (Figure 3 and Figure 4), but as q varies in actual
 273 routine operation it is necessary to use some form of temporal superposition and/or load aggregation
 274 (Claesson & Javed 2012) to determine the overall temperature change, $\Delta T(t)$ resulting from $q(t)$ over
 275 the lifetime of a geo-structure.



276

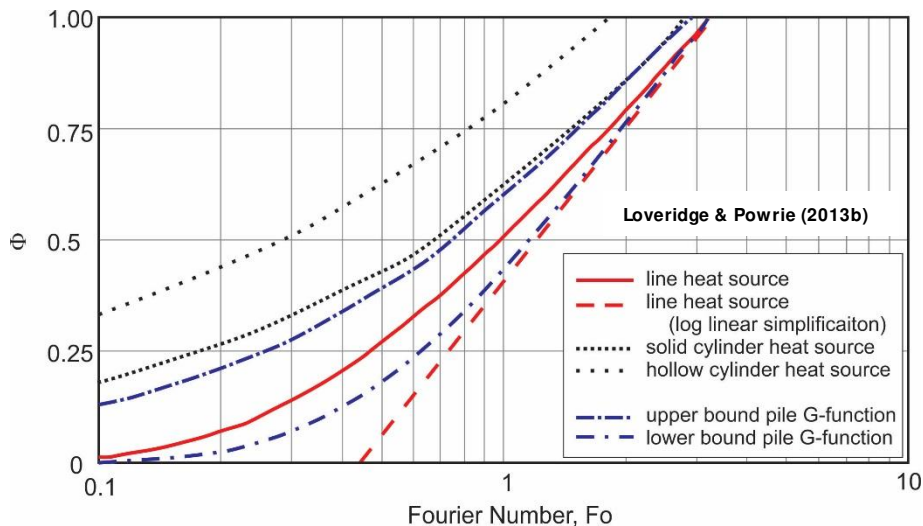
277 **Figure 2 Schematic of the classical G-function models: (a) infinite line source (ILS), (b) infinite**
 278 **cylindrical source (ICS), (c) finite line source (FLS). T_{∞} =far field temperature; H =heat exchanger**
 279 **length; h =depth below ground surface. Adapted from Bidarmaghz 2015.**

280



281

282 **Figure 3 Example G-functions showing development of long-term steady state conditions for heat**
 283 **exchangers of finite length. Aspect ratio = pile length / pile diameter**



284

285 **Figure 4 Different G-functions displayed at short time scales. Pile upper and lower bound G-**
 286 **functions after Loveridge & Powrie (2013b)**

287 *2.1.2.2 Pile Specific G-functions*

288 The SBM and other FLS approaches are perhaps the most commonly adopted type of G-function, being
 289 readily implemented in accessible borehole design software that is sometimes used for piles.
 290 However, this type of approach is not validated for piles and may over predict temperature changes
 291 (e.g. Wood et al. 2010a). This is due to (i) the short length of piles not being accommodated in routine
 292 GHE software which implements these analysis methods; and (ii) the accompanying use of a steady
 293 state resistance (see Section 2.1.2.3). However, it should be noted that such approaches remain
 294 conservative in terms of energy assessment. This means that a design would be safe, although the
 295 danger of over conservatism relates to increased payback times on investment.

296 The solid cylinder model has advantages for use with piles since it can capture flow of heat into the
 297 pile as well as into the ground. Solutions have been published for both the infinite and finite heat
 298 source scenarios (Man et al. 2010). However, this approach still requires validation, but it was

299 suggested that it may provide an upper bound for pile behaviour as shown in Figure 4 (Loveridge &
 300 Powrie 2013b).

301 Applying a similar approach to the SBM, Loveridge & Powrie (2013b) derived upper and lower bound
 302 G-functions based on pile geometries rather than a line source. While validated on short term thermal
 303 response tests of small diameter piles, the approach awaits longer term validation and critical
 304 assessment for piles with different length to diameter ratios.

305 All the finite heat source models described above are illustrated for short time periods in Figure 4. At
 306 long time periods the temperature response will converge on that of the finite line source (Figure 3),
 307 with the steady state value dependent on the aspect ratio. All these models also suffer some of the
 308 same limitations which need to be appreciated. They all assume a constant surface temperature as a
 309 boundary condition. This has two drawbacks. First, the near surface temperature distribution is not
 310 constant, but fluctuates throughout the year. For short GHEs such as energy piles this may be
 311 significant (e.g. Bidarmaghz et al. 2016). Second, most energy piles are buried beneath a building and
 312 boundary conditions at the pile head may be better represented as either insulated or as a small net
 313 flux representing heat loss from the building (Loveridge & Powrie 2013a). There are few datasets
 314 showing pile temperatures under buildings, but initial data from Mikhaylava et al. (2016c) and Habart
 315 et al. (2016) show fluctuations at the pile head. These temperature changes suggest some heat
 316 exchange with the building. However, uncertainty over the most appropriate boundary conditions also
 317 remains a barrier to further development (see also Section 3.1).

318 **Table 1 Main types of G-function for use with piles**

Model	References	Description	Comments
Infinite Line Source (ILS)	Carslaw & Jaeger (1959)	Assumes an infinitely long and thin heat source embedded in a homogeneous medium.	Infinite length means that long term steady state behaviour is neglected.
Infinite (Hollow) Cylindrical Source (ICS)	Carslaw & Jaeger (1959); Ingersol et al. (1954); Kakaç and Yener (2008); Bernier (2001)	Assumes an infinitely long hollow cylinder which acts as a heat source embedded in a homogeneous medium.	Infinite length means that long term steady state behaviour is neglected. Gives larger temperature changes than the ILS at short time periods. It is equivalent to the ILS at longer time periods.
Superposition Borehole Model (SBM)	Eskilson (1987)	Uses numerically exact calculation based on a finite line heat source, with superposition for multiple boreholes.	As calculated numerically, to be applied routinely the SBM G-functions must be pre-programmed into software codes for different combinations of multiple boreholes. This approach is widely used and well validated for borehole design (e.g. Cullin et al. 2015).
Analytical Finite Line Source (FLS)	Eskilson (1987) Zeng et al. (2002) Lamarche & Beauchamp (2007) Claesson & Javed (2011)	Using a mirrored virtual line sink approach to simulate the ground surface, these G-functions provide an analytically exact version of SBM.	Zeng et al. (2002) use the mid-depth of the heat exchanger as the reference temperature while later works use an average temperature which provides a better correlation to SBM. The more recent works concentrate on simplifying the mathematics

Model	References	Description	Comments
Solid Cylinder Model (SCM)	Man et al. (2010)	Heat flow into and out of the heat exchanger is simulated. The model has been presented in both infinite and finite forms.	Studies by Loveridge & Powrie (2013b) suggest that the SCM may provide a sensible upper bound for piles, providing the finite version of the model is used.
Pile G-Functions	Loveridge & Powrie (2013b)	Derived numerically in a similar way to SBM, these G-functions are then presented as appropriate upper and lower bound solutions to cater for the wide range of pile sizes and pipe configurations.	The functions typically fall between the SCM and the log linear simplification of the FLS (Figure 4).

319

320 2.1.2.3 Thermal Resistances

321 The pipe thermal resistance R_p can be readily calculated by analytical means as set out in Hellstrom
322 (1991) and Lamarche et al. (2010). Analytical, empirical or numerically based methods can be used to
323 calculate the resistance of the concrete part of the pile, a summary of which is given in Table 2.
324 Claesson & Hellstrom (2011)'s multipole method for calculation of the pile resistance, R_c , has been
325 shown to be the best solution for small diameter vertical GHEs (Lamarche et al. 2010) and is expected
326 to also perform well with larger diameter piles. Such an approach was adopted by the SIA (2005).
327 Additionally, numerically derived means of determining the pile resistance are proposed by Loveridge
328 & Powrie (2014) based on the results of simulations. These correspond well to the multipole method
329 for the two pipe cases.

330 However, R_c is a steady state parameter and a thermal steady state may not be present during
331 operation of the pile. Except for very small diameter piles a design approach based on a steady state
332 resistance is therefore unlikely to be a sensible assumption and would result in over prediction of the
333 temperature changes (Loveridge & Powrie 2013b) and hence underestimation of energy availability.
334 Consequently, transient methods are to be recommended for pile design where possible.

335 **Table 2 Methods for calculating ground heat exchanger steady state thermal resistance**

Approach	References	Description	Comments
Empirical	Paul (1996)	Shape factor approach using empirically derived values for different pipe configurations. Derived from in situ test data.	Empirical for boreholes so will not apply for larger diameter piles. Determines R_b
Analytical	Hellström (1991)	Direct analytical method based on line source theory. Assumes 2D heat flow.	Theoretical, therefore applicable to any geometry. Determines R_c
Analytical	Bennet et al. (1987); Claesson & Hellstrom (2011)	Line source method with multipole expansion correction. Assumes 2D heat flow.	Theoretical, therefore applicable to any geometry. Determines R_c

Analytical	Hellstrom (1991); Diao et al. (2004a)	Multipole method with correction for quasi-3D heat flow.	Theoretical, therefore applicable to any geometry. It determines R_c . Not significantly different from 2D case in most scenarios.
Numerically derived	Sharqawy et al. (2009)	Empirical method based on 2D numerical simulations for boreholes	Most pile geometries will be outside range of analysis carried out to determine relationships. Determines R_c
Numerically derived	Loveridge & Powrie (2014)	Empirical method based on 2D numerical simulations for piles	Specific for pile geometries. Determines R_c

336

337 2.1.2.4 Transient Pile Models

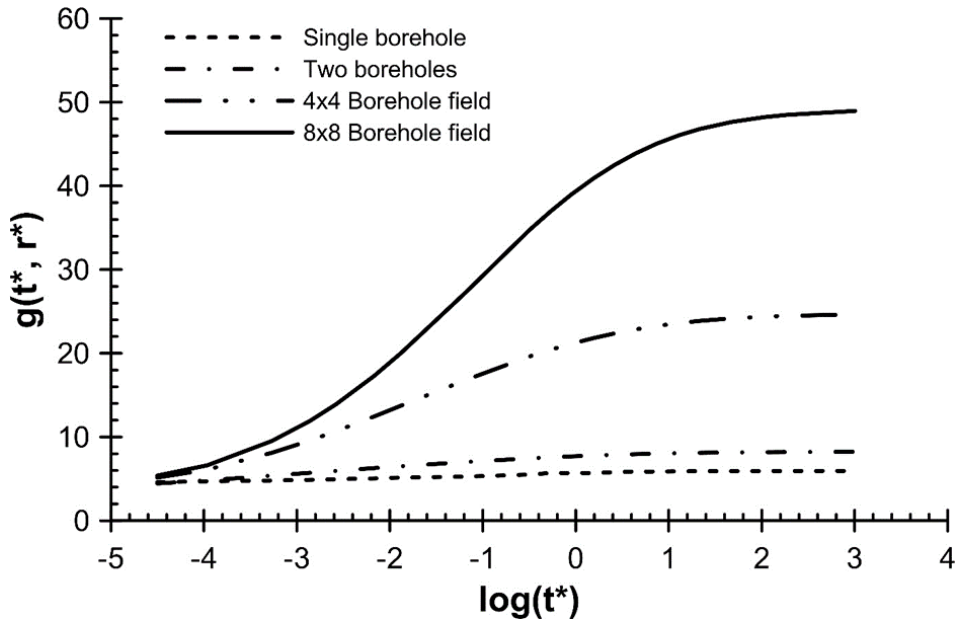
338 There are several alternatives to using a steady state pile resistance. Loveridge & Powrie (2013b)
 339 proposed adopting temperature response functions, like G-functions, to replace the constant value of
 340 R_c . They suggested upper and lower bound functions based on a range of numerical simulations.

341 Alternative transient analysis can be carried out which considers the ground and the pile concrete in
 342 one analysis. Li & Lai (2012) proposed composite G-functions based on superposition of several line
 343 sources (each representing a pipe) installed in a two-material medium containing the ground and the
 344 pile. These functions are an important step forward but would need pre-programming for a range of
 345 likely scenarios (as is done for SBM when implemented in popular borehole software tools).

346 2.1.2.5 Numerical Simulations

347 Despite the fact that analytical solutions have been developed to capture the thermal performance of
 348 GHE, most of the assumptions bring limitations. In response to these difficulties, numerical models
 349 solving the governing heat transfer equations have surged. This includes 1D finite difference models
 350 (e.g. Gehlin & Hellstrom 2003; Shonder & Beck 1999, 2000) and Finite Element (FE) models in 2D (e.g.
 351 Austin, 1998; Sharqawy et al. 2009) and 3D (e.g. Bidarmaghz 2015; Ozudogru et al. 2015; Raymond et
 352 al. 2011; Signorelli et al. 2007; Wagner et al. 2012). In the following section, selected 1D, 2D and 3D
 353 numerical models are briefly explained, with a focus on illustrating the main approaches taken. Several
 354 the examples have been developed for boreholes rather than piles, but the techniques used are
 355 equally as applicable in the latter case.

356 Eskilson developed pioneering work on numerical simulation of GHEs for boreholes, which has gone
 357 on to underpin much of current practice (Eskilson 1987; Eskilson & Claesson 1988) for both boreholes
 358 and piles. Numerical computation on a 2D radial-axial coordinate system was used to determine the
 359 temperature distribution around a single borehole with finite length and diameter. The mirror image
 360 method has been used to account for the constant temperature on the ground surface, as per the
 361 finite line source method. The temperature distribution in the ground region for a number of thermally
 362 interacting boreholes is then obtained by superimposing the temperature response of a single
 363 borehole in space. This is the basis of the Superposition Borehole Model (SBM) and led to the first G-
 364 functions, examples of which are given in Figure 5. However, by neglecting the detail of the GHE, the
 365 model is not suitable for use at short timescales.



366

367 **Figure 5 Example G-functions for different arrangements of boreholes (Bourne-Webb et al. 2016).**
 368 **t^* is the ratio of the elapsed time and time to steady state; r^* is the non-dimensional radial**
 369 **coordinate.**

370 Based on Eskilson's g-functions, Yavuzturk et al. (1999) developed a 2D finite volume numerical model
 371 that overcomes the short time step issues in Eskilson's model. Therefore, the thermal resistance and
 372 capacitance effects of the heat exchanger components are considered in this model. A constant heat
 373 flux per unit depth of the borehole was assumed for the pipe wall as the boundary condition due to
 374 the restriction of the code used. The fluid in the pipes is not explicitly modelled. Several other 2D
 375 models have been proposed for borehole heat exchanger fields (e.g., Muraya et al. 1996; Lazzari et al.
 376 2010).

377 Two dimensional models have also been employed to understand pile thermal behaviour. Some of the
 378 more notable cases include the 2D slice models of Loveridge & Powrie (2013b) and Loveridge & Powrie
 379 (2014) who used the results of their finite element (FE) simulation to develop pile specific G-functions
 380 and thermal resistance relationships. The models do not explicitly consider the pipes and apply a
 381 constant heat flux at the pipe outer boundary. Similar techniques were also used by Alberdi-Pagola
 382 et al. (2018) when interpreting thermal response tests of quadratic section energy piles.

383 Dupray et al. (2014) built a 2D model in the vertical plane to consider the potential thermal storage
 384 available for a group of piles beneath a building. This type of simplification is unusual in GHE analysis
 385 and reflects the adoption of plane strain for the coupled geomechanical part of the analysis. In the
 386 model the authors used a slab of fixed temperature underlain by a low conductivity insulating layer to
 387 represent the base of the building. The heat source was rather crudely incorporated throughout the
 388 area of the piles within the 2D domain. However, Sailer et al. (2018a) show this 2D plane approach to
 389 overestimate the temperature change that occurs. While this will be conservative, Sailer et al. (2018a)
 390 go on to develop conversion factors for 2D plane analysis to improve predictions made from this
 391 approach.

392 A transient 3D finite element model to simulate the thermal behaviour of the ground and the GHEs
 393 was developed by Marcotte et al. (2010) and Marcotte & Pasquier (2008). The model is limited in

394 depth to the length of the GHE. The carrier fluid, the U-pipes and the grout are considered in this
395 model, but instead of including an explicit pip bend at the base of the GHE, the pipes are simply
396 continued to the base of the model. The fluid temperature profile is obtained after integrating the
397 bottom horizontal face of the downward pipe, information that is then used as a boundary condition
398 for the lower face of the upward pipe. Despite being a 3D model, axial effects related to geometry (as
399 opposed to fluid flow) are ignored since the upper and lower boundaries are insulated. Therefore, the
400 model is only appropriate for short timescales.

401 Bidarmaghz, Narsilio and co-workers developed a truly 3D finite element model for both boreholes
402 and energy piles. This model explicitly considers the flow and heat transfer in the pipes embedded in
403 the GHE. The fluid flow within the pipes is modelled either in 3D or 1D and is fully coupled to the heat
404 diffusion in the concrete and the ground. The model has been validated against full scale experimental
405 data covering a range of conditions and then used to investigate optimisation (Bidarmaghz 2015,
406 Bidarmaghz et al. 2012, Bidarmaghz et al. 2016a, 2016b, Narsilio et al. 2012, Narsilio et al. 2018). Using
407 similar techniques, Ozudogru et al. (2015) also developed a 3D numerical model for simulating vertical
408 U-tube borehole GHEs.

409 Various authors have also applied 1D line or pipe elements to energy piles, including Choi et al. (2011),
410 Cecinato & Loveridge (2015), Batini et al. (2015) and Caulk et al. (2016). Rees & He (2013) took an
411 alternative approach to simplifying the pipe details within a borehole heat exchanger model. They
412 used a single layer of cells to represent the fluid within the U-tube. The thermal properties of the
413 material in these cells must be adjusted to make this representation appropriate.

414 Other numerical simulations have considered different physical processes in the soil surrounding
415 energy piles and geothermal heat exchangers to evaluate coupling between heat transfer and water
416 flow processes. For example, Wang et al. (2015a) evaluated the impact of coupled heat transfer and
417 water flow on the behaviour of an energy pile in unsaturated silt and compared results with those
418 from centrifuge physical modelling tests. Baser et al. (2018) evaluated the roles of enhanced vapour
419 diffusion and phase change in the coupled heat transfer and water flow in unsaturated soils
420 surrounding a borehole heat exchanger and found that consideration of these two variables leads to
421 a faster heating response and larger zone of influence of the heat exchanger. Further, heating of
422 unsaturated soil was found to lead to permanent drying that may cause changes in the transient
423 response during cyclic heating and cooling. Specifically, the drying effect leads to a decrease in thermal
424 conductivity and specific heat capacity of the unsaturated soil.

425 *2.1.2.6 Hybrid Models*

426 The Duct Storage Model (DST) was developed to consider an underground thermal store constructed
427 of many identical vertical GHE installed within a cylindrical area (Hellstrom 1989). The model
428 superimposes three solutions: a finite difference model for the long-term heat transfer between the
429 thermal store and the surrounding ground, a second finite difference model for the heat transfer
430 between GHEs and the ground within the store and finally an analytical model for the steady heat
431 transfer within the heat exchangers. Despite numerical implementation the model runs fast enough
432 for routine application. It has been implemented in the building energy software TRNSYS for borehole
433 applications and as a standalone application called PILESIM (Pahud 2007). PILESIM is commercially
434 available and one of the few tools validated for use with piles. The validation is based on the Zurich
435 Airport case study (Pahud & Hubbach 2007). However, many of the assumptions in the DST are not

436 appropriate for piles, which are typically installed on an irregular grid and may comprise different sizes
437 and lengths. The DST also assumes a steady state resistance which has been shown to overestimate
438 temperature changes.

439 Another technique which has proved successful is that of simulating the energy pile and the ground
440 as a series of resistances and capacitances using an electrical analogy. This approach has been
441 adopted by Zarrella et al. (2013) who initially developed a model for boreholes (De Carli et al. 2010,
442 Zarrella & De Carli 2013) and then extended it to be applicable to energy piles. The pile version uses
443 an equivalent U-tube simulation to account for a larger number of U-pipes connected in parallel. The
444 “electrical” circuit is 3D to include axial effects and is computed numerically but is dependent on input
445 parameters in term of values of the resistances that depend on the pile and pipe geometry. These
446 needed to be determined separately in advance and is usually done by application of a discretised
447 model based on the finite difference or finite element methods. A similar approach is presented for
448 piles with four pipes, without the U-tube simplification, by Maragna & Loveridge (2019).

449 *2.1.2.7 Pipe Arrangements and Pile Geometry*

450 Numerical simulation is a productive tool for sensitivity analysis and several authors have addressed
451 the issues of pipe arrangements and pile geometry (e.g., Makasis et al. 2018a, 2018b). Initial studies
452 (e.g. by Gao et al. 2008) focused on the relative efficiency of U, UU (parallel connection) or W (series
453 connection) shaped pipes being installed within the piles. However, more recent work by Cecinato &
454 Loveridge (2015) shows that the most important factor for maximising energy exchange in piles is to
455 install a greater number of pipes, hence either UU or W shaped arrangements will always be
456 preferable to a single U tube. The authors showed that following pipe numbers, the pile length was
457 the next most influential factor, followed by the pile thermal properties. The importance of pile length
458 is consistent with work by Batini et al. (2015), who also studied the influence of aspect ratio and other
459 factors on thermal and mechanical performance.

460 Recently there has been significant interest in the use of helical (or “spiral coil”) pipe arrangements
461 rather than standard vertical pipe installed as U-tubes (e.g. Park et al. 2013; Go et al. 2014; Man et al.
462 2011). Comparative studies have shown helical pipe arrangements to potentially offer greater heat
463 transfer rates compared to standard energy pile arrangements (Zarrella et al. 2013; Yoon et al. 2015).
464 At least some of this advantage is due to the greater pipe lengths that can be accommodated within
465 the pile using the spiral arrangement.

466 Contiguous flight auger (CFA) piles with short steel cages which prevent full depth installation of heat
467 transfer pipes have also given rise to an alternative pipe layout. In these cases, to permit a full depth
468 pipe installation U-tubes are attached to a separate steel bar and plunged centrally into the concrete
469 following insertion of the short cage (Amis et al. 2014). However, due to the closer proximity of the
470 pipes such central arrangements of pipes will always be less energy efficient than a standard
471 arrangement (Loveridge & Cecinato 2016).

472 Further discussion of pile types and pipe arrangements is considered from a field data perspective in
473 Section 3.1.1.1.

474 2.1.3 Energy Walls

475 2.1.3.1 Overview

476 The last five years has seen an increased interest in energy retaining walls. These are most typically
477 diaphragm walls, but also include piled walls. These embedded retaining walls may be constructed to
478 support building basements, metro stations or shallow cut and cover tunnels. Depending on the end
479 use of the excavation space in front of the wall, their thermal behaviour may vary and consequently
480 it is important to correctly understand the nature of this space and what boundary conditions it may
481 impose on the energy wall. This additional boundary condition is the most important difference when
482 considering the thermal performance of energy walls as opposed to piles which are surrounded by the
483 ground. Consequently, some consideration is given to determining this condition before looking
484 specifically at analytical and numerical methods applied to thermal analysis for energy walls.

485 2.1.3.2 The Excavation Space

486 Building basements may be subject to damped seasonal variations if they are not temperature
487 controlled, or they could approximate constant temperature environments if they are subject to
488 climate conditioning. On the other hand, metro stations or shallow tunnels may exhibit strong
489 convective conditions due to the movement of trains or other vehicles, and there might be sources of
490 heat, like train braking or passengers. When undertaking such an analysis, the excavation space
491 therefore needs thermal characterisation. The space may be represented by one of three boundary
492 conditions. An adiabatic condition suggests that there is no heat transfer to this space and is
493 potentially conservative in the long term if the space is considered a positive source of energy.
494 However, the space can also be a sink and reduce efficiency due to heat losses, in which case this
495 assumption may not be conservative. The alternative extreme is a constant (or time varying)
496 temperature boundary condition. This will give the highest heat transfer rates. Finally, a convective
497 condition may be assumed, with use of a heat transfer coefficient to determine the magnitude of the
498 heat transfer occurring within the excavation space. Very high heat transfer coefficients, applicable to
499 scenarios with high air flow conditions, will approximate a temperature boundary.

500 Bourne-Webb et al. (2016b) studied the difference between a temperature and a convective boundary
501 using a 2D steady state finite difference simulation. They showed a potential four-fold difference in
502 heat transfer rates from 20 W/m^2 to 80 W/m^2 between the extreme conditions. However, the steady
503 state analysis may not be representative of long-term behaviour. Transient analysis over two months
504 by Piemontese (2018) showed a much smaller discrepancy between these conditions, generally less
505 than 5 W/m^2 .

506 Current experience shows a variety of approaches taken to the excavation space boundary condition.
507 Many analyses have assumed a constant (or time varying) temperature condition, for example the
508 basement applications considered by Kürten et al. (2015a), Kürten (2014) and Sterpi et al. (2017), and
509 the metro stations studied by Soga et al. (2014), Rui & Yin (2018) and Rammal et al. (2018). Heat
510 transfer coefficients representing a convective boundary have been used more rarely, notably by
511 iCConsulten (2005) when assessing metro stations and tunnels and by Bourne-Webb et al. (2016b) in
512 their sensitivity study. More recently, adiabatic conditions have been assumed for metro station
513 studies in Torino (Barla et al. 2018) and Melbourne (Narsilio et al. 2016a, 2016b).

514 Field data with which to validate analysis approaches remain relatively rare (see also Section 3).
515 Angelotti & Sterpi (2018) used data from a diaphragm wall forming a basement wall in northern Italy
516 to validate their numerical simulations. They found that a time varying temperature boundary was
517 appropriate over the four months of data available. To provide the best fit they applied a damping
518 coefficient to reduce the fluctuations of air temperature in the locality to an appropriate value to
519 approximate conditions within the basement. The constant temperature approach used by Kurten et
520 al. (2015a) during numerical simulation was also validated, but this time with reference to model test
521 data (refer to Section 4). No longer-term validations are available.

522 2.1.3.3 Numerical Simulations

523 Numerical simulation is the most common approach for analysis of the thermal capacity of energy
524 walls. Several different approaches have been applied. Bourne-Webb et al. (2016b) used 2D steady
525 state finite difference analysis with fixed temperature values on the pipe boundary conditions.
526 Rammal et al. (2018) approximated the heat transfer process by assuming a constant temperature in
527 the energy wall in the 3D finite difference analysis. More common, however, is the use of 1D line
528 elements to simulate the heat transfer pipes within a 3D finite element analysis, for example in the
529 studies of Sterpi et al. (2017), Di Donna et al. (2016a), Narsilio et al. (2016a, 2016b) and Barla et al.
530 (2018). 3D finite volume analysis was carried out by Shafagh & Rees (2018), including meshed pipe
531 detail.

532 Not all the approaches are fully validated by field data. Di Donna et al. (2016a) used the published
533 short-term thermal performance test data from Xia et al. (2012) to validate their model. Sterpi et al.
534 (2018) and Shafagh & Rees (2018) both use longer data sets. The former from 4 months of monitoring
535 from a real case in Italy and the latter from a 38-day multi-stage thermal response test in Spain.

536 2.1.3.4 Analytical Methods

537 While numerical simulation is a common research tool, and has also been used by researchers
538 supporting practice (e.g. Narsilio et al. 2016a, 2016b; Rammel et al. 2018), more accessible analytical
539 techniques for analysis of energy walls have yet to be fully developed for routine deployment

540 First Sun et al. (2013) proposed the first analytical solution based on heat conduction. The model
541 contains many familiar assumptions from the analysis of energy piles, with the addition of a convective
542 heat transfer boundary condition for the inside face of a retaining wall. The model was tested against
543 full numerical simulation and the thermal performance test data from the Shanghai Museum of
544 Nature History (Xia et al. 2012). However, poor fit was found at short time periods (<12 hours)
545 suggesting the details of the heat exchanger are insufficiently well captured.

546 Subsequently, Kurten et al. (2015b) used an electrical analogy to develop a thermal resistance model
547 for energy walls. They took account of pipe positioning and used a numerical model to compute the
548 resistance. The approach was then validated against full numerical simulation and model scale
549 laboratory tests. More recently Shafagh & Rees (in review) have developed a more general resistance
550 model for a rectangular shape with an irregular hole. The truly analytical approach, which assumes
551 either isothermal or convective boundary conditions, would be application to energy wall applications.

552 While the thermal resistance models deal only with the internal heat transfer within the wall, a
553 composite model has also been developed by Shafagh & Rees (2018) based on the Dynamic Thermal
554 Network (DTN) approach. The network describes the relationship between temperature and fluxes at

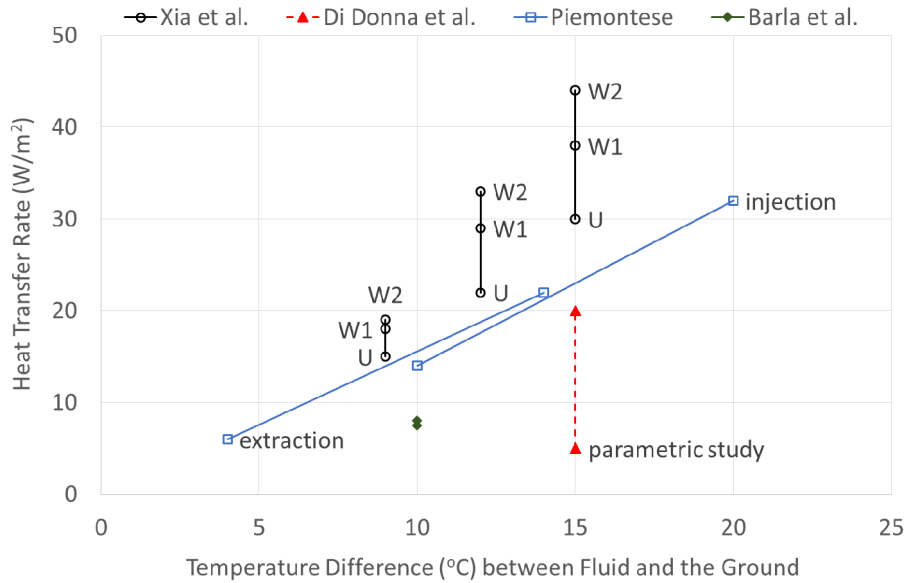
555 surfaces, with these surfaces specified as the ground, the excavationspace and the heat transfer pipes.
556 DTN is a response factor method and therefore represents transient conduction in terms of the surface
557 fluxes and temperature variables only. In this approach the current state is expressed entirely in terms
558 of the current and past temperatures (Rees & Fan, 2013). Each transient heat flux is dependent on
559 weighed averaged nodal temperatures which are calculated using weighting factors. Shafagh & Rees
560 (2018) calculated these weighting factors using their finite difference model. However, once the
561 weighting factors are pre-determined based on the geometry then the run time is fast. The model was
562 then validated against a long-term thermal response test.

563 *2.1.3.5 Pipe Arrangements*

564 Various sensitivity analyses have shown the benefit of W as opposed to U shaped pile installations
565 within the walls (Xia et al. 2012, Barla et al. 2018) based on field and numerical testing (Figure 6).
566 However, slinky-like arrangements, where many turns are made to maximise the amount of pipe
567 included in the wall are also popular in some countries, and analyses show these may have the
568 greatest benefit in terms of heat transferred (Sterpi et al. 2017). Reducing the pipe spacing or
569 increasing the length of pipe attached to a given wall panel will also often increase energy efficiency
570 (Kurten 2011, Di Donna et al. 2016a, Barla et al. 2018). However, pipe length alone is an insufficient
571 measure and pipe arrangement must also be considered in combination (Sterpi et al. 2017).

572 The above pipe optimisation studies were mostly are short-term analyses. The statistical based
573 parametric analysis by Di Donna et al. (2016a), on the other hand, suggests that the importance of
574 pipe spacing and arrangement will decrease in the longer term. As more time progresses, the
575 temperature difference between the ground and the excavation space becomes of prime significance
576 instead. This is consistent with the steady-state analysis of Bourne-Webb et al. (2016b) and the long-
577 term transient analyses of Narsilio et al. (2016a). Again, this highlights that the temperature response
578 of the structure (and hence the energy exchanged) to be highly dependent on this internal excavation
579 space boundary condition. Finally, the temperature difference between the heat transfer fluid and the
580 soil is key for determining the heat transfer rate (Xia et al. 2012, Piemontese 2018), Figure 6. This
581 confirms the importance of balancing thermal loads to maintain maximum temperature differences
582 during operation (e.g., Narsilio et al. 2016a).

583



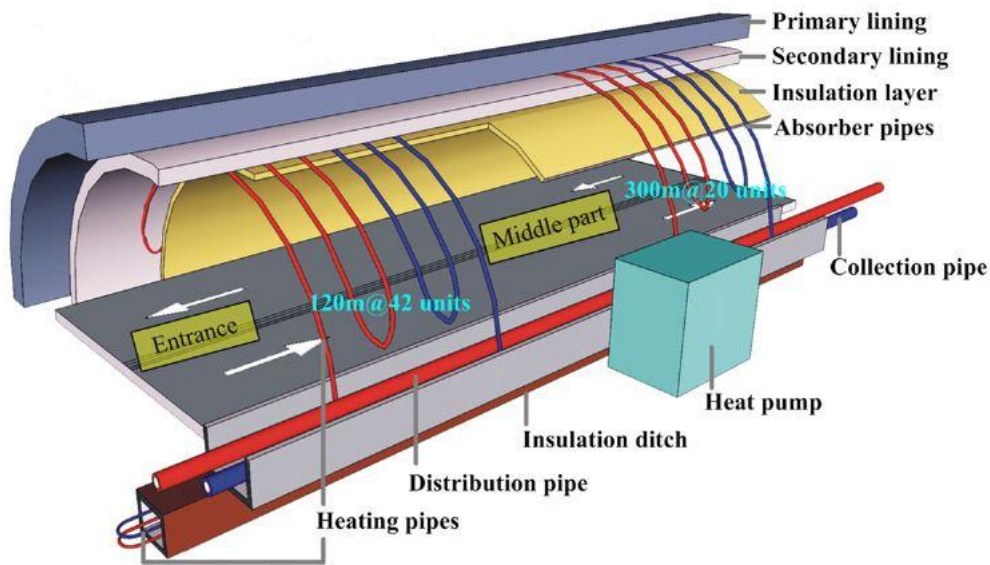
584

585 **Figure 6 Effect of pipe arrangements and temperature difference between fluid and the ground on**
 586 **the heat transfer rate obtained from energy walls. (U = single U tube; UU = two U-tubes connected**
 587 **in parallel; W 1 or W 2 = two U-tubes connecting in series; parametric study includes both U and UU**
 588 **arrangements).**

589 2.1.4 Energy Tunnels

590 2.1.4.1 Overview

591 Like retaining walls acting as heat exchangers, tunnel linings equipped with heat transfer pipes are
 592 relatively rare and there is still no routinely adopted design and analysis practice, although some
 593 guiding principles have been offered in the literature (e.g., Frodl et al. 2010, Nicholson et al. 2014a,
 594 Tinti et al. 2017). Figure 7 shows a schematic example of an energy tunnel. However, there is an
 595 increasing interest on the potential use of energy tunnels, driven by sustainability and innovation
 596 requirements found in large infrastructure projects. Pilot and trial tunnel sections are most typically
 597 encountered in metro rail projects, with pipe heat exchangers embedded on the tunnel linings shortly
 598 after shotcreting or in tunnel segments. Depending on the primary intended end-use of the tunnel
 599 heat exchangers, that is, to exchange heat with the ground or to exchange heat with the tunnel air
 600 space (i.e., providing heating or cooling to the tunnel space), their thermal behaviour may vary and
 601 consequently it is also important to correctly understand the nature of this use and the boundary
 602 conditions that are to be prescribed on the energy tunnels models. Like with energy walls, the
 603 boundary condition against the air space of the tunnel is the most important difference with borehole
 604 ground heat exchangers and energy piles, and due consideration must be given in any analytical or
 605 numerical analysis for energy tunnels. The role of groundwater flow and its predominant direction
 606 also impact on the thermal energy yield.



607

608 **Figure 7 Schematic view of a energy tunnel. Absorber pipes are embedded into the tunnel lining**
 609 **(adapted from Zhang et el. 2013, reproduced with permission, Licence Number 4585510080214)**

610 *2.1.4.2 The Tunnel Space*

611 Like with energy walls, the tunnel space needs careful thermal characterisation. The environmental
 612 conditions of the tunnel air space vary on a case by case basis. They are typically not subjected to
 613 climate conditioning; however, ventilation is common in metro and vehicle tunnels. Unventilated or
 614 “hot” tunnels also exist, such as those in the London Underground (Nicholson et al. 2013; Stephen,
 615 2016, Mortada et al. 2018). These conditions are important when considering thermally activating the
 616 tunnels. Even in hot tunnels, convective conditions may exist due to the movement of trains or other
 617 vehicles, and additional sources of heat arising from train braking or passengers may also exists. In
 618 sewage tunnels (liquid as oppose to gas, air) convection is also important.

619 The tunnel space may be represented by one of three boundary conditions. When there is no heat
 620 exchange with this space, an adiabatic condition shall be considered. This boundary condition implies
 621 thermal insulation has been incorporated in the tunnel lining, which is not typically the case for tunnels
 622 and carries additional material and construction costs (and in the case of metro, passengers and cargo
 623 tunnels, materials must be fire resistant as well). For the common case of no thermal insulation, the
 624 tunnel air space can also be a heat sink or source, and the analysis can be carried either modelling the
 625 space air convective-conductive heat transfer (most comprehensive) or by (un-conservatively)
 626 prescribing a constant or time varying temperature boundary condition. The latter approach under-
 627 or over-estimate the heat transfer of the thermally activated tunnel lining, scenarios with high
 628 air/sewage flow convention, will approximate a temperature boundary.

629 *2.1.4.3 Numerical Simulations*

630 Full scale data with which to validate analysis approaches remain relatively rare (see also Section 3).
 631 Bidarmaghz et al. (2017) and Bidarmaghz and Narsilio (2018) used data from an energy tunnel pilot
 632 project in Germany summarised in Buhmann et al. (2016) to validate their numerical simulations. Lee
 633 at al. (2016) and Zhang et al. (2013, 2016a, 2017) performed field scale and laboratory scale thermal

634 performance tests to validate and extend their own numerical and analytical models respectively.
635 They found that a constant or time varying temperature boundary was appropriate for highly
636 ventilated tunnels or for short term testing, but this is an area of active research in which longer-term
637 validations and representativeness of the boundary conditions adopted are still under investigation.

638 While the published literature on energy tunnels is still quite limited, one can see that numerical
639 modelling has been adopted to undertake technical feasibility studies and or better understand results
640 from laboratory and field testing (e.g., Nicholson et al. 2014a, Narsilio et al. 2016a, 2016b, Barla et al.
641 2016, Baralis et al. 2018). Numerical simulations are used to assess temperature changes in the ground
642 and the tunnel space, and heat transfer rates. Studies have been conducted in both two (Franzius &
643 Pralle 2011) and three dimensions (Nicholson et al. 2014a). Again, the structure internal boundary
644 condition is very important. Zhang et al. (2014) have observed the importance of the air inside the
645 tunnel as a heat source, with subsequent analysis linking tunnel air speed and heat transfer rates
646 (Zhang et al. 2016a, 2017). This is reflected in the study of Nicholson et al. (2014a) where the trains
647 running within the tunnel were positively taken as a source of heat. However, Franzius & Pralle (2011)
648 neglected heat transfer into the tunnel which is a significant over simplification. Di Donna & Barla
649 (2016), Barla et al. (2016), Lee et al. (2016), Bidarmaghz et al. (2017) and Bidarmaghz and Narsilio
650 (2018) have also used 3D numerical simulations with 1D pipes to reduce computational effort to
651 perform parametric studies, including the effect of ground and groundwater conditions on the energy
652 efficiency of energy tunnels.

653 *2.1.4.4 Analytical Methods*

654 An analytical solution has also been proposed by Zhang et al. (2013) based on a model in radial
655 coordinates. This accounted for the internal boundary condition via a sinusoidal varying temperature
656 condition determined from monitoring of road tunnels. The model was successfully validated against
657 field data, but only over a limited time frame. In addition, empirical models have been used by Tinti
658 et al. (2017) for high level estimations of thermal yields for sections of tunnels linking Italy and Austria.

659 Analytical methods offer much quicker alternatives for the analysis and design of energy tunnels than
660 detailed finite element simulations, the most common numerical technique adopted to date for this
661 purpose (previous section). Clearly, research on analytical techniques for energy tunnels is
662 underdeveloped at present.

663 *2.1.4.5 Pipe Arrangements*

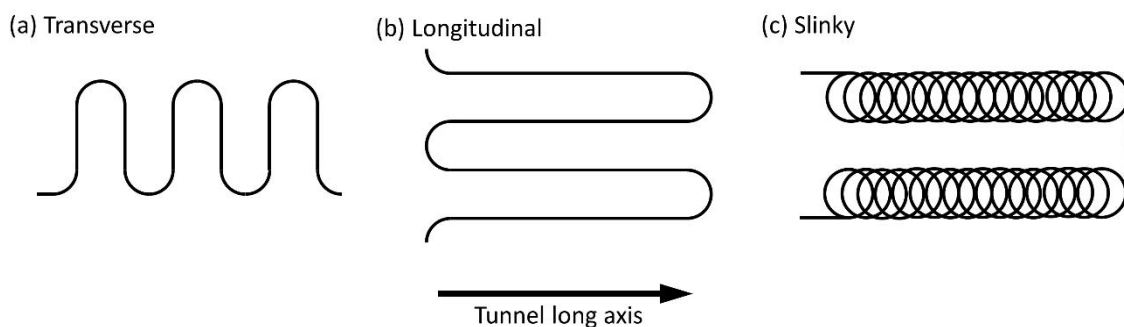
664 As it is the case for other types energy geostructures, pipe arrangements must suit constructability
665 and minimise or avoid overall construction program delays. Currently, there are three main means to
666 embedded absorber pipes into tunnels, with similar pipe configuration arrangements. These are also
667 reflective of the excavation method:

- 668 • Installation of absorber pipes between the outer and inner (shotcrete or other) lining or in the
669 inner lining. This solution is best suited to be used in drill and blast or punctual mechanised
670 excavation systems. Examples included the pilot geothermal system of Stuttgart's Fasanenhof
671 underground station in Germany (Geimer 2013, Buhmann et al. 2016) and of Yakeshi's
672 Linchang tunnel in Inner Mongolia (Zhang et al. 2014).

- 673 • Installation of precast energy textile or energy fleece, also suitable for drill and blast
674 excavations (Lee et al. 2016). The first application of this type can be found in Vienna's Lainzer
675 tunnel (2003) in Austria (Adam and Markiewicz 2009).
- 676 • Installation of absorber pipes within precast lining segments: suitable for Tunnel Boring
677 Machine (TBM) excavations. The first GSHP system using thermally activated lining segments
678 was installed in Austria, in the Stuttgart-Jenbach tunnel (Frodl et al. 2010; Franzius & Pralle
679 2011).

680 In all three cases, absorber pipes are placed in a meandering fashion, with the pipes either
681 predominately parallel to the main axis of the tunnel (longitudinal meandering) or perpendicular to it
682 (transverse meandering). The slinky pipe arrangement has only been tested in prefabricated energy
683 textiles (see Figure 8).

684 Adam & Markiewicz (2009) and Brandl et al. (2010) placed heat exchanger pipes on a geotextile
685 between the primary and secondary tunnel lining for a Vienna metro tunnel constructed using the
686 New Austrian Tunnelling Method (NATM), Schneider & Moorman (2010) incorporated geothermal
687 heat exchangers into panels in a Stuttgart metro tunnel that were connected with coupling joints that
688 provide both mechanical interlocking and hydraulic connections, and Nicholson et al. (2014a)
689 incorporated heat exchanger tubing into segmental panels for the London Crossrail tunnel.



690
691 **Figure 8 Typical layout of absorber pipes in energy tunnels: (a) longitudinal meandering pipe, (b)**
692 **transverse, and (c) slinky (only found in energy textiles to date).**

693 2.1.5 Other Geotechnical Structures

694 Energy ground anchors have been suggested and in one case successfully trialled (Adam & Markiewicz
695 2009, Mimouni et al. 2014). Analysis to date appears to be mainly based on numerical simulations,
696 although their axisymmetric nature would mean they are well suited to similar design approaches
697 applied to energy piles. Energy base slabs have also been constructed (e.g. Brandl 2006) and design
698 approaches would be similar to retaining walls. However, because slabs do not have the benefit of the
699 embedded part of retaining walls, which are surrounded by soil on both sides, they will always have
700 lower rates of heat transfer. Recent in situ monitoring of walls and slabs by Angelotti & Sterpi (2018)
701 show almost three times lower heat transfer rates for the slabs, in the range of 3 to 9 W/m². This
702 compares well to the average rate of 5 W/m² reported from various sites by Kipry et al. (2009).

703 Excavations for shallow foundations have also been utilised for ground heat transfer and storage. In
704 Korea, heat transfer pipes have been trialled at the base of concrete shallow foundations, with
705 subsequent numerical simulation validated against experimental data (Nam & Chae 2014). In the

706 United States, Oak Ridge National Laboratory led a project to place horizontal pipes within the
707 excavations already being made for shallow foundations for domestic house (Hughes & Im 2013), so
708 called Foundation Heat Exchangers. The project was supported by analysis by Oklahoma State
709 University and others who developed numerical simulation and implemented the results in the
710 software EnergyPlus for routine application (Cullin et al. 2014, Xing et al. 2012, Spitler et al. 2011).

711 Shallow geothermal systems can also be used to prevent snow accumulation and/or ice formation on
712 bridges, roads, sidewalks, and similar structures. For example, geothermal systems for bridge de-icing
713 generally envisage energy piles for the bridge foundation, loops embedded in the abutment
714 embankment for additional heat exchange with the ground, and loops in the bridge deck that will
715 maintain the surface warm to prevent ice formation (e.g. Olgun & Bowers, 2013). A brief review on
716 geothermal energy for bridge deck and pavement de-icing is presented in Yu et al. (2016). Detailed
717 numerical analyses and feasibility studies are presented elsewhere (e.g. Ho and Dickson, 2017; and
718 Han and Yu 2018).

719 **2.2 Geomechanical and Structural Analysis**

720 2.2.1 Overview

721 The geotechnical design of energy geostructures focuses primarily on both ensuring their ultimate
722 capacity to safely exceed building loading demands, and their long-term serviceability in terms of
723 deformation response. In the case of energy piles, depending on the restraints provided by the
724 overlying superstructure and the mobilised side shear stresses and end bearing stresses specific to the
725 subsurface stratigraphy, temperature changes associated with geothermal heat exchange may lead to
726 thermally-induced changes in axial stress and deformations. The thermally-induced changes in axial
727 stress may increase the building loading demands on the energy pile, while the thermally-induced
728 deformations may lead to changes in the long-term serviceability. Furthermore, depending on the
729 magnitude of the axial stress before heat exchange processes commence, cyclic heating and cooling
730 may lead to permanent deformations that need to be characterised. Accordingly, it is critical to
731 accurately estimate the thermally-induced changes in axial stress and deformations expected for an
732 energy pile under the site-specific end-restraint boundary conditions and subsurface stratigraphy. For
733 other energy geostructures such as tunnels and walls, a similar design philosophy may be adopted,
734 but it is expected that the restraint boundary conditions will differ from those encountered for energy
735 piles.

736 2.2.2 Piles

737 The two major approaches to predict the thermally-induced axial stresses and deformations in energy
738 piles are load transfer analysis and FE analysis. Load transfer analysis is a simplified approach to
739 consider axial soil-structure interaction phenomena that relies upon assumed shapes of the mobilised
740 side shear stress and end bearing stress versus deformation curves (Coyle & Reese 1966). Although
741 semi-empirical, this approach permits characterisation of nonlinear soil-structure interaction that may
742 be difficult to consider in finite element analyses. However, a challenge in this analysis is the definition
743 of the head restraint boundary conditions and the role of radial stresses. Load transfer analysis has
744 been used successfully to represent the observed mechanical and thermo-mechanical behaviour of
745 energy piles in the field and centrifuge by Knellwolf et al. (2011), McCartney (2015) and Chen &
746 McCartney (2016). It has also been used to evaluate the role of cyclic heating and cooling (Pasten &

747 Santamarina 2014; Suryatriyastuti et al. 2014). It is important to note that there has not been sufficient
748 experimental data collected to validate these predictions. These studies did identify that piles that are
749 loaded closer to their ultimate capacity will show greater amounts of permanent deformations due to
750 ratcheting effects. Ouyang et al. (2011) used a hybrid load transfer analysis that combined the axial
751 stress-strain response of individual energy piles obtained from a load transfer analysis with an elastic
752 continuum solution to model interaction between energy piles.

753 Finite element analyses have been widely used to study the thermo-mechanical behaviour of energy
754 piles, considering a range of different constitutive relationships for the energy pile, soil, and interface,
755 as well as considering different physical processes such as heat flow and thermally-induced pore water
756 flow. Although FE analyses can consider the impacts of more complex phenomena, they require more
757 parameters for the constitutive relationships. Although the focus of many energy pile designs is on
758 the pile performance considering the soil-pile interface, the behaviour of the surrounding soil may
759 have long-term implications on the energy pile performance. Laloui et al. (2014) and Coccia &
760 McCartney (2016a, 2016b) provided a review of different constitutive relationships that can be
761 considered for the thermo-mechanical behaviour of soils and soil-pile interfaces. Several constitutive
762 relationships used in FE analyses of soils do not consider thermo-mechanical behaviour but account
763 for different ways to incorporate soil nonlinearity during mechanical loading. Specifically,
764 Suryatriyastuti et al. (2016) used a hyperbolic model to represent the behaviour of the soil without
765 consideration of temperature effects. Saggiu & Chakraborty (2015), Olgun et al. (2014) and Ozudogru
766 et al. (2015) used an elasto-plastic formulation with the Mohr-Coulomb yield criterion, while Ng et al.
767 (2015) used an incremental nonlinear hypoplastic model specific to sand. On the other hand, fewer
768 models have incorporated thermo-elasto-plastic soil behaviour. Specifically, Rotta Loria & Laloui
769 (2016a) used a linear thermo-elastic model for the soil, Laloui et al. (2006) used a thermo-elasto-plastic
770 model with the Drucker-Prager yield criterion, and Di Donna et al. (2016b) used a thermo-elasto-
771 plastic model with the Mohr-Coulomb criterion. It was not possible to validate whether the soil
772 constitutive model influenced the axial soil-structure interaction predictions, but all the constitutive
773 models used in the previous studies still resulted in good matches in terms of the predicted axial
774 stresses and strains in the energy piles. Laloui et al. (2006), Laloui and Nuth (2006), and Rotta Loria &
775 Laloui (2016a) assumed that the pile and soil were rigidly connected (a perfectly rough interface),
776 Suryatriyastuti et al. (2012) and Ozudogru et al. (2015) used an elastic-perfectly plastic soil-pile
777 interface element, Saggiu & Chakraborty (2015) and Ng et al. (2015) used an interface friction angle
778 smaller than that of the soil and a refined mesh near the interface, while Suryatriyastuti et al. (2016)
779 used a bounding surface plasticity formulation for the interface. Gawecka et al. (2016, 2017) used a
780 full-coupled thermo-hydro-mechanical FE model to model the impact of transient heat transfer and
781 water flow on soil-structure interaction in energy piles and found that thermally-induced stresses in
782 energy piles dissipate with time as the surrounding subsurface reacts to the changes in pile
783 temperature. Cyclic effects have been considered in several finite element analyses, with plastic
784 deformations obtained through the constitutive model of the soil (Ng et al. 2015) or through the soil-
785 pile interface constitutive model (Suryatriyastuti et al. 2016). Many of the models mentioned above
786 were validated using field data from Laloui et al. (2006) or Bourne-Webb et al. (2009), although Rotta
787 Loria et al. (2015a, 2015b) found that FE analyses could also be validated using centrifuge modelling
788 results.

789 A significant advantage of FE simulations over load transfer analyses is the ability to consider heat flow
790 analyses and their impacts on the thermo-hydro-mechanical response of the subsurface surrounding

791 the energy pile. Laloui et al. (2006) was able to predict the deformations of the soil surrounding an
792 energy pile while Di Donna et al. (2016b) and Rotta Loria & Laloui (2016a) were able to characterise
793 the thermal and thermo-mechanical interactions between pile groups. Wang et al. (2015a) simulated
794 the coupled flow of heat and water away from a centrifuge-scale energy pile in unsaturated silt, while
795 Akrouch et al. (2016) simulated coupled heat and mass transfer in unsaturated soil away from
796 laboratory-scale energy piles. In both cases, the changes in degree of saturation surrounding the
797 energy pile will lead to a change in effective stress and a corresponding change in the ultimate side
798 shear stress at the soil-pile interface, similar to that observed experimentally by Goode and McCartney
799 (2015). Changes in saturation also lead to changes in the soil thermal properties and heat transfer
800 from the energy pile.

801 Different methods of analyses have been used to consider the behaviour of energy pile groups than
802 those used for individual energy piles. Rotta Loria et al. (2016a) used a modified interaction factor
803 approach to consider group effects, while Suryatriyastuti et al. (2016), Di Donna et al. (2016b), and
804 Rotta Loria & Laloui (2016b) used FE analyses. The interaction factor approach can be used readily in
805 design calculations, while finite element analysis requires more in-depth site-specific testing to
806 determine material properties. The critical variables in the design of energy pile groups are the spacing
807 and diameter of the energy piles, and the relative stiffness of the pile, soil, and overlying slab which
808 may lead to changes in thermal and mechanical interaction. Although these studies identify that there
809 may be differential movements or changes in the stresses in the overlying slab if one of the energy
810 piles operates while the others do not, this effect is lessened when the temperature changes of the
811 energy piles are the same. It may not be possible to achieve similar changes in pile temperature in
812 practice, so some differential displacements or stresses are expected. Thermal interaction may lead
813 to a decrease in the thermal efficiency of the energy piles in terms of a balanced seasonal heat
814 exchange, so it is still important to have an adequate spacing between energy piles in groups if
815 possible.

816 Several analyses have been conducted quite recently focused on the behaviour and performance of
817 groups of energy piles (i.e. Rotta Loria and Laloui 2016a, 2016b, 2017a, 2017b, 2017c). It was shown
818 that the vertical displacement of energy piles can increase because of thermally-induced group effects
819 induced by the interactions among piles (Rotta Loria and Laloui, 2017b; Rotta Loria and Laloui, 2017c).

820 New challenges in the analysis of energy piles may arise when they are applied in soft soil, expansive
821 soil, or unsaturated soil settings, during lateral loading of energy piles, or when different materials are
822 used in the construction of energy piles. For example, McCartney & Murphy (2017) presented 6 years
823 of monitoring results from a pair of energy piles in saturated claystone that may have expansive
824 characteristics and observed a long-term dragdown effect superimposed atop the thermo-mechanical
825 behaviour of the energy pile. This dragdown could have been due to the natural settlement of the
826 soils on site under the building load, but they may also have been induced by the ground temperature
827 changes. Ghaaowd et al. (2018) evaluated the impact of heating on the pullout response of energy
828 piles from soft clays and observed an increase in pullout capacity that corresponded with a decrease
829 in void ratio of the clay surrounding the energy piles. This was attributed to the impact of permanent
830 contraction during drained heating of the clay on the undrained shear strength, which was
831 characterized experimentally for the same clay by Samarakoon et al. (2018). Analyses of these new
832 challenges will undoubtedly require the use of advanced finite element software for the long-term
833 design of energy piles.

834 2.2.3 Other Energy Gestructures

835 The thermo-mechanical response of energy walls is expected to be similar to energy piles, with an
836 exception that the lateral expansion at the ends of the wall will induce a 3D stress field that may be
837 more complex to evaluate than in energy piles (Soga et al. 2015). Further, structural restraints in the
838 case of basement walls may lead to differential thermal volume changes that are not observed in the
839 1D axial analysis of energy piles. While it may be possible to use load transfer analyses for energy
840 walls, it is expected that FE analyses would be required to evaluate their thermo-mechanical response.
841 However, Nicholson et al. (2014a) found that the temperature changes within the space enclosed by
842 a tunnel have a much greater effect than the temperature changes in the wall due to typical levels of
843 heat extraction.

844 As described in Section 2.1.4.5, different methods have been proposed to incorporate geothermal
845 heat exchangers into tunnel linings to extract heat from both the interior of the tunnel as well as from
846 the surrounding ground, depending on the method of tunnel construction. These different designs
847 may have different thermo-mechanical performance due to the geometry of the concrete section
848 surrounding the energy pile. The FE analyses developed for energy piles can be adapted to study
849 energy tunnels, with the main technical difference expected would be a change in the hoop stresses
850 and strains in the tunnel during heat extraction along with the tensile stresses around the heat
851 exchangers and between joints (Nicholson et al. 2014a). The surrounding subsurface may provide a
852 different restraint to thermal strains than in energy piles, and thermal deformations may affect
853 arching and stress distributions around the tunnel, although these changes likely already occur in the
854 tunnels without the incorporation of heat exchangers due to changes in ambient tunnel temperature
855 (Nicholson et al. 2014b). Sailer et al. (2018b) used FE analyses to compare hydro-mechanical FE
856 analyses where an energy wall expands and contracts during temperature changes without
857 temperature effects on the soil, and thermo-hydro-mechanical FE analyses where an energy wall
858 expands and contracts during temperature changes considering temperature effects on the soil. The
859 changes in pore water pressure of the soil in the latter analysis were found to have major effects on
860 the stress state in the soil and led to differences in the axial forces in the wall and the vertical
861 displacement of the wall. Barla et al. (2018) used FE analyses to study the thermal and thermo-
862 mechanical behaviour of energy walls and also found that the bending moment and horizontal
863 displacement increase at the top of an energy walls during heating, but with magnitudes within
864 acceptable structural limits.

865

866 **3 Field Scale Testing**

867 **3.1 Pile Thermal Tests**

868 3.1.1 Thermal Performance Tests

869 In this discussion thermal performance tests, which aim at obtaining the energy capacity of a system,
870 are differentiated from thermal response tests, which have their origin in the need to determine the
871 soil thermal conductivity in situ. Thermal performance tests have been further subdivided into short
872 term tests, usually conducted over a few days, and longer-term observations, typically conducted
873 during full operation of a system. This distinction is important, since short term tests commonly
874 provide an overestimate of energy capacity compared with operational conditions. Short term tests

875 nonetheless can be useful, especially for making comparisons of design aspects such as pile types and
 876 configurations.

877 *3.1.1.1 Short Term Tests*

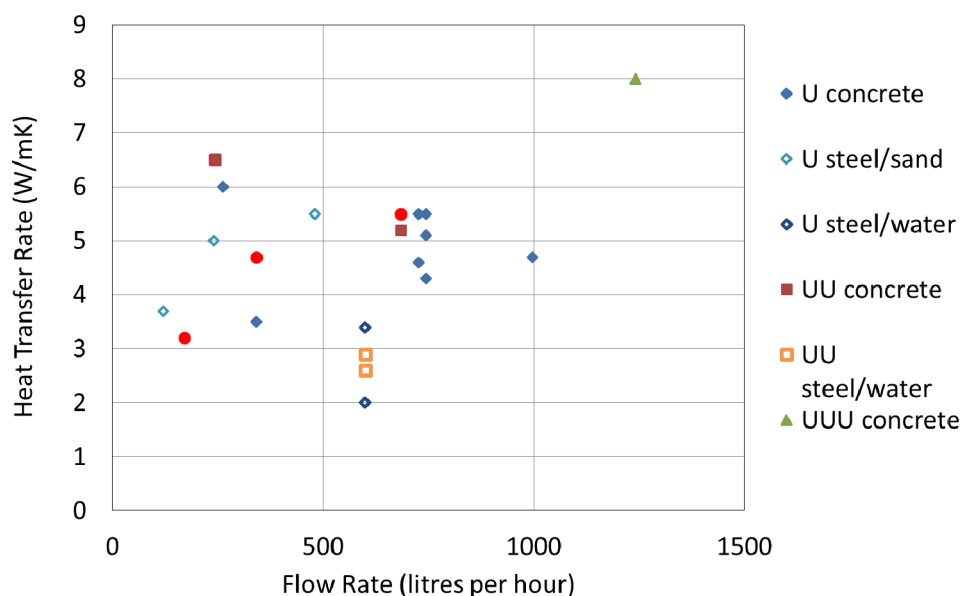
878 In this context short term test are defined as those where the duration of the experiment is no more
 879 than three months (although typical such tests are less than one week long). The performance of the
 880 pile heat exchanger is tested by circulating fluid, usually entering the pile at constant temperature,
 881 through the heat transfer pipes and recording the resulting outlet temperature. From the outlet
 882 temperature and knowledge of the fluid flow rate and thermal properties it is possible to calculate the
 883 heat transferred to the heat exchanger and the ground. Seven examples of this type of test have been
 884 identified for a variety of different piles as summarised in Table 3. The resulting heat exchange rates,
 885 expressed in W/m, vary substantially and depend on a range of factors including the pile construction,
 886 the number and arrangements of pipes, the flow rate, the ground conditions, the temperature
 887 difference between the fluid and the ground and the test duration. Complete information is not
 888 always available about all these factors, but nonetheless some overarching trends can be identified.

889 **Table 3 Summary of pile thermal performance tests**

Reference	Pile Type	Pile Diameter (mm)	Pipe No & Arrangement*	Flow Rate (L/h)	Temperature Difference* (°C)	Heat Transfer Rate (W/m)
Jalaluddin et al. (2011)	Steel screw pile, sand filled	140	U	120, 240, 480	10	37 - 55
Hamada et al. (2007)	Hollow pre-cast concrete, mortar filled	300	U, UU	244, 263	9 - 10	54 - 69
Morino & Oka (1994)	Steel, water filled	400	Direct use	1800	15 - 25 5 - 12 (extraction)	120 - 140 70 - 85
Nagano et al. (2005)	Steel, water filled	400	U, UU, direct use	300 - 1800	7 - 14	14 - 95
Gao et al. (2008)	Concrete, cast in situ	600	U, UU, W	171, 342, 684	17	55 - 115
Colls (2013)	Concrete, cast in situ	600	U, UUU	726 - 1242	3 - 16	4 - 8
Katsura et al. (2009)	Hollow steel, water filled	267, 400, 600, 800, 1200	U	480, 960, 1440	9 - 14	70 - 90
Murphy et al. (2015)	Concrete, bored cast in situ	610	U, W, UUU	381 - 1249	1.3 - 8.8	90 - 139
Brettmann & Amis (2011)	Concrete, continuous flight auger (augercast)	300, 450	UU	N.R.	N.R.	73 - 80
Ooka et al. (2007)	Concrete, bored cast in place	1500	8 U	N.R.	N.R.	100 - 120
Singh et al. (2015)	Concrete, bored cast in place	600	U	600	~4	

890 + between the fluid inlet temperature and the undisturbed ground temperature
 891 * Notes on pipe arrangements:
 892 U = single U-tube (2 pipes); UU = two U-tubes in parallel (4 pipes); UUU = three U-tubes in parallel (6 pipes); W = two U-
 893 tubes in series (4 pipes); Direct use = two open ended pipes inserted into the water filled pile, water infill part of circulation
 894 system.
 895 N.R. = Not reported.
 896

897 Several studies show increasing heat transfer with both increasing flow rate and increasing heat
 898 exchanger diameter (Gao et al. 2008, Katsura et al. 2009, Jaluddin et al. 2011, Nagano et al. 2005).
 899 However, when the pile capacity is normalised by temperature difference between the inlet fluid and
 900 the undisturbed ground, the trends in flow rate are less clear due to scatter relating to other factors
 901 (Figure 9). The study of Gao et al. (2008) also illustrates how an increasing number of U-tubes in series
 902 will increase the heat transfer capacity for the same flow rate. This verifies numerical studies by
 903 Cecinato & Loveridge (2015). However, Gao et al. (2008) also show that using multiple U-tubes in
 904 parallel is not necessarily advantageous unless the total flow rate to the pile is also increased so that
 905 the same flow rate to each U-tube can be maintained. The type of heat exchanger is also important.
 906 The highest rates of heat transfer in Table 3 are both associated with the direct use of infill water in
 907 steel piles as part of the heat exchanger (Morino & Oka 1994, Nagano et al. 2005). This is not surprising
 908 since this type of pile will be able to exploit any thermally driven convection within the water
 909 contained inside the steel pile. What is perhaps more surprising is that the cases of closed loop U-
 910 tube installations within water filled steel piles also reported by Nagano et al. (2005) have a much
 911 lower unit extraction rate compared to other installations (Figure 9). Overall, most pile exhibit a heat
 912 transfer rate in the range of 3 to 6 (W/mK). The effect of intermittent and continuous operating modes
 913 on the thermal behaviour of a full-scale geothermal energy pile was investigated by Faizal et al. (2016a,
 914 2016b).



915

916 **Figure 9 Unit heat exchange rates from short term performance tests of piles. Data taken from the**
 917 **sources listed in Table 3.**

918 3.1.1.2 Long Term Tests and Operation

919 Long term monitoring data for operational energy pile schemes is relatively rare. Six cases where heat
 920 transfer rates have been recorded over periods of months or years are included in Table 4. One
 921 notable factor is that most long-term studies consider concrete piles that have been bored and cast in
 922 situ, whereas many of the thermal performance tests were conducted to examine other types of piles,
 923 especially steel piles. Four of the case studies (Wood et al. 2010a,2010b; Kipry et al. 2009; Pahud 2007;
 924 Pahud & Hubbach 2007; Henderson et al. 1998) show significantly lower heat exchange rates than
 925 shorter term tests, in the range 15 to 35 W/m. This is to be expected and is in line with recommended
 926 ballpark figures (e.g., SIA, 2005). More surprising are the two studies with higher heat exchange rates
 927 (Murphy & McCartney 2015; Sekine et al. 2007) of 90 to 220 W/m which fall outside of expected
 928 ranges. However, it must also be noted that without full information about the thermal loads at all
 929 the sites, as well as the temperature differences between the fluid and the ground it is not possible to
 930 make full comparisons between the case studies. Generally enhanced heat transfer rates would be
 931 expected where the thermal load is highly intermittent and includes a balance of heat injection and
 932 extraction, where the temperature difference between source and sink is high and where the ground
 933 has beneficial thermal properties.

934 Other notable observations from the studies include relatively uniform temperature profiles with
 935 depth down the piles (Murphy & McCartney 2015; McCartney and Murphy 2017) and the favourable
 936 comparison between piles and boreholes forming part of a combined system (Henderson et al. 1998).
 937 The first point suggests that largely radial heat flow is occurring (at least within the two-year timescale
 938 of the study), although the authors do note that the influence of ambient conditions is noticeable for
 939 the instrumented pile closest to the building edge. In the second study, Henderson et al. (1998) were
 940 able to compare the energy exchanged by an approximately equal total length of borehole and pile
 941 heat exchangers. They found the piles beneath their building to be supplying 56% of the heating and
 942 70% of the cooling, which they attributed to the absence of interaction with ambient conditions due
 943 to the building positioned above the pile heat exchangers.

944

945 **Table 4 Summary of operational pile performance**

Reference	Pile Type	Pile Diameter (mm)	Pile Length (m)	No Pipes	Monitoring Period	COP / SPF*	Heat Transfer Rate (W/m)
Henderson et al. (1998)	Steel tubes with concrete infill	200	26	2	12 months		16.4 extraction 18.3 injection
Wood et al. (2010a, b)	Bored cast in situ	300	10	2	7 months		26
Murphy and McCartney (2015); McCartney and Murphy (2017)	Bored cast in situ	910	15, 13	4, 8	6 years		91, 95

Pahud & Hubbach (2007)	Bored cast in situ	900 - 1500	26 - 27	10	24 months	2.7 to 3.9 (SPF)	15 extraction 16 rejection
Sekine et al. (2007)	Bored cast in situ	1500	20	8	15 months	3.2 extraction (COP) 3.7 injection (COP)	120 extraction 100 – 220 rejection
Kipry et al. (2009)	Various schemes					3 to 6.5 (SPF)	<30 extraction <35 injection

946 * COP = coefficient of performance and is the ratio of useable energy to the electricity supplied to the heat pump; SPF =
947 seasonal performance factor and is the ratio of the useable energy to the electricity supplied to the heat pump and
948 associated circulation pumps used in the system.

949 3.1.2 Thermal Response Tests

950 Thermal response testing is an in-situ technique designed to characterise the thermal properties of
951 the ground heat exchanger and the surrounding soil or rock to enable appropriate values to be used
952 in design. The technique as it is commonly deployed now, using mobile tests rigs, was developed for
953 borehole heat exchangers in the 1990's by two groups working independently, one at Oklahoma State
954 University (Austin, 1998) and the other at Lulea University of Technology in Sweden (Gehlin 2002).
955 Both groups developed an idea first proposed by Mogensen (1983) which proposed applying a
956 constant rate of heating or cooling to a GHE via the circulating fluid and using the resulting
957 temperature change to determine both the ground thermal conductivity and the borehole thermal
958 resistance. The test is directly analogous to a pumping test in groundwater engineering to determine
959 aquifer properties.

960 For the case of borehole heat exchangers, the test has now become relatively routine and there are a
961 number of relevant national and international standards for its implementation and interpretation
962 (Sanner et al. 2005; IGSHA 2007, 2009; GSHPA 2011; Banks 2012). Additionally, Spitler & Gehlin
963 (2015) provide a useful review of the development of the test method and equipment as well as a
964 review of interpretation methods and uncertainties. The most commonly used analytical model for
965 interpretation of the test remains the simplified infinite line source. In this model the relationship
966 between change in temperature and time is log-linear which makes interpretation straight forward.
967 The thermal conductivity can be determined from the gradient of the straight line and the thermal
968 resistance from the intercept on the temperature change axis. The thermal conductivity can therefore
969 be determined independently of the thermal resistance, which is not possible in other more
970 sophisticated parameter estimation techniques. However, the simplified infinite line source approach
971 has a key disadvantage when applied to pile heat exchangers. For the log-linear relationship to be
972 valid a certain amount of time must have elapsed, usually taken as $5r_b^2/\alpha$ where r_b is the heat
973 exchanger radius and α is the soil thermal diffusivity. This ensures that the mathematical simplification
974 behind the log-linear relationship is valid, and that the heat exchanger is at a thermal steady state (i.e.
975 the thermal resistance is constant). While this criterion is typically a few hours for boreholes, it may
976 be days or weeks for piles given the dependence on the square of the radius. The consequence of this
977 is that longer test times or different interpretation techniques are required for large diameter piles
978 (Loveridge et al. 2014a). Longer test times mean greater expense and reliable alternative

979 interpretation techniques for large diameter piles are still under development (e.g. Loveridge et al.
 980 2015).

981 The following sections summarise the work that has been done on thermal response testing for piles
 982 in recent years, as well as reporting published test datasets.

983 *3.1.2.1 Case Studies*

984 Seven notable pile thermal response test case studies are highlighted in Table 5 below. Other tests
 985 have been performed but those summarised in the table are more comprehensively reported and
 986 contain some alternative measure of the ground thermal conductivity with which to compare the in-
 987 situ results. In almost all cases the in-situ results for thermal conductivity are higher than those
 988 measured in the laboratory (Figure 10). There are several factors which may be causing this effect.
 989 First assuming the inlet temperature is typically higher than the ambient air temperature, thermal
 990 response tests can lose heat to the atmosphere between the application of the heat input and the
 991 point at which the circulation fluid enters the ground. This can cause overestimation of the applied
 992 thermal power and hence over estimation of the thermal conductivity and/or thermal resistance (see
 993 e.g., Jensen-Page et al. 2018). This effect can be minimised by reducing the distance between the test
 994 rig and the GHE, by better insulating hoses, and by positioning the fluid temperature sensors as close
 995 to the ground as possible. Of course, underestimation of the power is also possible when tests are
 996 conducted in the peak of summer or in particularly warm climates. Secondly, real temperature
 997 response functions for piles are expected to have reduced gradients compared with the idealised ILS
 998 model (Figure 4). Therefore, fitting of the ILS will lead to artificially low line source gradients and hence
 999 overestimations of thermal conductivity.

1000 Furthermore, samples taken from sites will have lost confining stress and also potentially lost moisture
 1001 before they are tested. Both these factors could result in underestimation of thermal conductivity
 1002 from laboratory tests. Consequently, quality of thermal response test and quality of soil sample can
 1003 both affect the accuracy of laboratory – field comparisons. Similar comparisons from borehole thermal
 1004 response testing have shown that better comparisons can be achieved when appropriate care is taken
 1005 with respect to quality (Witte et al. 2002, Breier et al. 2011). However, it is likely that the larger
 1006 diameter and shorter length of piles will contribute to potential errors in thermal response tests
 1007 results due to additional divergence from line heat source theory. Recently, Akrouch et al. (2015)
 1008 proposed the ‘thermal cone test’ to determine in-situ the thermal properties of soils. This technique
 1009 upgrades the well-known cone penetrometer test (CPT), typically used to determine the geotechnical
 1010 engineering properties of soils to gather their thermal properties as well. Finally, it is also worth
 1011 highlighting the two orders of magnitude difference in scale between needle probes often used in the
 1012 laboratory and in situ tests.

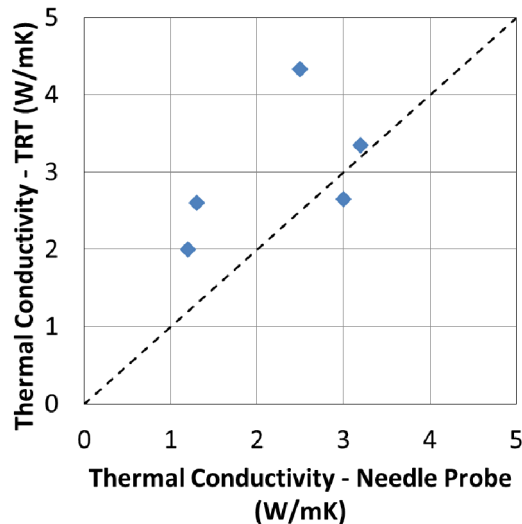
1013 **Table 5 Summary of pile thermal response tests**

Reference	Pile Type	Pile Dia. (mm)	Pile Length (m)	No Pipes	Test Duration	Field Thermal Conductivity (W/ mK)	Laboratory Thermal Conductivity (W/ mK)	Comments
Hemmingway & Long (2013)	Bored cast in situ	250, 350	14.5	2	13 hours	3.2/ 3.5 (line source injection & recovery) 5.8 (GPM)	3.2 (needle) ~ 2.3 (literature)	Sands and gravels; tests curtailed due to overheating

Reference	Pile Type	Pile Dia. (mm)	Pile Length (m)	No Pipes	Test Duration	Field Thermal Conductivity (W/ mK)	Laboratory Thermal Conductivity (W/ mK)	Comments
		300	6	2	20 hours	2.9/2.6 (line source injection & recovery) 2.9 (GPM)	~ 2.2 (literature)	
Alberdi-Pagola et al. (2018)	Square, precast concrete	300	15	2	96 hours	2.4 (simulation) 2.1 (line source)	~ 2.0 (literature)	Two test sites, one in organic clay and sand, one in fill over till.
Loveridge et al. (2014b); Low et al. (2015)	Cast in situ	300	26	2	72 hours	2.5/2.7(line source injection & recovery) 2.4/2.9 (G-function injection & recovery)	1.3 (needle)	London Clay; extended time period between sampling and lab testing
Loveridge et al. (2015)	Bored cast in situ	300, 450	18	2, 4	70 – 100 hours	2.6 – 2.7 (line source) 3.1 ±10% (G-functions)	3.0 (needle)	Silty and sandy clay over dense sand; see also Brettmann et al. 2010, 2011
Park et al. (2015)	Hollow concrete cylinder, grout fill	400	13, 14	4, 6	13 hours	2.2 (simulation)	2.0 (needle)	Residual soil, over weather and unweathered gneiss.
Bouazza et al. (2013)	Bored, cast in situ	600	16	2 6 6	3 days 9 days 52 days	4.2 (line source) 5.0 (line source) 3.8 (line source)	2 to 3 (needle)	Dense sands; power variations may have effected results
Murphy et al. (2014)	Bored cast in situ	610	15	6	20 days	2.0 (line source)	1.2 (needle)	Sandstone; field thermal conductivity corrected for pipe run out length

1014

1015



1016

1017

Figure 10 Comparison of Thermal Conductivity derived from Laboratory Testing and Thermal Response Testing (TRT) on Energy Piles. Laboratory values from the needle probe, using a weighted average where different soil units are present. TRT results from line source interpretations, average where there are multiple tests or injection and recovery values.

1018

1019

1020

1021

3.1.2.2 Recommendations

1022

Given the test results in Table 5 it is clear that due care is required in the interpretation of pile thermal response tests. Some better results have been obtained from smaller diameter piles and given the costs of long tests on larger diameter piles it is recommended that practical application be restricted to smaller diameters until better interpretation methods are available. Loveridge et al. (2014a) and Loveridge et al. (2015) have suggested that to limit test durations to 100 hours, then pile diameters should be kept to 300mm or possibly 450mm at the most. Routine pile thermal response testing also has project programme implications since time must be provided in the construct schedule for the concrete heat of hydration to dissipate, which will take longer in larger diameter piles. An alternative approach is to use a borehole for thermal response testing at site investigation stage. However, this has its own drawbacks given that the pile lengths are unlikely to be known this early in the project planning. Further research in this area would therefore assist with providing better guidance, especially for larger diameter piles.

1023

1024

1025

1026

1027

1028

1029

1030

1031

1032

1033

1034

1035

3.2 Pile Geomechanical Tests

1036

3.2.1 Single Piles

1037

Several tests have been performed on full-scale energy piles in the field, including both individual energy pile tests before construction of the building (Laloui et al. 2003; Laloui et al. 2006; Bourne-Webb et al. 2009; Amatya et al. 2012; Akrouch et al. 2014; Wang et al. 2015b; Bouazza et al. 2011; Laloui 2011; Sutman et al. 2014) as well as tests on energy piles beneath constructed buildings (Brandl 2006; McCartney & Murphy 2012; Murphy et al. 2015; Murphy & McCartney 2015; Faizal et al. 2018a, 2018b). Quantitative observations from these studies have been summarised in recent review papers (e.g., Olgun & McCartney 2014; Bourne-Webb et al. 2019), so this discussion focuses on the range of conditions that were investigated in these studies. Although most of the field-scale pile tests were on

1038

1039

1040

1041

1042

1043

1044

1045 the compression response of bored cast-in place (drilled shaft) energy piles or augercast energy piles,
1046 Akrouch et al. (2014) investigated the application of tensile loads to energy micropiles. The soil profiles
1047 in most of the cases were heavily overconsolidated clays or weak rock, which are the best suited for
1048 bored pile installation. There were not any studies in soft clay, but Akrouch et al. (2014) evaluated the
1049 response of energy piles in highly expansive clay and observed a pronounced creep effect during
1050 application of tensile loads. Most of the individual loading tests on energy piles included a loading
1051 frame at the ground surface using other pipes for reaction support, while Bouazza et al. (2011)
1052 presented the only study on an energy pile that used an Osterberg cell embedded at the toe to push
1053 upward and measure side shear stresses and end bearing independently. A wide range in
1054 instrumentation has been used in the piles, including thermistors and fiberoptic sensors for
1055 temperature changes, vibrating wire strain gages and fiberoptic sensors for axial and radial strain
1056 changes, and load cells for axial stress changes. The fiberoptic sensors have a significant advantage of
1057 being able to monitor continuous profiles of strain and temperature, permitting evaluation of the
1058 impacts of individual subsurface strata on the axial thermo-mechanical response of energy piles.

1059 3.2.2 Pile Groups

1060 Consistent with conventional pile groups, there are relatively few full-scale case histories on energy
1061 pile groups. Two relevant studies have been performed by Mimouni & Laloui (2015) and Rotta Loria
1062 and Laloui (2016b). Rotta Loria & Laloui (2016b) assessed the impact of stresses imposed on other
1063 piles during of a single pile beneath a building load, while Mimouni & Laloui (2015) evaluated the
1064 response of piles without a head restraint and restrained in a group by a slab and investigated heating
1065 of all the piles as a group. Heating all the piles doubled the degree of freedom and led to greater
1066 upward pile heave during heating. However, this also corresponded to lower differential
1067 displacements and associated stresses.

1068

1069 3.3 Energy Walls

1070 There have now been a number of energy walls constructed around the world. These include at least
1071 four diaphragm walls for commercial buildings and two other embedded retaining walls for rail
1072 infrastructure in Austria (Brandl, 1998, 2006), two building basements in the UK (Amis et al, 2010,
1073 Nicholson et al, 2014b), metro station applications in London and Paris (Soga et al, 2015, Delerabee
1074 et al, 2018), a public building in Shanghai (Xia et al, 2012) and a recent commercial building in Northern
1075 Italy (Angelotti & Sterpi, 2018). However, by contrast to piles, few of these case studies report on the
1076 thermal capacity or performance. Those that are published also tend to be reported with fewer details
1077 making it harder to learn broader lessons. The sections below identify relevant data that are available.

1078 3.3.1 Thermal Performance

1079 The only true short-term thermal performance test for an energy wall is the case of the Shanghai
1080 Natural History Museum. Xia et al. (2012) present the thermal performance test results for the
1081 constructed diaphragm wall with heat transfer pipes installed on both the front and rear sides of the
1082 panel. Three different types of pipe arrangements were tested at three different inlet water
1083 temperatures. Two of the arrangements involved four pipes with two each on the excavated and
1084 retained sides, while the third arrangement included only the two pipes on the retained side. The
1085 experiments also investigated the effects of flow rate and intermittent operation. The results are

1086 presented in terms of energy exchanged per metre of installed heat transfer pipe and range between
1087 30W/m and 150 W/m depending on the conditions tested. As would be expected the four pipe
1088 arrangements, intermittent operations, higher temperature differences and higher flow rates all lead
1089 to greater heat exchange.

1090 Table 6 converts the results of Xia et al. (2012) to exchanged power in W/m^2 and compares them with
1091 the operational case of Angeloltti & Sterpi (2018) and numerical experiments reported in the
1092 literature. Angeloltti & Sterpi (2018) present four months of data for heat extraction from a diaphragm
1093 wall in Tradate in Northern Italy. Each 2.4m wide panel contain a single loop of pipe but arranged in
1094 three overlapping coils at the back of the wall to maximise pipe lengths. The heat transfer rates for
1095 this operational case are 12 – 15 W/m^2 based on monthly averages and correspond to the lower range
1096 of data presented by Xia et al. (2012). This is unsurprising since longer term studies would be expected
1097 to have lower heat transfer rates. The numerical studies also presented in Table 6 have a similar lower
1098 bound to the field data. However, many studies include the effects of groundwater flow which
1099 theoretically give a substantial increase in available power.

1100 Total energy obtained from two notable bored pile wall case studies are reported by Brandl (2006)
1101 and Nicholson et al. (2014b). These operational schemes in are located in Vienna and Oxford
1102 respectively. In the Vienna scheme the bored pile wall forms part of a railway tunnel, where 59 piles
1103 of 17 m length are connected to the energy system and used to heat an adjacent school. One heating
1104 period yielded 214 MWh of thermal energy. In Oxford 61 bored piles of 450mm in diameter were
1105 equipped with heat transfer pipes. Heating of an associated building was achieved with a COP of 5.8
1106 for cooling and 3.9 for heating.

Table 6 Summary of wall thermal performance

Reference	Approach (Field / Simulation Type / Excavation BC)	Wall Type	Excavation Space	Dimensions	Retained Height	Pipe No & Arrangement t*	Flow Rate (L/h)	Temperature Difference ⁺ (°C)	Duration	Heat Transfer Rate (W/m ²)
Xia et al. (2012)	Field Thermal Performance Test	Diaphragm wall	Open to air when tested	2.25m long x 1m wide x 38m deep	18.5m	U or W	706	+9 +12 +15	50 hours	15 (U); 18 – 19 (W) 22 (U); 29 – 33 (W) 30 (U); 38 – 44 (W)
Angelotti & Sterpi (2018)	Operational Case	Diaphragm wall	Building basement	0.5m wide x 2.4m long x 15.2m deep	10.8m	1 loop with 3 overlapping coils in 0.8m width	NR	NR	4 months (Winter)	12 – 15 (extraction)
Bourne-Webb et al. (2016b)	2D steady state FDA; Constant temperature or convection	Diaphragm wall	NR	0.8m wide	Not modelled	U UU	Not modelled	+15	Steady state	13 – 22 20 - 80
Di Donna et al. (2016a)	3D FEA; Constant Temperature	Diaphragm wall	NR	Variable width, 20m deep	Variable	U or UUU	353 - 2121	+8	60 days	5 – 20
Makasis et al. (2018c)	3D FEA & Machine Learning; Varying thermal load; thermally insulated wall	Diaphragm wall	Metro station, basement	13m long x 1m wide x 22m deep	Variable: 5, 10, 20, and 30m	Meandering (W)	330	NR	5 years, monthly analysis	4 – 22 (NR, personal communication)
Piemontese (2018)	3D FEA; Constant Temperature or convection	Diaphragm wall	NR	2.5m long x 1m wide x 20m deep	10m	W	469	+10 to +20 -4 to -14	30 days	14 – 32 (injection) 6 – 22 (extraction) (up to 48 with gw flow)
Rammal et al. (2018)	3D transient FDA; Adiabatic	Diaphragm wall	Metro station	1.2m wide x 32.5m deep	22m	Not modelled	Not modelled	+11 (summer) -5 (autumn) -9 (winter) +7 (spring)	3 year seasonal analysis	12 (100 with gw flow)

Reference	Approach (Field / Simulation Type / Excavation BC)	Wall Type	Excavatio n Space	Dimensions	Retained Height	Pipe No & Arrangemen t*	Flow Rate (L/h)	Temperature Difference* (°C)	Duration	Heat Transfer Rate (W/m ²)
Barla et al. (2018)	3D transient FEA; Adiabatic	Diaphragm wall	NR	0.8m wide x 15.5m deep	9.5m	W Slinky	706	-10	30 days	7.5 8
Barla et al. (2018)	3D transient FEA; Adiabatic	Diaphragm wall	NR	0.8m wide x 15.5m deep	9.5m	Slinky	291	+13 to -13 (seasonal sinusoidal)	6 years seasonal analysis	7 – 20 (extraction) 10 – 25 (injection) (up to 50 with gw flow)

FEA = finite element analysis; FDA = finite difference analysis; FVA = finite volume analysis.

N.R. = Not reported.

+ between the fluid inlet temperature and the undisturbed ground temperature

* Notes on pipe arrangements:

U = single U-tube (2 pipes); UU = two U-tubes in parallel (4 pipes); UUU = three U-tubes in parallel (6 pipes); W = two U-tubes in series (4 pipes); Slinky = 1 loop with meandering pipes

Heat transfer rates in absence of groundwater (gw) flow unless stated.

1 3.3.2 Thermal Response Tests

2 Few thermal response tests have been reported on energy walls. This may be because the absence of easily
3 applied analytical solutions for their interpretation means that generating meaningful results from a wall
4 thermal response test more challenging. Equally, given these challenges, there may be simpler methods of
5 obtaining site specific design parameters, including borehole thermal response tests and laboratory testing.

6 A number of test have been carried on diaphragm walls constructed as part of the Crossrail project in London,
7 although the data is not publicly available. As part of the GEOTECH project, an extended thermal response
8 test was carried out on a 17m deep diaphragm wall constructed to support a 6.5m deep basement in Spain.
9 Four loops were installed at 0.4m spacing to a depth of 15.6m. Multiple thermal tests were carried out
10 consecutively at an applied power of 2kW with pulses of varying durations from a few hours to several days.
11 In total the experiment ran for over one month. The data is reported in Shafagh & Rees (2018) where it is
12 used for model validation purposes rather than for explicit determination of the ground thermal properties.
13 Nonetheless, in the absence of other soil information, fitting their Dynamic Thermal Network model to the
14 test data did allow derivation of the wall and ground thermal properties. It is worth noting that the analyses
15 used fully transient techniques to capture the thermal behaviour, which, like piles, would be essential for
16 avoidance of model errors related to the capacitance of the heat exchanger.

17 3.4 Energy Tunnels

18 Similarly to energy walls, there have now been a few pilot and testing energy tunnels constructed around the
19 world and a few operational energy tunnels. These include notable test sections constructed in Austria and
20 Germany at the Katzenburg, Lainzer and Jenbach tunnels (Schneider & Moormann 2010; Adam & Markiewicz
21 2009; Franzius & Pralle 2011); a tunnel heat exchanger constructed in Inner Mongolia to transfer heat from
22 deeper within the tunnel to the tunnel portal regime where there is a risk of freezing during cold winter
23 conditions (Zhang et al. 2013), and a series of energy geotextile installed inside a disused tunnel in Korea (Lee
24 et al. 2012).

25 Typically, thermal performance tests are conducted. Although the construction of the above structures has
26 been well reported, details of their thermal performance is just becoming available and complement other
27 numerical (or model scale) results being published. The scarcity of published data in this emerging field of
28 research makes it hard to generalised broader lessons. Nevertheless, the sections below identify relevant data
29 that are available.

30 3.4.1 Thermal Performance Tests

31 A number of thermal performance tests have been carried out and reported on a 200 m section of the Linchang
32 tunnel in the city of Yakeshi in Inner Mongolia, starting from about 2013. Results have been used by the same
33 research group conducting the tests and others to assist with validation of analytical models for heat transfer
34 around the tunnel (Zhang et al. 2014) as well as to validate and contrast against results of various numerical
35 models (e.g., Barla et al. 2016; Barla and DiDonna 2018). A number of constant temperature inlet tests were
36 carried out, each over about two-day period. These showed a linear relationship between the inlet
37 temperature and the heat exchanged, with resulting rates of 24 to 60 W/m length of the heat exchange pipes,
38 depending on the temperature difference and flow rate used. Not surprisingly, these figures are similar to
39 those obtained for diaphragm walls.

40 Longer thermal performance tests were conducted on the Stuttgart's Fasanenhof tunnel, where two blocks of
41 10 m each were thermally activated by imbedding meandering absorber pipe between outer and inner
42 shotcrete linings. Tests were run for about half a year at constant inlet temperature with flow rates kept
43 constant for 5 months and then almost doubled for a further 2 months. The heat transfer rates were found
44 to be between $30\text{W}/\text{m}^2$ and $5\text{W}/\text{m}^2$ of activated tunnel depending on operational conditions (Buhmann et al.
45 2016,). These results were used by others to validate numerical models and explore the impact on nearby
46 borehole ground heat exchangers (Bidarmaghz et al. 2017) and the impact of groundwater flow (Barla and
47 DiDonna 2018, Bidarmaghz and Narsilio 2018). The results from these field scale tests in Fasanenhof are
48 consistent with the average heat transfer yield reported for the 54m long energy tunnel segmental lining of
49 Stuttgart's Jenbach tunnel, of about $15\text{W}/\text{m}^2$ on average (Frodl et al. 2010; Buhmann et al. 2016).

50 Short term and longer-term tests were also performed on six variants of energy geotextiles attached to the
51 abandoned tunnel in South Korea, near Seocheon. The pipe arrangement included similar pipe lengths of both
52 transverse and longitudinal meandering pipe (see Section 2.1.4.5) and greater lengths of pipe in slinky
53 configuration, and also tested proximity of the absorber pipes to the tunnel space. Both constant power and
54 varying inlet temperature to represent operational conditions. The heat transfer rates were found to be up
55 to around $40\text{W}/\text{m}^2$ of geotextile on average, with higher yield rendered by the slinky configurations. Again,
56 this is similar to conditions found for diaphragm walls. The field data gathered from the tunnel lining also
57 showed clearly that the air temperature inside the tunnel had a large impact on the temperatures in the
58 circulating fluid, emphasising the importance of understanding this boundary condition. This has been also
59 flagged by the German-Austrian experienced.

60 While not explicitly addressed by the current field scale energy tunnel literature, numerical simulations built
61 upon these experimental results strongly suggest that the groundwater flow velocity and the degree of tunnel
62 air ventilation and thermal insulation have a significant impact on the thermal yield of energy tunnels. Table
63 7 summarises such observations and provides more details of field and full-scale testing, as well as other
64 means to assess the thermal aspects of energy tunnels.

Table 7 Summary of tunnel thermal performance

Reference	Approach	Heat Exchanger Type	Tunnel Location	Dimensions	Equivalent Tunnel Diameter (m)	Pipe No & Arrangement*	Flow Rate (L/h) (per pipeline)	Temperature Difference+ (°C)	Duration	Heat Transfer Rate (W/m ²)
	(Field Simulation Type / BC)									
Zhang et al. 2014	Field Thermal Performance Test	Cast in situ - Fixed between outer and inner tunnel lining	Linchang tunnel, Yakeshi city, Inner Mongolia	NR (~70 m ² estimated) (8 m long)	7.7	Longitudinal meandering, 1m and 0.5m pipe spacing	487 to 1250	2 to 6	42 hours	25 to 50
Buhmann et al. 2016	Field Thermal Performance Test	Cast in situ - Fixed to outer tunnel lining	Stuttgart-Fasanenhof, Germany	360 m ² (20 m long)	9.6	Longitudinal meandering	580 (5 months) to 1085 (2 months) (Re 2400 to 4330)	3.6	6 months (Summer)	30 to 5
Frodl et al. 2010; Buhmann et al. 2016	Field Thermal Performance Test / Operation	Tunnel segmental lining	Stuttgart-Jenbach, Germany	2,200 m ² (54 m long)	13	Transversal Meandering	500	4.6	2 months (Winter)	15
Lee et al. 2016	Field Thermal Performance Test (and Numerical model)	Cast off site - Fixed on inner tunnel lining	Abandoned railroad tunnel, Seocheon, South Korea	~90 m ²	NR	6 types: including longitudinal meandering, transverse and slinky	30 to 60 (heating) 90 to 120 (cooling)	4 to 5 (heating) and 12 (cooling)	2.5 months (heating) + 2 months (cooling)	Transverse: 4-6 (Heating) and 24-34 (Cooling) Longitudinal: 5-10 (Heating) and 24-28 (Cooling) Slinky: 11 (Heating) and 37 (Cooling)

Reference	Approach	Heat Exchanger Type	Tunnel Location	Dimensions	Equivalent Tunnel Diameter (m)	Pipe No & Arrangement*	Flow Rate (L/h) (per pipeline)	Temperature Difference+ (°C)	Duration	Heat Transfer Rate (W/m ²)
	(Field Simulation Type / BC)									
Zhang et al. 2016a; Zhang et al. 2017	Laboratory TRT	Cast in situ - external to outer lining	Laboratory study (1/20th scale)	NR (~20 m ² estimated scaled up) (18 m long scaled up)	8 (scaped up, 0.4 m in model)	Longitudinal and transverse meandering, 1m (scaled up) pipe spacing	360 to 1800 (estimated equivalent)	7, 12, 17	1 to 4 days	30 to 60
Zhang et al. 2013	Analytical model	Cast in situ - Fixed between outer and inner tunnel lining	Linchang tunnel, Yakeshi city, Inner Mongolia	NR (~3,500 m ² estimated) (200 m long)	12	Meandering	290 to 1470 (750 recommended)	varies	2 to 90 days	~12 (average, estimated)
Tinti et al. 2017	Analytical (empirical) model	Cast in situ - Fixed between outer and inner tunnel lining	Mules Access Tunnel of the Brenner Base Tunnel (BBT) system, Eastern Alps, Italy	~37,000 m ² (1,265 m long)	9.5	Meandering	800	10 (varies)	NR	11 to 32
Nicholson et al. (2014a)	FEM Numerical model	Within tunnel lining	Cross-rail London, UK	~4800 m ² (33 rings) (250 m long)	6.3	Longitudinal Meandering	216 to 432	2 to 10 (varies)		10 to 30
Barla et al. 2016; DiDonna & Barla 2016; Barla & DiDonna 2018	3D FEM Numerical model	Tunnel segmental lining	Metro Torino line 1, Italy	~30,000 m ² (1350 m long)	7.4	Transversal Meandering	600	3 to 4	1 month	53 (Winter) to 74 (Summer)
Bidarmaghz and Narsilio 2018; Bidarmaghz et al. 2017	3D FEM Numerical model	Within tunnel lining	Stuttgart-Fasanenhof, Germany	240 m ² (10 m long)	10	Longitudinal meandering, 0.4m pipe spacing	560	NR	5 years	12 to 40

67 **3.5 Other Energy Geostructures**

68 The use of basement slabs as heat exchangers is well known from the literature (e.g. Adam & Markiewicz,
69 2009, Katzenbach et al. 2014), but there are few details of well recorded case studies providing details of
70 thermal performance. Katzenbach et al. (2014) suggest that slabs are less thermally effective compared to
71 other geostructures, but that they nonetheless remain attractive due to their low installation costs. These
72 points are supported by recent in situ monitoring of walls and slabs by Angelotti & Sterpi (2018) and Kipry et
73 al. (2009), as discussed in Section 2.1.5.

74 Large diameter sewer pipes adapted as energy geostructures have also been successfully trialled at full scale.
75 As reported by Adam & Markiewicz (2009), the heat transfer pipes are placed in the material of the base of
76 the pipe. Initial results of a trial section showed dependency of the peak power obtained on the effluent level
77 in the sewer, its flow rate and temperature.

78 **4 Model Scale Testing**

79 Although field-scale testing of energy piles permits consideration of the effects of actual construction
80 techniques and real soil conditions, there are limitations to this type of testing. In addition to issues with
81 expense, time, and site coordination, there are many uncertainties in the field that may not permit a
82 comprehensive understanding of the thermal or thermo-mechanical process of interest. Model testing in
83 either laboratory-scale or centrifuge-scale provides an opportunity to understand the mechanisms of energy
84 pile behaviour under carefully controlled conditions (material properties, geometric features), and dense
85 instrumentation arrays can be used to detect heat transfer, water flow, and changes in stress or strain.
86 Furthermore, boundary conditions can play a critical role in both the thermal and thermo-mechanical
87 evaluation of energy piles and other energy geostructures. From a thermal perspective, boundary conditions
88 at the surface, far field, and within the embedded heat exchangers can affect the heat transfer process and
89 should be well-characterised. From a geomechanical perspective, the restraint provided at the head and toe
90 of the structure have major effects on the magnitude and location of the thermally-induced stresses. In the
91 field, it is often difficult to ensure that the toe of the foundation is completely clean, which may result in a
92 softer restraint at the toe than expected from the characteristics of the intact material (Murphy et al. 2015).
93 In addition, it is difficult to assess the restraint provided to the top of the foundation by an overlying slab or
94 beam. For example, the head deformations of energy piles will affect the response of other energy piles in a
95 group. The thermal and mechanical boundary conditions in laboratory-and centrifuge-scale testing can be
96 carefully controlled, which provides them with a major advantage over field testing. Finally, the parameters
97 governing the failure of a foundation may play an important role in the prediction of the thermo-mechanical
98 soil-structure interaction behaviour. Axial or lateral loading tests to failure are relatively simple to perform in
99 the laboratory or centrifuge (e.g., McCartney & Rosenberg 2011; Wang et al. 2011, 2012a; Yavari et al. 2014a;
100 Goode et al. 2014a; Goode and McCartney 2015), while they may be very complex in the field.

101 Due to the advantages mentioned above, the information gained for model scale testing can potentially be
102 used to provide trust-worthy calibration or validation data for numerical or analytical models describing
103 energy geostructure behaviour. Of these model testing options, laboratory-scale testing permits realistic
104 simulation of heat transfer processes and can potentially be used to study thermo-mechanical effects for some
105 soil types. Centrifuge testing is more suited for evaluation of thermo-mechanical soil-structure interaction due
106 to scaling issues with heat flow that will be discussed later. However, some thermo-hydro-mechanical
107 processes that depend on the stress state such as thermally-induced excess pore water pressure during
108 undrained heating may be considered in centrifuge testing. All the model scale testing conducted by

109 researchers so far has been limited to energy piles except for the work by Kurten (2011), who assessed the
110 thermal behaviour of energy walls, and the work by Zhang et al. (2016b), who performed an experimental
111 study of nonisothermal tunnel linings.

112 **4.1 Model Test on Piles**

113 4.1.1 Laboratory Scale Tests (1-g)

114 4.1.1.1 *Overview*

115 Laboratory-scale testing in tanks permits both careful control of the preparation of soil layers, use of different
116 heating sources and loading mechanisms for energy piles, and potentially visualisation of different
117 phenomena. A summary of the different laboratory-scale tests that will be discussed in this section is
118 presented in Table 8. Most laboratory-scale experiments on energy piles have been performed on reduced-
119 scale models, typically $\frac{1}{4}$ to $\frac{1}{2}$ scale systems. In many cases the scaled diameter of the model energy pile can
120 be similar to energy piles in the field, but the length is typically shorter than in the field. Although there has
121 not been a detailed evaluation of scaling relationships for reduced-scale energy piles tested under self-weight
122 conditions (1-g), there have been studies in the earthquake engineering field that may provide some insight
123 into potential scaling relationships. Most work on this topic has built upon the scaling relationships of Rocha
124 (1957) and Lai (1988). The main concept of their relationships is that the constitutive relationship that governs
125 the mechanical response of the soil should be scaled, and thus both stresses and strains (strain which is already
126 dimensionless) in the model are linearly related through a scalar scaling parameter. This approach was
127 proposed because many soils when tested under low effective stresses will exhibit dilative, strain softening
128 behaviour. By using a looser soil in the scaled model, the stress strain curve under lower effective stresses will
129 have a closer shape to that expected in the full-scale model. They found that their scaling relationships work
130 well for small-strain behaviour where the soil can be considered as an elastic body. A similar scaling conflict
131 for heat flow to that encountered in centrifuge modelling, which will be discussed later, may be encountered
132 as the length is scaled in their approach. Nonetheless, the scaling conflict may have less of an effect than in
133 centrifuge tests. Further research is needed to evaluate scaling relationships for laboratory testing of energy
134 piles, either through re-interpretation of available data or through numerical modelling of physical models (Ko
135 1988).

136 4.1.1.2 *Evaluation of Heat Transfer in Laboratory-scale Tests*

137 One of the earliest laboratory-scale tests to consider the role of heat flow around an energy pile was
138 performed by Ennigkeit & Katzenbach (2001), who evaluated heat flow processes. They developed a solution
139 to the heat equation assuming that the primary mode of heat transfer is conduction and were able to obtain
140 a good match to their data. Their work showed the utility of incorporating dense instrumentation arrays
141 around a carefully prepared soil layer to validate analytical models. Thermal tests on scale-model energy piles
142 have since been performed by Kramer and Basu (2014a, 2014b) and Kramer et al. (2015), who processed their
143 heat flow results to interpret the heat flux from the energy pile into the soil. Akrouch et al. (2016) performed
144 a coupled heat transfer and water flow analysis for energy piles in unsaturated clay and found that heating of
145 the energy pile results in a drying effect of the soil surrounding the energy pile. This drying effect also served
146 to lead to a slight reduction in the thermal conductivity of the soil. An innovative technique to study heat flow
147 in laboratory-scale models developed by Black & Tatari (2015) involves the use of transparent soils and digital
148 image analysis. Transparent soils consist of particles saturated with a fluid having a compatible refractive index
149 that leads to transparent conditions and have been used together with lasers and digital image analysis to

150 study deformation problems in geotechnical engineering. Black & Tatari (2015) found that temperature
151 changes led to a change in the refractive index and a loss of optical clarity of the fluid, which can be used as a
152 beneficial attribute of transparent soil to study heat transfer processes around energy piles.

153 4.1.1.3 *Evaluation of Soil-structure Interaction in Laboratory-scale Tests*

154 Several studies have been performed on energy piles in laboratory-scale tanks. Wang et al. (2011, 2012a)
155 performed tests at various temperatures on small-scale steel energy piles, with an innovative setup that
156 permits the pile to be loaded upward from the base after heating. This approach permits the role of the side
157 shear stress to be isolated. They evaluated the behaviour of the model energy piles in loosely-compacted, dry
158 N50 fine sand, partially saturated N50 fine sand, and partially saturated 300WQ silica flour. During heating,
159 the authors observed no change in shaft resistance with the dry sand and a decrease in shaft resistance with
160 the partially saturated sand and with the partially saturated 300WQ silica flour. The changes in shaft resistance
161 may be due to some mobilisation of side friction during the thermal expansion of the steel, which led to less
162 additional axial stress required to reach the ultimate capacity of the energy pile during mechanical loading.

163 Kalantidou et al. (2012) performed a thorough evaluation of a multi-stage test on an aluminium model-scale
164 energy pile in a dry sand layer. They tracked the head displacement of the energy pile during heating-cooling
165 cycles, and during mechanical loading after heating to different temperatures. They observed a hysteretic
166 response during heating and cooling, which indicates that some plastic deformations occurred at the soil-pile
167 interface during the temperature changes. This effect is likely overemphasised due to the relatively large
168 thermal expansion of the aluminium, which has a coefficient of thermal expansion that approximately double
169 that of most soils and reinforced concrete. Tang et al. (2014) performed similar tests to Kalantidou et al. (2012)
170 but focused on the role of the applied load on the foundation head. Application of a greater foundation load
171 will lead to a greater initial mobilisation of side shear resistance and end bearing, which can influence the
172 subsequent thermo-mechanical response. However, the magnitude of thermal stress will depend on the
173 restraint provided by the overlying structure (i.e., the head stiffness) more than the applied load on the
174 foundation head. Yavari et al. (2014a) performed complimentary tests to those of Kalantidou et al. (2012)
175 using similar a similar dry sand, but incorporated strain gages to infer soil-structure interaction behaviour.
176 They were able to measure strain profiles that are consistent with those measured in full-scale energy piles.
177 Subsequently, Yavari et al. (2014b) performed a simplified finite element analysis of the energy pile tests and
178 found good agreement between the calibrated model and the laboratory-scale results. Marto & Amaludin
179 (2015) performed tests on aluminium energy piles in compacted Kaolinite and observed similar compression
180 curves for different temperatures. However, their model scale energy pile and soil container were relatively
181 small compared to other laboratory-scale tests.

182 The characteristics of the energy pile can have a major effect on the soil-structure interaction response
183 because the displacement required to mobilise the side shear resistance may be relatively small. Accordingly,
184 tests on reinforced concrete will provide closer response to actual energy piles in the field. Kramer & Basu
185 (2014b) and Kramer et al. (2015) reported results from small-scale tests on a precast concrete pile tested
186 under 1-g using F50 Ottawa sand and observed a slight increase in pile capacity at increased temperatures.
187 Although a relatively large layer of sand must be prepared in their tank-scale tests, their results permit the
188 evaluation of the failure conditions of energy piles in addition to their thermal response. Di Donna et al. (2015)
189 performed direct shear tests under different temperatures to evaluate the effects of cyclic temperature
190 changes on soil-structure interaction mechanisms. They found that a sand–concrete interface was affected
191 by cyclic degradation (i.e., deformations induced by temperature changes) but not affected directly by
192 temperature. Conversely, the response of a clay–concrete interface changed at different temperatures. They

193 observed an increase of interface strength with increasing temperature because of clay volume changes
 194 associated with the changes in temperature.

195 Laboratory-scale tests have provided interesting insight into energy pile behaviour in some settings, which
 196 have also matched well with modelling results. However, the scaling relationships of Rocha (1957) have not
 197 been considered when extrapolating the trends from laboratory-scale (low stress) conditions to full-scale piles
 198 that are also influenced by installation effects. Although 1-g tests have not been performed on saturated clays,
 199 pore water pressure development and thermal consolidation in saturated clays can alter the stress state and
 200 result in deformations around a heat exchanger pile. In energy piles, the rate of heating and the rate of
 201 dissipation of excess pore water pressures must be carefully considered. Fast heating may lead to undrained
 202 heating and pore water pressure increases that may cause a decrease in pile capacity. Slow heating may lead
 203 to drained heating and thermal consolidation that may cause an increase in pile capacity. The role of the initial
 204 effective stress state is an important issue to consider in these conditions (Ghaaowd et al. 2017), which may
 205 not be completely captured in a tank scale test.

206 A different approach was followed Eslami et al. (2017) to study the effect of the temperature on the variation
 207 on the bearing capacity of thermo-active piles. A mini-pressurimeter test was conducted in the laboratory in
 208 in a container with controlled temperatures ranging from 1 to 40 C. It was observed that as temperature
 209 increased, the pressurimeter modulus (E_p) slight decreased, and both, the limit pressure (p_i) and creep (p_i)
 210 significantly decreased. Murphy and McCartney (2014) developed a thermal borehole shear device to evaluate
 211 the impact of temperature on the soil-concrete interface shear behaviour in-situ and found negligible effect
 212 of temperature on the frictional behaviour of the interface with a sandy soil. This negligible impact of
 213 temperature on the drained interface shear strength in cohesionless is consistent with the negligible increase
 214 in ultimate capacity of energy piles in sands with increasing pile temperature observed by Goode and
 215 McCartney (2015).

216

217

Table 8 Summary of laboratory-scale tests on energy piles

Study	Tank dimensions	Pile/ heater material	Pile type	Soil type	Purpose
Ennigkeit and Katzenbach (2001)	1 m diameter, 2.4 m height	Aluminum	Heating rod	Dry sand	Heat flow analysis
Wang et al. (2011, 2012a)	0.272 m diameter, 0.15 m height	Steel	End-bearing	Moist sand, silica flour	Upward loading for side shear evaluation
Kalantidou et al. (2012), Tang et al. (2014)	0.57 m diameter, 0.85 m height	Aluminum	Semi-floating	Dry sand	Cyclic heating and cooling, loading to failure
Yavari et al. (2014a)		Aluminum	Semi-floating	Dry sand	Cyclic heating and cooling
Kramer and Basu (2014a, 2014b); Kramer et al. (2015)	1.83 m × 1.83 m square, 2.13 m height	Reinforced concrete	Semi-floating	Dry sand	Heating, effect of temperature of load-settlement curve

Study	Tank dimensions	Pile/ heater material	Pile type	Soil type	Purpose
Black & Tatari (2015)	0.6 m × 0.5 m rectangle, 0.4 m height	Aluminum	Semi-floating	Transparent soil	Heat flow visualization
Marto and Amaludin (2015)	0.27 m diameter, 0.25 m height	Metal	Semi-floating	Compacted clay	Effect of temperature on pile head displacement

218

219 4.1.2 Centrifuge Tests on Energy Piles (N-g)

220 4.1.2.1 Overview

221 Because soil properties are very sensitive to self-weight conditions, laboratory-scale tests may not accurately
 222 capture the soil behaviour that may affect the thermo-mechanical response of a full-scale energy pile. This is
 223 particularly the case in sands, where a change in the mean effective stress can change the shape of the shear
 224 stress-strain curve and volumetric strain response significantly, potentially converting from contractive, strain-
 225 hardening behaviour at high mean effective stress to a dilative, strain-softening behaviour at low mean
 226 effective stress. Accordingly, a geotechnical centrifuge can be used to increase the self-weight of a soil layer,
 227 and more accurately consider the role of mean effective stress in the soil layer. A summary of the different
 228 centrifuge tests that will be discussed in this section is presented in Table 9.

229 Centrifuge physical modelling is based on the concept of geometric similitude. In this case, the lengths of
 230 geometric features in a model L_m can be scaled down from the lengths of geometric features in a full-scale
 231 prototype L_p , as follows:

$$L_m = \frac{L_p}{N} \quad (7)$$

232 where N is the acceleration ratio, defined as follows:

$$N = \frac{\omega^2 r}{g} \quad (8)$$

233 where g is the acceleration due to earth's gravity, ω is the angular velocity of the centrifuge, and r_e is the
 234 effective radius (typically at the centre of the energy pile). Using the concept of geometric similitude, the
 235 effective stresses in a centrifuge-scale model σ_m can be shown to be the same as those in a prototype σ_p , as
 236 follows:

$$\sigma_m = \rho g N z_m = \rho g N \left(\frac{z_p}{N} \right) = \rho g z_p = \sigma_p \quad (9)$$

237 where r is the density of the soil and z_m and z_p are the depths from the surface of the soil layer in the model
 238 or prototype. Similarly, the strains in a centrifuge-scale model ε_m are also equal to those in a prototype ε_p , as
 239 follows:

$$\varepsilon_m = \frac{\Delta L_m}{L_m} = \frac{\Delta L_m}{N} \frac{N}{L_m} = \frac{\Delta L_p}{L_p} = \varepsilon_p \quad (10)$$

240

241 Accordingly, the stress and strains in a centrifuge-scale model are expected to be the same as those in a
242 prototype. This also includes the thermal axial strains in an energy pile, as the coefficient of thermal expansion
243 of an energy pile is not expected to depend on self-weight.

244 Although the centrifuge is effective at increasing the self-weight of the soil layer, and thus affecting any aspect
245 of soil behaviour that is stress-dependent, it is not effective at scaling other features that do not depend on
246 self-weight, such as heat flow and diffusion-based flow processes. Experimental evaluations of heat flow in
247 the centrifuge will be discussed in the next section, but an implication of the fact that heat flow does not scale
248 is that the zone of influence of heat flow in the centrifuge will be greater than that in the prototype. Another
249 way of considering this is that during heating for a certain time period, heat will have travelled over a greater
250 scaled distance in the centrifuge model than in the prototype. Accordingly, most engineers use a scaling factor
251 for the time in the centrifuge scale model t_m compared with the time for heat flow in the prototype t_p . This
252 scale factor can be assessed using Fick's law as follows:

253

$$\frac{dT_m}{dt_m} = \alpha_m \frac{d^2T_m}{dz_m^2} \quad (11)$$

254 where T_m is the temperature in model scale, z_m is the length in model scale, and α_m is the thermal diffusivity.
255 Using a similar equation for the prototype, the following relationships between the times in model and
256 prototype scales can be derived:

257

$$t_m = \left(\frac{z_m}{z_p}\right)^2 t_p = N^2 t_p \quad (12)$$

258 where z_p is the length in prototype scale. Accordingly, when scaling results from a centrifuge model to
259 prototype scale, heat will be transferred N^2 times faster than in the actual prototype soil layer.

260 An implication of temperature scaling is that a greater volume of soil surrounding the model-scale foundation
261 will be affected by changes in temperature. Soils change in volume with temperature, so if a greater zone of
262 soil around the foundation is affected then the effects of differential volume change of the foundation and
263 soil may be emphasised. From this perspective, centrifuge modelling will provide a worst-case scenario. A
264 solution to address the scaling issue is to calibrate numerical simulations of the tests using the data from
265 model scale. However, if the goal of testing is to evaluate the impact of temperature on the load-settlement
266 curve of the foundations, time should be provided to reach steady-state conditions. However, if the goal is to
267 evaluate the impact of temperature on the axial strain distribution in the foundation, tests can be performed
268 until strains stabilize while the foundation temperature is held constant. This amount of time depends on the
269 soil type.

270 4.1.2.2 Evaluation of Heat Transfer and Water Flow in Centrifuge-scale Tests

271 One of the earliest uses of centrifuge modelling for the evaluation of the thermo-hydro-mechanical response
272 of soil surrounding a heat source was performed by Maddocks & Savvidou (1984), who were interested in the
273 disposal of nuclear waste canisters in soft clay deposits offshore. The study was complimented by an
274 assessment of scaling relationships for heat and water flow in the centrifuge by Savvidou (1988) and the
275 development of an analytical solution for coupled heat flow and thermal consolidation by Booker & Savvidou
276 (1984; 1985). Although this experimental situation is perhaps the most complex setting that can be
277 encountered by an energy pile in the field, the lessons learned from these studies are still useful for

278 understanding different processes that may occur in soil surrounding an energy pile. As the study was focused
279 on soft clay soils, it was found that heating of a cylindrical source will lead to diffusive heat flow due to
280 conduction, which is affected by the scaling issue mentioned in the previous section. However, they also
281 observed the generation of excess pore water pressures during undrained heating. These will dissipate with
282 time leading to volume changes. Furthermore, Savvidou (1988) observed that for soils with high Rayleigh
283 numbers (i.e., soils with relatively high hydraulic conductivity) such as saturated sand, convective heat flow
284 may occur due to buoyancy driven flow of water in the soil layer, this phenomenon has been also observed in
285 numerical simulations (Bidarmaghz & Narsilio 2016; Diao et al. 2004b). Because convective heat flow is
286 associated with the flow of water, this process can lead to non-similar conditions between a model and
287 prototype. This behaviour is not expected for dry sands or lower permeability soils (i.e., clays or unsaturated
288 soils). Because of complexities that may be encountered in some soil layers (e.g. because of volume change or
289 convection), the approach suggested by Ko (1988) can be used to confirm the scaling relationships proposed
290 by Savvidou (1988) when conducting tests in the centrifuge involving heat transfer. Specifically, soil layers
291 having different thicknesses and energy piles with different diameters can be tested in the centrifuge
292 container at different g-levels so that each model represents the same prototype system. As each model is
293 theoretically similar to the same prototype, they should have the same behaviour in prototype scale if the
294 scaling relationships are valid.

295 The geotechnical centrifuge is an ideal setting for the evaluation of the change in pore water pressure
296 encountered during undrained heating of saturated soils. Centrifuge modelling not only permits formation of
297 a NC clay deposit that has a similar stress state to a prototype soil layer in the field (zero effective stress at the
298 surface and increasing effective stress with depth), but also permits a dense instrumentation array to
299 characterize the heat transfer and water flow processes and extensive in-situ characterization to evaluate
300 thermo-hydro-mechanical processes. Because studies such as Ghaaowd et al. (2017) showed that the
301 magnitude of excess pore water pressures induced in saturated soils is closely linked with the initial effective
302 stress, the effective stress profile in the centrifuge model will ensure that the pore water pressures that
303 develop with depth will be closer to those expected in the field than in laboratory-scale consolidation
304 chambers under constant mean stress.

305 Several centrifuge studies have been performed on energy piles in dry sand. In these soil layers, the heat flow
306 is expected to be insensitive to the g-level. This was confirmed by the study of Krishnaiah & Singh (2004) who
307 performed spatial and temporal measurements of temperature in dry quartz sand surrounding a cylindrical
308 heat source during centrifugation at different g-levels. Their results confirm that centrifugation does not lead
309 to a change in the heat flow process, and that application of geometric similitude to the model measurements
310 will lead to a greater zone of influence of the heat source. However, dry sands are not expected to undergo a
311 significant thermal volume change during heating and cooling, so this greater zone of influence may not have
312 a major effect. Rosenberg (2010) presented results from heat flow around an energy pile in unsaturated silt,
313 and subsequent analyses by Kaltreider et al. (2015) using model-scale dimensions confirm that conduction
314 was the primary mode of heat transfer.

315 *4.1.2.3 Evaluation of Soil-Structure Interaction in Centrifuge-Scale Tests*

316 There are several experimental studies which investigated the temperature effects on the load-displacement
317 curve and soil-structure interaction response of centrifuge-scale energy piles. McCartney et al. (2010) and
318 McCartney & Rosenberg (2011) performed early centrifuge-scale on reinforced-concrete, semi-floating energy
319 piles in unsaturated, compacted silt, focusing on changes in the load settlement curve after a heating-cooling
320 cycle and after monotonic heating to steady-state conditions, respectively. McCartney et al. (2010) found that

321 the capacity of the energy pile after a heating-cooling cycle was greater than that of an unheated energy pile.
322 McCartney & Rosenberg (2011) found that the capacity of the energy pile increased with temperature.
323 Although the observations of McCartney & Rosenberg (2011) were initially proposed to be due to radial
324 expansion of the energy pile, leading to a change in normal stress on the sides of the pile, later tests found
325 that heating of the energy pile led to thermally-induced water flow in the unsaturated silt and a corresponding
326 increase in effective stress. The compaction of the soil around the foundations may have led to an initially high
327 radial stress that may not be representative of energy piles in the field.

328 A later series of centrifuge tests were performed in a layer of the same compacted silt but with an end-bearing
329 energy pile having embedded strain gages (Stewart & McCartney 2012, 2014). Stewart & McCartney (2014)
330 provided an interpretation of the thermally induced strains, stresses, and displacements in the energy pile.
331 Although, the concrete mix design of the energy pile evaluated by Stewart & McCartney (2012, 2014) led to a
332 relatively low Young's modulus and coefficient of thermal expansion, the trends in the results corresponded
333 well with those observed in full-scale energy piles (McCartney 2013). Stewart & McCartney (2014) also
334 observed a reduction in water content near the test pile due to thermally induced water flow. McCartney
335 (2013) reported the results from a semi-floating energy pile having the same Young's modulus as that of
336 Stewart & McCartney (2014) and observed lower compressive stresses in the energy pile due to the lower
337 restraint provided by the relatively compressible soil at the toe of the semi-floating pile. Small-scale testing
338 also presents opportunities to evaluate different technologies to assess soil-structure interaction effects. For
339 example, Khosravi et al. (2012) performed non-destructive load-response tests on the scale-model, end-
340 bearing energy pile developed by Stewart & McCartney (2014) in compacted silt and found that a slight
341 increase in the speed of a compressive wave was observed due to the greater restraint of a heated energy
342 pile.

343 Goode et al. (2014), Goode & McCartney (2014) and Goode & McCartney (2015) developed a new pair of end-
344 bearing and semi-floating energy piles with a slightly larger diameter than that evaluated by Stewart and
345 McCartney (2014) that permitted a stiffer concrete mix design that had thermo-mechanical properties close
346 to that expected in an energy pile in the field. The centrifuge tests performed by Goode et al. (2014) and
347 Goode & McCartney (2015) on semi-floating energy piles in dry Nevada sand indicate that the shape of the
348 compression curve does not change significantly with temperature. They also observed that the thermal axial
349 strains in the pile were close to the free-expansion strain due to the relatively low restraint provided by the
350 medium-dense sand. A null point near the centre of the energy pile was observed from an integration of the
351 strains with depth. Goode and McCartney (2014) evaluated the role of head restraint (load control and
352 stiffness control) for an end-bearing energy pile in dry Nevada sand, and found that stiffness control conditions
353 lead to higher thermal axial stresses due to the greater restraint provided for the energy pile. Goode &
354 McCartney (2015) also compared the behaviour of semi-floating and end-bearing energy piles in dry sand and
355 compacted silt and found that higher stresses were observed in the compacted silt. The strain distributions in
356 the energy piles in compacted silt were more nonlinear with depth, likely due to greater side shear stresses.
357 Goode and McCartney (2015) also performed loading-unloading tests on an end-bearing energy pile in dry
358 sand after heating to different temperatures and did not observe a noticeable change in the slope of the
359 recompression curve.

360 Ng et al. (2014) and Ng et al. (2015) performed centrifuge tests on aluminium energy piles in saturated clay
361 and saturated sand layers, respectively, focusing both on the impact of cyclic heating and cooling and on the
362 role of temperature on the compression curve. Different from the observations of Goode et al. (2014) for
363 semi-floating energy pile tests in dry sand, Ng et al. (2015) observed an increase in the ultimate bearing
364 capacity of semi-floating energy piles in saturated sand heated to higher temperatures.

365 The effect of cyclic temperature-induced changes in energy pile performance is another area of research.
 366 During its lifetime, an energy pile is exposed to daily and seasonal temperature changes which result in
 367 expansion and contraction of the pile itself. These relative deformations between the soil and the pile can
 368 induce slip at the soil-pile interface which can affect the shear stress transfer between the soil and the pile.
 369 Further, ratcheting mechanisms may occur for semi-floating foundations that lead to continued thermally-
 370 induced settlements or heave after multiple cycles. In addition, the soil surrounding the energy pile is exposed
 371 to temperature changes which can induce excess pore pressures, volume changes and degradation of the
 372 strength of the soil at the pile interface. Progressive migration away from energy piles in unsaturated soils can
 373 reduce the thermal conductivity and cause desaturation of the soil at the pile interface. The role of cyclic
 374 heating and cooling has been studied by Stewart and McCartney (2014) and Ng et al. (2014). Little
 375 permanent head displacements were noted by Stewart and McCartney (2014) for an end-bearing energy pile
 376 in compacted silt. However, Ng et al. (2014) observed that continued downward displacements were observed
 377 for a semi-floating energy pile in saturated clay, albeit approaching a shakedown behaviour after several
 378 cycles. Further tests need to be performed to evaluate whether ratcheting conditions may occur during cyclic
 379 heating of energy piles in over-consolidated clay or dense sand.

380 In addition to help clarify the role of different variables (soil type, saturation conditions, cyclic loading, restraint
 381 at the head or toe of the energy pile), the results from the centrifuge modelling are also useful to calibrate
 382 and validate numerical simulations. Wang et al. (2012b, 2015) used a coupled thermo-hydro-mechanical
 383 model to evaluate the thermal axial stresses and strains in the energy pile results presented by Stewart and
 384 McCartney (2014). A good match between the calibrated model and the experimental results was obtained
 385 when the model was performed using model-scale results. Rotta Loria et al. (2015) used a finite element model
 386 with the Mohr-Coulomb failure criterion to evaluate the centrifuge results for semi-floating energy piles in
 387 sand presented by Goode et al. (2014), and a good match between the model and experimental results was
 388 obtained. The promising match between the observations from centrifuge data and numerical simulations
 389 emphasizes the usefulness of centrifuge modelling in the development of new numerical simulation tools.

390 **Table 9 Summary of centrifuge-scale tests on energy piles**

Study	Pile/ heater material	Pile/ heater type	Soil type	Purpose
Maddocks & Savvidou (1984)	Steel	Thin heating rod	Saturated clay	Thermo-hydro-mechanical process characterization
Krishnaiah & Singh (2004)	Steel	Thin heating rod	Dry sand	Heat flow evaluation at different g-levels
McCartney et al. (2010)	Reinforced concrete	Semi-floating	Compacted silt	Temperature effects on load-settlement curve
McCartney & Rosenberg (2011)	Reinforced concrete	Semi-floating	Compacted silt	Temperature effects on load-settlement curve
Stewart and McCartney (2012, 2014)	Reinforced sand-cement	End-bearing	Compacted silt	Soil-structure interaction, cyclic effects
Khosravi et al. (2012)	Reinforced sand-cement	End-bearing	Compacted silt	Dynamic load-response test
McCartney (2013)	Reinforced sand-cement	Semi-floating	Compacted silt	Soil-structure interaction

Study	Pile/ heater material	Pile/ heater type	Soil type	Purpose
Goode et al. (2014)	Reinforced concrete	Semi-floating	Dry sand	Soil-structure interaction, temperature effects on load-settlement curve
Goode & McCartney (2014)	Reinforced concrete	End-bearing	Dry sand	Role of head restraint
Goode & McCartney (2015)	Reinforced concrete	Semi-floating and end-bearing	Dry sand and compacted silt	Soil-structure interaction, temperature effects on load-settlement curve
Ng et al. (2014)	Aluminum	Semi-floating	Saturated clay	Soil-structure interaction, cyclic effects
Ng et al. (2015)	Aluminum	Semi-floating	Saturated sand	Soil-structure interaction, temperature effects on load-settlement curve
Ghaaowd et al. (2018)	Aluminum	End-bearing anchor	Saturated clay	Temperature effects on load-settlement curve

391

392 4.2 Model Scale Tests on Other Energy Geostructures

393 Kurten et al. (2015a) present results of energy performance testing carried on a model energy wall.
394 Constructed within a sand box of dimensions 3m x 3m x 2m the model walls contained both U and W shaped
395 pipe arrangements. It was possible to control the temperature conditions on both sides of the wall. The results
396 showed the overall pipe length to be more important than the actual pipe arrangements, with heat exchange
397 rates of between 20 W/m and 100 W/m of pipe. These short-term results are compatible with the full-scale,
398 short-term tests performed by Xia et al. (2012). Overall energy outputs from the model tests were quoted as
399 36 W/m² to 150 W/m².

400 Zhang et al. (2016b) completed a model scale sand box experiment on a geothermal tunnel lining subjected
401 to cross flow of groundwater (see Table 7). The experiment was 1/20th scale and construction within a 1.4 m
402 x 1.2 m x 1.2 m tank. The authors investigated both the spacing and nature of the arrangement of the heat
403 transfer pipes, the temperature difference between the inlet temperature and the ground and the role of
404 groundwater based on sensitivity to Darcy velocity. The issue of scaling was not addressed in detail, but it was
405 noted that the groundwater flow velocity in the model is 20 times that in the prototype and hence values were
406 chosen with this factor in mind. Overall the results showed that significant groundwater flow both lowers the
407 temperature change at the tunnel and spreads the temperature increment over a wider area. It also reduces
408 the time to steady state and increases the degree of recovery during intermittent operation. Instrumentation
409 within the tunnel also showed the significant heat transfer occurring between the model geostructure and the
410 air within the tunnel, again showing the importance of this boundary condition. It is commented that the
411 results of the model test are consistent with those from the full-scale tests carried out by the same authors
412 (Zhang et al. 2016b, Zhang et al. 2014).

413 5 Discussion

414 It follows from the preceding material that geoprofessionals indeed contribute to the development of GSHP
415 technology and the dual use of geostructures as load bearing and as heat exchanger elements (as well as the
416 thermal optimisation of borehole GHEs). By doing so, peak energy demand is lowered and/or flatted via this
417 efficient heating and cooling of residential, commercial and industrial buildings. Moreover, using

418 geostructures remove the need for construction of (or minimise the number of) special purpose GHEs, further
419 contributing to reduce capital costs for shallow geothermal energy systems.

420 The GSHP technology has been primarily driven by colleagues specialising in Mechanical Engineering and the
421 Heating, Ventilation and Air Conditioning (HVAC) industry with limited input from Geotechnical Engineering.
422 This situation is rapidly changing. While there is still further research and development opportunities for the
423 design and installation of borehole GHEs, there exist today a swathe of thermal design approaches developed
424 for boreholes. In contrast, much fewer guidelines are available for the design and construction of energy piles
425 and for other energy geostructures such as retaining walls or tunnel linings. When it comes to thermal
426 analyses for geostructures, particularly for energy piles, a number of lessons can be imported, albeit with
427 limitations, from existing knowledge for GSHP systems that use boreholes, as highlighted in Section 2.1.2.
428 However, regarding thermo-geomechanical considerations, the existing GSHP literature developed for
429 boreholes is of limited use.

430 For thermal analysis and design of energy piles (and other geostructures) appropriate analytical models are
431 still required. An analytical solution which is solved transiently in radial coordinates has been proposed by
432 Javed & Claesson (2011). The model was developed for boreholes but is potentially suitable for adaption for
433 piles. One aspect which would require reconsideration is the simplification of the pipe details to an annulus
434 to permit adoption of radial coordinates. In addition, the model has a uniform surface boundary temperature
435 and assumes homogeneous and isotropic ground conditions which for 'short' piles (relative to typical deeper
436 boreholes) poses issues. Regardless of the model employed, in energy piles analytical models dealing with the
437 short term transient behaviour are yet to be effectively developed. Numerical simulations (Section 2.1.2.5),
438 hybrid models (Section 2.1.2.7) or other novel techniques such as Machine Learning (Makasis et al. 2018c,
439 2018d) may guide these analytical developments in the view of the current limited access to full scale and
440 model scale testing data.

441 For the thermo-geomechanical analysis of energy piles (and other geostructures), ensuring that their ultimate
442 bearing capacity is not exceeded by the combined building and thermally induced forces, and that their long-
443 term serviceability is maintained have driven the core of the research by geoprofessionals. Although published
444 long term experimental data is lacking in general, Sections 2.2, 3 and 4 and the long-term experience from
445 Switzerland and Austria (e.g., Brandl's work) suggest negligible or manageable thermo-mechanical effects
446 arising from GSHP system operations. However, special attention and further research is needed when dealing
447 with soft, normally consolidated and/or unsaturated soils.

448 In all cases, there has not been sufficient experimental data collected to validate predictions. This situation is
449 also changing. The largest field instrumented program in shallow geothermal research is believed to be
450 running in Australia (Johnston et al. 2014, Narsilio et al. 2014, Aditya et al. 2018), but it mostly accounts for
451 borehole GHEs and the GSHP industry there is not as developed as in other parts of the world. Although not
452 in a systematic and coordinated manner as in the Australian case, a number of other isolated monitored full
453 scale tests were conducted and are being conducted around the globe, particularly in North America, parts of
454 Europe (e.g., Switzerland, UK, Spain) and parts of Asia (e.g., Korea, China). These testing account for borehole
455 GHEs and energy piles mostly. Not only a larger dataset is still needed, but also other energy geostructures
456 are required to be tested to advance knowledge and validate and calibrate numerical and analytical models,
457 alongside constructability. The absence of standard thermal performance testing makes generalisations hard
458 to be derived, which is also compounded by the incomplete site characterisation and knowledge of soil
459 conditions.

460 Similar limitations and difficulties arise in *in situ* thermal response testing for determining soil conditions.
461 Perhaps more importantly are the limitations of the test itself, initially developed for slender boreholes, when
462 attempted on energy piles or retaining walls, with vastly different geometrical ratios and more subjected to
463 influences from the elements (e.g. Bidarmaghz et al. 2016b, Jensen-Page et al. 2018). For the log-linear
464 relationship to derive *in situ* thermal parameters at steady state conditions to be valid, it may be days or weeks
465 for energy piles (as oppose to 1-2 days for boreholes), or different interpretation techniques are still required,
466 with a few currently just under development (e.g. Loveridge et al. 2015).

467 Model scale testing offer good opportunities to overcome the disadvantages of field scale testing as
468 highlighted in Section 4. However, there still exist scaling issues and scaling compatibility amongst the different
469 physical processes involved. Materials' thermo-mechanical mismatches with prototypes, for example on the
470 materials used for energy pile centrifuge models, have been generally overlooked, and while still providing
471 useful information, there are opportunities to perform more realistic model testing (e.g. Minto et al. 2016).

472 Clearly practical tools for geoengineers and practitioners are still required. GSHP technology and energy
473 geostructures are starting to be implemented more widely and seriously considered in large scale
474 infrastructure projects (e.g. Cross Rail in London, Metro extensions in Melbourne, Paris and Torino). Tools for
475 design as well as for management and constructability of energy geostructure are desperately required
476 alongside guidelines, which would eventually lead to standards. While some solid research bases have been
477 already developed perhaps for a first generation 'practical' design tool, there is still much to learn for a routine
478 application of GSHP technology. Even more so, when larger scale implementation of the technology is sought
479 (see for example, Nicholson et al. 2013, Ryżyński & Bogusz 2016, Mortada et al. 2018). The development and
480 implementation of guidelines for the structural and geotechnical design of energy geo- structures is another
481 critical component of this activity that need more work. Perhaps the first effort in this area corresponds to the
482 SIA-D0190 (2005) Swiss guide that deals with the design of energy piles. A similar standard was developed in
483 the United Kingdom by the Ground Source Heat Pump Association (GSHPA 2012). Most recently the
484 'CFM S' SYNTEC INGENIERIE/ SOFFONS-FNTP' (2017) was proposed in France. Following the Eurocodes, the
485 French guidelines consider a performance-based design approach, which is a significant difference respect to
486 the Swiss and British standards, which are basically prescriptive approaches. Undoubtedly more effort and
487 advances are necessary in this area as well.

488 **6 Summary**

489 An overview on the most relevant and recent advances on energy geo-structures was presented in this paper.
490 Aspects covering the design and analysis of thermo-active geostructures were discussed in this contribution
491 with particular attention to the influence of temperature changes on pile, surrounding soils and other
492 components of the system. Analytical functions and approaches (e.g. G-functions, thermal resistances)
493 generally used in the design of energy piles were presented and analysed in detail together with numerical
494 solution typical used to tackle this type of problem. The discussion did not limit to energy piles, because other
495 energy geostructures were also considered, including, retaining walls, tunnels and bridges (i.e. deck de-icing).
496 The paper also reviews recent developments in terms of laboratory and field testing associated with thermo-
497 active structures, encompassing, lab 1-g tests, centrifuge experiments; and large-scale/field tests. Finally, the
498 discussion focused on highlighting the main findings and progress in the last few years in this very active area,
499 as well as on identifying present and future challenges related to the interaction between energy
500 geostructures and the ground.

501

502 **References**

- 503 Adam, D. & Markiewicz, R. (2009) Energy from earth-coupled structures, foundations, tunnels and sewers,
504 *Geotechnique*, 59 (3), 229-236.
- 505 Aditya, G. R., Narsilio, G. A. & Johnston, I. W. (2018) Full-scale instrumented ground source heat pump
506 experiments in Melbourne, Australia. Symposium of Energy Geotechnics in Switzerland in September 2018,
507 185-191, doi:10.1007/978-3-319-99670-7_24
- 508 Akrouch, G., Sánchez, M., & Briaud, J-L. (2014) Thermo-mechanical behaviour of energy piles in high plasticity
509 clays. *Acta Geotechnica*, 9(3), 399–412.
- 510 Akrouch, G.A., Briaud, J-L, Sánchez, M., and Yilmaz, R. (2015) Thermal Cone Test to Determine Soil Thermal
511 Properties. *Journal of Geotechnical and Geoenvironmental Engineering* 10.1061/(ASCE) GT.1943-
512 5606.0001353, 04015085
- 513 Akrouch, G.A., Sanchez, M.A., and Briaud, J-L. (2016) An experimental, analytical, and numerical study on the
514 thermal efficiency of energy piles in unsaturated soils. *Computers and Geotechnics* 71, 207-220.
- 515 Akrouch, G.A., Sanchez, M.A., and Briaud, J-L. (2018) Performance of a Shallow Geothermal Energy System
516 under Cooling-Dominated Conditions". *Renewable Energy* (under review).
- 517 Alberdi-Pagola M; Erbs Poulsen S; Loveridge F; Madsen S; Lund Jensen R (2018) Comparing heat flow models
518 for interpretation of precast quadratic pile heat exchanger thermal response tests. *Energy*, 145, 721-733.
- 519 Amatya, B.L., Soga, K., Bourne-Webb, P.J., Amis, T., and Laloui, L. (2012) Thermo-mechanical behaviour of
520 energy piles. *Géotechnique*, 62(6), 503–519.
- 521 Amis, T., Robinson, C. & Wong, S. (2010) Integrating Geothermal Loops into the Diaphragm Walls of the
522 Knightsbridge Palace Hotel Project. *EMAP – Basements and Underground Structures 2010*, 10p.
- 523 Amis, T. & Loveridge, F. (2014) Energy piles and other thermal foundations for GSHP – Developments in UK
524 practice and research, *The REHVA European HVAC Journal*, January, 32 – 35.
- 525 Amis, T., McCartney, J.S, Loveridge, F., Olgun, C. G., Bruce, M.E & Murphy, K. (2014) Identifying Best Practice,
526 Installation, Laboratory Testing, and Field Testing, *DFI Journal*, 8 (2), 74-83.
- 527 Angelotti, A. & Sterpi, D. (2018). On the performance of energy walls by monitoring assessment and numerical
528 modelling. *ICE Environmental Geotechnics*. <https://doi.org/10.1680/jenge.18.00037>.
- 529 Arulrajah, A., Narsilio G., Kodikara, J., and Orense, R. (2015), "Key issues in environmental geotechnics:
530 Australia–New Zealand", *Environmental Geotechnics*, 2 (6), 326-330.
- 531 Austin, W.A. (1998) Development of an in situ system for measuring ground thermal properties. Masters
532 Thesis. Oklahoma State University. Stillwater, OK.
- 533 Banks, D. (2012) *An Introduction to Thermogeology, Ground Source Heating and Cooling*, 2nd Edition, Wiley
534 Blackwell, Chichester, UK.
- 535 Baralis, M, Barla, M., Bogusz, W., Di Donna, A., Rzyżyński, G. & Żeruń, M. (2018) Geothermal potential of the
536 NE extension Warsaw (Poland) metro tunnels. *Environmental Geotechnics*, 2018 (in press, Published Online:
537 August 17), 1-13. <https://doi.org/10.1680/jenge.18.00042>
- 538 Barla, M., Di Donna, A. & Perino, A. (2016) Application of energy tunnels to an urban environment.
539 *Geothermics*. 61, 104-113.

540 Barla, M. & Di Donna, A. (2018) Energy tunnels, concepts and design aspects, *Underground Space*, 3(4), 268-
541 276.

542 Barla, M., Di Donna, A. & Santi, A. (2018). Energy and mechanical aspects on the thermal activation of
543 diaphragm walls for heating and cooling. *Renewable Energy*. <https://doi.org/10.1016/j.renene.2018.10.074>.

544 Başer, T., Dong, Y., Moradi, A.M., Lu, N., Smits, K., Ge, S., Tartakovsky, D., and McCartney, J.S. (2018) Role of
545 water vapor diffusion and nonequilibrium phase change in geothermal energy storage systems in the vadose
546 zone. *Journal of Geotechnical and Geoenvironmental Engineering*. 144(7), 04018038.

547 Batini, N., Rotta Loria, A. F., Conti, P., Testi, D., Grassi, W. & Laloui, L. (2015) Energy and geotechnical behaviour
548 of energy piles for different design solutions, *Applied Thermal Engineering*, 85, 199-213.

549 Black, J., & Tatari, A. (2015) Transparent soil to model thermal processes: An energy pile example. *ASTM*
550 *Geotechnical Testing Journal*. 38 (5), GTJ20140215.

551 Bennet, J, Claesson, J, Hellstrom, G., 1987. Multipole method to compute the conductive heat flow to and
552 between pipes in a composite cylinder. Report. University of Lund, Department of Building and Mathematical
553 Physics. Lund, Sweden.

554 Bernier, M. (2001) Ground Coupled Heat Pump System Simulation, *ASHRAE Transactions*, 107 (1), 605-616.

555 Bidarmaghz, A. (2015) 3D numerical modelling of vertical ground heat exchangers, PhD Thesis, University of
556 Melbourne.

557 Bidarmaghz, A., Narsilio, G.A. (2016), Shallow geothermal energy: emerging phenomena in permeable
558 saturated soils, *Geotechnique Letters*, Proceedings of the Institution of Civil Engineers ICE (UK), 6(2), pp. 119-
559 123. DOI: 10.1680/jgele.15.00167

560 Bidarmaghz, A., Narsilio G. A., and Johnston, I. W. (2012), Numerical modelling of ground loop configurations
561 for direct geothermal applications", In Narsilio, G. A., Arulrajah, A., and Kodikara, J. (eds.), Proceedings of the
562 11th Australia New Zealand Conference on Geomechanics (ANZ-2012). ISBN 978-0-646-54301-7. Melbourne,
563 Australia, July 15-18, 614-619.

564 Bidarmaghz, A, Makasis, N, Narsilio, G.A., Francisca, F.M., and Carro Pérez, M.E. (2016a), "Geothermal Energy
565 in Loess", *Environmental Geotechnics*, Proceedings of the Institution of Civil Engineers ICE (UK), 3(4), 225-236.

566 Bidarmaghz, A., and Narsilio G., (2018). "Heat exchange mechanisms in energy tunnel systems." *Geomechanics*
567 *for Energy and the Environment*, 16(December), 83-95.

568 Bidarmaghz, A., Narsilio, G. A., Johnston, I.W. & Colls, S. (2016b) The importance of surface air temperature
569 fluctuations on long-term performance of vertical ground heat exchangers, *Geomechanics for Energy and the*
570 *Environment*, 6, 35-44.

571 Bidarmaghz, A., Narsilio G., Buhmann P., Moormann C., and Westrich B. (2017) Thermal interaction between
572 tunnel ground heat exchangers and borehole heat exchangers. *Geomechanics for Energy and the*
573 *Environment*. 10(June), 29-41. Doi: 10.1016/j.gete.2017.05.001

574 Booker, J.R. & Savvidou, C. (1984) Consolidation around a spherical heat source. *Int J Solids Struct*. 20(11-12):
575 1079-1090.

576 Booker, J.R. & Savvidou C. (1985) Consolidation around a point heat source. *Int J Numer Anal Meth*. 9(2): 173-
577 184.

578 Bouazza, A., Wang, B. & Singh, R.M. (2013) Soil effective thermal conductivity from energy pile thermal tests.
579 Coupled Phenomena in Environmental Geotechnics: Proceedings of the International Symposium, Torino,
580 Italy, 1-3 July 2013, Taylor & Francis, London, pp. 211-219.

581 Bouazza, A., Singh, R.M., Wang, B., Barry-Macaulay, D., Haberfield, C., Chapman, G., Baycan, S. & Carden, Y.
582 (2011) Harnessing on site renewable energy through pile foundations. *Australian Geomech. J.*, 46(4), 79–90.

583 Bouazza, A., Wang, B. & Singh B. M. (2013) Soil effective thermal conductivity from energy pile thermal tests,
584 In: *Coupled Phenomena in Environmental Geotechnics*, Manessero et al. (Eds), Taylor and Francis Group,
585 London. 211-219pp.

586 Bourne-Webb, P.; Burlon, S.; Javed, S.; Kürten, S.; Loveridge, F. (2016) Analysis and design methods for energy
587 geostructures. *Renewable and Sustainable Energy Reviews*, 65, 402-419

588 Bourne-Webb, P.J., Bodas Freitas, T.M. & da Costa Gonçalves, R.A. (2016) Thermal and mechanical aspects of
589 the response of embedded retaining walls used as shallow geothermal heat exchangers. *Energy and Buildings*.
590 doi: 10.1016/j.enbuild.2016.04.075.

591 Bourne-Webb, P., Amatya, B., Soga, K. & Payne, P. (2009) Energy pile test at Lambeth College, London:
592 geotechnical and thermodynamic aspects of pile response to heat cycles, *Géotechnique* 59(3), 237-248.

593 Bourne-Webb, P.J., Freitas, T.M.B., Assunção, R.M.F. (2019) A review of pile-soil interactions in isolated,
594 thermally-activated piles. *Computers and Geotechnics* 108, 61-74.

595 Brandl, H. (2006) Energy foundations and other thermo active ground structures, *Geotechnique*, 56 (2), 81 –
596 122.

597 Brandl, H., Adam, D., Markiewicz, R. Unterberger, W. & Hofinger, H. (2010) Massivabsorbertechnologie zur
598 Erdwärmennutzung bei der Wiener U-Bahnlinie U2, Osterr. Ingenieur- und Architekten- Zeitschrift, 155, Heft
599 7-9/2010 und Heft 10-12/2010, 1-7.

600 Breier, R.A., Smith, M.D. & Spitler, J.D. (2011) Reference data sets for vertical boreholes ground heat exchanger
601 models and thermal response tests analysis, *Geothermics*, 40, 79 – 85.

602 Brettmann, T. and Amis, T. (2011) Thermal conductivity evaluation of a pile group using geothermal energy
603 piles, *Proc. Geo-Frontiers 2011 Conf.*, Dallas, TX, USA, March, ASCE, 499–508.

604 Buhmann, P., Moormann, C., Westrich, B., Pralle, N. & Friedemann, W. (2016) Tunnel geothermics—A German
605 experience with renewable energy concepts in tunnel projects. *Geomechanics for Energy and the Environment*
606 8, 1-7. DOI: 10.1016/j.gete.2016.10.006

607 Carslaw HS and Jaeger JC (1959) *Conduction of Heat in Solids*. Second Edition, Oxford University Press.

608 Caulk, R., Ghazanfari, E., & McCartney, J.S. (2016) Parameterization of a calibrated geothermal energy pile
609 model. *Geomechanics for Energy and the Environment*. 5(3), 1-15.

610 Cecinato, F. & Loveridge, F. (2015) Influences on the thermal efficiency of energy piles. *Energy*, 82, 1021-2023.

611 Chen, D. & McCartney, J.S. (2016) Calibration parameters for load transfer analysis of energy piles in uniform
612 soils. *ASCE International Journal of Geomechanics*. 1-17. 10.1061/(ASCE)GM.1943-5622.0000873. 04016159.

613 Choi, J.C., Lee, S.R. & Lee, D.S. (2011) Numerical simulation of vertical ground heat exchangers: Intermittent
614 operation in unsaturated soil conditions, *Computers and Geotechnics*, 38, 949-958.

615 CIBSE (2013) *Ground Source Heat Pumps TM51:2013*, Chartered Institute of Building Services Engineers,
616 London, UK.

617 Claesson, J. & Javed, S. (2011) An analytical method to calculate borehole fluid temperatures for time-scales
618 from minutes to decades. *ASHRAE Transactions*, 117(2), 279-288.

619 Claesson, J. & Hellström, G. (2011) Multipole method to calculate borehole thermal resistances in a borehole
620 heat exchanger. *HVAC & R Research*, 17(6), 895-911.

621 Claesson, J. & Javed, S. (2012) A load aggregation method to calculate extraction temperatures of borehole
622 heat exchangers, *ASHRAE Trans*, 118(1), 530–9.

623 Coccia, C.J.R. & McCartney, J.S. (2016a) Thermal volume change of poorly draining soils I: Critical assessment
624 of volume change mechanisms. *Computers and Geotechnics*. 80: 26-40. 10.1016/j.compgeo.2016.06.009.

625 Coccia, C.J.R. & McCartney, J.S. (2016b) Thermal volume change of poorly draining soils II: Constitutive
626 modelling. *Computers and Geotechnics*. 80(December), 16-25. 10.1016/j.compgeo.2016.06.010.

627 Colls, S. (2013) *Ground heat exchanger design for direct geothermal energy systems*, PhD Thesis, University of
628 Melbourne, Australia.

629 Coyle, H.M. & Reese, L.C. (1966) Load transfer for axially loaded piles in clay. *J. Soil Mech. Found. Div.*, 92(2),
630 1–26.

631 CFM S/ SYNTEC INGENIERIE/ SOFFONS-FNTP (2017) *Recommandations pour la conception, le dimensionnement
632 et la mise en oeuvre des géostructures thermiques*. Version 1; pp 120.

633 Cullin J. R., Spitler J. D., Montagud C. et al. (2015) Validation of vertical ground heat exchanger design
634 methodologies. *Science and Technology for the Built Environment*, 21(2), 137-149

635 Cullin, J. R., Spitler, J. D., & Gehlin, S. E. A. (2014) Suitability of foundation heat exchangers for ground source
636 heat pump systems in European Climates, *REHVA Journal*, January 2014, 26-40.

637 De Carli, M., Tonon, M., Zarrella, A. & Zecchin, R. (2010) A computational capacity resistance model (CaRM)
638 for vertical ground-coupled heat exchangers, *Renewable Energy*, 35 (7), 1537-1550.

639 Delerabee, Y. & Rammal, D., Mroueh, H., Burlon, S., Habert, J. & Froitier, C. (2018). Integration of
640 Thermoactive Metro Stations in a Smart Energy System: Feedbacks from the Grand Paris Project.
641 *Infrastructures*. 3. 56.

642 Di Donna, A. & Barla, M. (2016) The role of ground conditions on energy tunnels' heat exchange,
643 *Environmental Geotechnics*, 3 (4), 214 – 224. <http://dx.doi.org/10.1680/jenge.15.00030>

644 Di Donna, A., Cecinato, F., Loveridge, F. & Barla, M. (2016a) Energy performance of diaphragm walls used as
645 heat exchangers, *Proceedings of the Institution of Civil Engineers, Geotechnical Engineering*.

646 Di Donna, A., Rotta Loria, A.F., Laloui, L. (2016b) Numerical study of the response of a group of energy piles
647 under different combinations of thermo-mechanical loads. *Computers and Geotechnics*. 72, 126-142

648 Di Donna, A., Ferrari, A. & Laloui, L. (2015), Experimental investigations of the soil–concrete interface: physical
649 mechanisms, cyclic mobilization, and behaviour at different temperatures. *Can. Geotech. J.*, 53(4), 659-672

650 Diao, N. R., Zeng, H. Y. & Fang, Z. H. (2004a) Improvements in modelling of heat transfer in vertical ground
651 heat exchangers, *HVAC&R Research*, 10 (4), 459-470.

652 Diao, N., Li, Q. & Fang, Z. (2004b) Heat transfer in ground heat exchangers with groundwater advection. Int. J.
653 Therm. Sci. 43, No. 12, pp. 1203–1211.

654 Do, S.L. & Haberl, J.S. (2010) A Review of Ground Coupled Heat Pump Models Used in Whole-Building
655 Computer Simulation Programs. Energy Systems Laboratory (<http://esl.tamu.edu>). Available electronically
656 from <http://hdl.handle.net/1969.1/93221>.

657 Dupray, F., Laloui, L. & Kazangba (2014) Numerical analysis of seasonal heat storage in an energy pile
658 foundation, Computers and Geotechnics, 55, 67-77.

659 Ennigkeit, A., & Katzenbach, R. (2001) The double use of piles as foundation and heat exchanging elements.
660 Soil Mechanics and Geotechnical Engineering. Proc. 14th International Conference on Soil Mechanics and
661 Geotechnical Engineering. Taylor and Francis. London. Vol. 2. 893-896.

662 Eskilson, P. (1987) *Thermal analysis of heat extraction boreholes*. Doctoral Thesis, Department of
663 Mathematical Physics, University of Lund, Sweden.

664 Eskilson, P. & Claesson, J. (1988) Simulation model for thermally interacting heat extraction boreholes.
665 Numerical Heat Transfer, 13, pp. 149-165.

666 Eslami, H., Rosin-Paumier, S., Abdallah, A. & Masrouri, F. (2017) Pressuremeter test parameters of a
667 compacted illitic soil under thermal cycling. Acta Geotechnica:1-14.

668 Faizal M, Bouazza A, Singh RM. (2016a) Heat transfer enhancement of geothermal energy piles. Renewable
669 and Sustainable Energy Reviews 57: 16–33. <http://dx.doi.org/10.1016/j.rser.2015.12.065>.

670 Faizal M, Bouazza A, Singh RM. (2016b) An experimental investigation of the influence of intermittent and
671 continuous operating modes on the thermal behaviour of a full scale geothermal energy pile. Geomechanics
672 for Energy and the Environment, 8: 8-29. <https://doi.org/10.1016/j.gete.2016.08.001>.

673 Faizal, M., Bouazza, A., McCartney, J.S., & Haberfield, C. (2018a) Axial and radial thermal responses of an
674 energy pile under a 6-storey residential building. Canadian Geotechnical Journal. <https://doi.org/10.1139/cgj-2018-0246>.

675

676 Faizal, M., Bouazza, A., Haberfield, C., & McCartney, J.S. (2018b) Axial and radial thermal responses of a field
677 scale energy pile under monotonic and cyclic temperatures. Journal of Geotechnical and Geoenvironmental
678 Engineering. 144(10), 04018072.

679 Fadejev, J., Simson, R., Kurnitski, J. & Haghigat, F. (2017). A review on energy piles design, sizing and
680 modelling. Energy 122, 390-407

681 Fisher, D.E., Rees, S.J., Padhmanabhan, S.K. & Murugappan, A. (2006) Implementation and validation of
682 ground-source heat pump system models in an integrated building and system simulation environment,
683 HVAC&R Research, 12 (1), 693-710.

684 Franzius, J.N. & Pralle, N. (2011) Turning segmental tunnels into sources of renewable energy, Proceedings of
685 the ICE Civil Engineering, 164, 35-40.

686 Frodl, S., Franzius, J. N. and Bartl, T. (2010). Design and construction of the tunnel geothermal system in
687 Jenbach /. Geomechanik Tunnelbau | Geomechanics and Tunnelling, 3(5), 658-668.
688 doi:10.1002/geot.201000037

689 Gao, J., Zhang, X., Liu, J., Li, K. & Yang, J. (2008). Numerical and experimental assessment of thermal
690 performance of vertical energy piles: an application, Applied Energy, 85, 901-910.

691 Garber, D., Choudhary, R. & Soga, K. (2013) Risk based lifetime costs assessment of a ground source heat pump
692 (GSHP) system design: Methodology and case study, *Building and the Environment*, 60, 66 – 80.

693 Gawecka et al. (2016), Effects of transient phenomena on the behaviour of thermo-active piles. Proc. 1st Int.
694 Conf. Energy Geotechnics, ICEGT 2016, 71-78

695 Gawecka et al. (2017), Numerical modelling of thermo-active piles in London Clay, *ICE Geotechnical*
696 *Engineering*, 170, 201-219

697 Gehlin, S. (2002) Thermal response test, model development and evaluation, Doctoral Thesis, Lulea Technical
698 University.

699 Gehlin & Hellstrom (2003) Influence on thermal response test by groundwater flow in vertical fractures in hard
700 rock. *Renewable Energy* 28(14): pp. 2221-2238.

701 Geimer, C., 2013. Metro tunnels enable geothermal-air conditioning – BINE information service, Projektinfo
702 09/2013, FIZ Karlsruhe – Leibniz Institute for Information Infrastructure, Germany (ISSN 0937-8367)

703 Ghaaowd, I., Takai, A., Katsumi, T., and McCartney, J.S. (2017) Pore water pressure prediction for undrained
704 heating of soils. *Environmental Geotechnics*. 4(2), 70-78.

705 Ghaaowd, I., McCartney, J.S., Huang, X., Saboya, F., & Tibana, S. (2018) Issues with centrifuge modeling of
706 energy piles in soft clays. 9th International Conference on Physical Modelling in Geotechnics. London, England.
707 Jul. 17-20. 1-6.

708 Glassley, W. (2010) *Geothermal energy: renewable energy and the environment*. 2010, Florida, USA: CRC
709 Press. 320 Pages. ISBN 9781420075700

710 Go, G-H., Lee, S-R., Yoon, S., Kang, H-B. (2014) Design of spiral coil PHC energy pile considering effective
711 borehole thermal resistance and groundwater advection effects, *Applied Energy*, 125, 165-178.

712 Goode, J.C., III, Zhang, M. & McCartney, J.S. (2014) Centrifuge modeling of energy foundations in sand. *Physical*
713 *Modeling in Geotechnics: Proc. 8th International Conference on Physical Modelling in Geotechnics*. Perth,
714 Australia. Jan. 14-17. C. Gaudin & D. White, eds. Taylor and Francis. London. 729-736.

715 Goode, J.C., III, & McCartney, J.S. (2014) Evaluation of head restraint effects on energy foundations. Proc.
716 *GeoCongress 2014 (GSP 234)*, M. Abu-Farsakh & L. Hoyos, eds. ASCE. Pp. 2685-2694.

717 Goode, J.C., III, & McCartney, J.S. (2015) Centrifuge modeling of boundary restraint effects in energy
718 foundations. *ASCE Journal of Geotechnical and Geoenvironmental Engineering*. 141(8), 04015034-1-13.

719 GSHPA (2012) *Thermal pile design installation and materials standards*, Issue 1.0. Ground Source Heat Pump
720 Association, Milton Keynes, UK, p. 85.

721 GSHPA (2011) *Closed-loop Vertical Borehole Design, Installation & Materials Standards Issue 1.0*, September
722 2011. Ground Source Heat Pump Association, Milton Keynes, UK.

723 Habert, J., El'Mejahed, M. & Bernard J-B. (2016) Lessons learned from mechanical monitoring of a
724 thermoactive pile, In: *Energy Geotechnics: Proceedings of the 1st International Conference on Energy*
725 *Geotechnics*, F. Wuttke, S. Bauer, M. Sanchez, eds. ICEGT 2016, Kiel, Germany, 29-31 August 2016.

726 Hamada, Y., Saitoh, H., Nakamura, M., Kubota, H., & Ochifuji, K. (2007) Field performance of an energy pile
727 system for space heating, *Energy and Buildings*, 39, 517-524.

728 Hellstrom, G. (1989) *Duct Ground Heat Storage Model, Manual for Computer Code*. Department of
729 Mathematical Physics, University of Lund, Sweden.

730 Hellstrom, G., 1991. Ground Heat Storage, Thermal Analysis of Duct Storage Systems, Theory. Department of
731 Mathematical Physics, University of Lund, Sweden.

732 Hemmingway, P. & Long, M. (2013) Energy piles: site investigation and analysis, Proc. Inst. Civil. Eng.
733 Geotechnical Engineering 166(6), 561-575.

734 Henderson, H.I., Carlson, S.W. & Walburger, A.C. (1998) North American monitoring of a hotel with room sized
735 GSHPs, Proc IEA Room Size Heat Pump Conference, Canada, 1998.

736 Han C. & Yu X. (2018) An innovative energy pile technology to expand the viability of geothermal bridge deck
737 snow melting for different United States regions: Computational assisted feasibility analyses, Renew. Energy
738 123: 417-427.

739 Ho I.H. & Dickson M. (2017) Numerical modeling of heat production using geothermal energy for a snow-
740 melting system, Geomech. Energy Environ. 10: 42-51.

741 Hughes, P. & Im, P. (2013) Foundation heat exchanger final report: demonstration, measured performance,
742 and validated model and design tool, Oak Ridge National Laboratory, Available online
743 [http://web.ornl.gov/sci/ees/etsd/btrc/publications/ORNL-](http://web.ornl.gov/sci/ees/etsd/btrc/publications/ORNLFHX%20Final%20Report_Jan%202012%20for%20Distribution_rev_01152013.pdf)
744 [FHX%20Final%20Report_Jan%202012%20for%20Distribution_rev_01152013.pdf](http://web.ornl.gov/sci/ees/etsd/btrc/publications/ORNLFHX%20Final%20Report_Jan%202012%20for%20Distribution_rev_01152013.pdf)

745 ICConsulten (2005) Wirtschaftliche optimierung von tunnelthermieabsorberanlagen,
746 grundlagenuntersuchung und planungsleitfaden, 23.12.2005. Rev 1, 84 pp.

747 IGSHA (2009) Ground Source Heat Pump Residential and Light Commercial Design and Installation Guide,
748 Oklahoma State University, Stillwater, USA.

749 IGSHA (2007) Closed-loop/geothermal heat pump systems: Design and installation standards, International
750 Ground Source Heat Pump Association/ Oklahoma State University.

751 Ingersoll, L.R., Zobel, O.J. & Ingersoll, A.C. (1954) Heat Conduction with Engineering and Geological
752 Applications. 3rd Edition, McGraw-Hill, New York.

753 Jalaluddin, Miyara, A., Tsubaki, K., Inoue, S., & Yoshida, K. (2011) Experimental study of several types of ground
754 heat exchanger using a steel pile foundation, Renew Energy, 36, 764–771.

755 Javed S and Claesson J (2011) New analytical and numerical solutions for the short-term analysis of vertical
756 ground heat exchangers. *ASHRAE Transactions*, 117(1), 3-12.

757 Jensen-Page, L, Narsilio G., Bidarmaghz, A., and Johnston, I., (2018). Investigation of the effect of seasonal
758 variation in ground temperature on Thermal Response Tests Renewable Energy, 125, 609-619.

759 Johnston, I.W., Narsilio, G.A., Colls, S., Valizadeh Kivi, A., Payne, D., Wearing-Smith, M. & Noonan, G. (2014)
760 Direct geothermal energy demonstration projects for Victoria, Australia IPENZ Transactions (NZ) (ISSN 1179-
761 9293) 41, pp. 1-10.

762 Kakaç, S. & Yener, Y. 2008. Heat conduction, 4rd Edition, Taylor and Francis Group, Boca Raton FL, USA,

763 Kalantidou, A., Tang, A.M., Pereira, J.-M., & Hassen, G. (2012) Preliminary study on the mechanical
764 behaviour of heat exchanger pile in physical model." *Géotechnique*. 62 (11), 1047–1051.

765 Kaltreider, C., Krarti, M. & McCartney, J.S. (2015) Heat transfer analysis of thermo-active foundations. *Energy*
766 *and Buildings*. 86, 492-501.

767 Katsura, T., Nakamura, Y., Okawada, T., Hori, S. & Nagano, K. (2009) Field test on heat extraction or injection
768 performance of energy piles and its application, *Proceedings of EFFSTOCK*, 2009.

769 Katzenbach, R., Olgun, C.G., Loveridge, F., Suttman, M., Bowers, G. A., McCartney, J.S., Laloui, L., Mimouni, T.,
770 Dupray, F., Spitler, J. D., Clauss, F., Meyer, L. L. & Akrouch, G. (2014) *New Technologies and Applications;*
771 *Materials and Equipment in Near Surface Geothermal Systems*, *DFI Journal*, 8 (2), 93-107.

772 Khosravi, A., Abdelrahman, S., & McCartney, J.S. (2012) Evaluation of thermal soil-structure interaction in
773 energy foundations using an impulse-response test. *Proc. GeoCongress 2012 (GSP 225)*. R.D. Hryciw, A.
774 Athanasopoulos-Zekkos, & N. Yesiller, eds. ASCE. 4466-4475.

775 Kipry, H., Bockelmann, F., Plessner, S. & Fisch, M.M. (2009) Evaluation of optimisation of UTESsystem of energy
776 efficient buildings, *Proceedings of EFFSTOCK*, 2009.

777 Knellwolf, C., Peron, H., & Laloui, L. (2011) Geotechnical analysis of heat exchanger piles. *J. Geotech*
778 *Geoenviron Eng.* 137(10):890–902.

779 Ko, H-Y. (1988) Summary of the state-of-the-art in centrifuge model testing. *Centrifuges in Soil Mechanics*.
780 W.H. Craig, R.G. James, & A.N. Schofield, eds., Balkema, Rotterdam, Netherlands, 11–18.

781 Kramer, C.A. & Basu, P. (2014a) Experimental characterization of energy output from a model geothermal pile.
782 *Proc. GeoCongress 2014*. ASCE, Reston, VA. 3703-3712.

783 Kramer, C.A. & Basu, P. (2014b) Performance of a model geothermal pile in sand. *Proceedings of 8th*
784 *International Conference on Physical Modelling in Geotechnics*. Perth, Australia. Jan. 14-17. C. Gaudin & D.
785 White, eds. Taylor and Francis. London. 771–777.

786 Kramer, C.A., Ghasemi-Fare, O. & Basu, P. (2015) Laboratory thermal performance tests on a model heat
787 exchanger pile in sand. *Geotechnical and Geological Engineering*. 33 (2), 253-271.

788 Krishnaiah, S., & Singh, D.N. (2004) Centrifuge modelling of heat migration in soils. *International Journal on*
789 *Physical Modeling in Geotechnics*. 4 (3), 39–47.

790 Kurten, S. (2011) Use of geothermal energy with thermo-active seal panels, *Geotechnical Engineering: New*
791 *Horizons, Proc 21st European Young Geotechnical Engineers Conference*, Rotterdam, 2011.

792 Kurten, S., Mottaghy, D. & Ziegler, M. (2015a) Design of plane energy geostructures based on laboratory tests
793 and numerical modelling. *Energy and Buildings*, 107, 434 – 444.

794 Kurten, S., Mottaghy, D. & Ziegler, M. (2015b) A new model for the description of the heat transfer for plane
795 thermo-active geotechnical systems based on thermal resistances. *Acta Geotechnica*, 10 (2), 219 – 229.

796 Lai, S. (1988) *Smilitude for Shaking Table Tests on Soil-Structure-Fluid Model in 1G Gravitational Field*. Report
797 to the Port and Harbour Research Institute. Report 27.3. 3-24.

798 Laloui, L., Olgun, C.G., Suttman, M., McCartney, J.S., Coccia, C.J.R., Abuel-Naga, H.M., and Bowers, G.A. (2014)
799 Issues involved with thermo-active geotechnical systems: Characterization of thermo-mechanical soil
800 behaviour and soil-structure interface behaviour. *The Journal of the Deep Foundations Institute*. 8(2), 107-
801 119.

802 Laloui, L., Nuth, M., and Vulliet, L. (2006) Experimental and numerical investigations of the behaviour of a heat
803 exchanger pile. *Int. J. Numer. Anal. Methods Geomech.*, 30(8), 763–781.

804 Laloui & Di Donna. (2013) *Energy geostructures*. John Wiley & Sons.

805 Laloui, L. (2011) In-situ testing of heat exchanger pile. *GeoFrontiers 2011*, Geotechnical special publication
806 211, J. Han and D. E. Alzamora, eds., ASCE, Reston, VA, 410–419.

807 Laloui, L., Moreni, M., and Vulliet, L. (2003) Comportement d'un pieu bifonction, fondation et échangeur de
808 chaleur. *Can. Geotech. J.*, 40(2), 388–402.

809 Laloui, L., and Nuth, M. (2006) Numerical modeling of some features of heat exchanger pile. *Foundation
810 Analysis and Design: Innovative Methods*. Geotechnical Special Publication 153. R.L. Parsons, L. Zhang, W. D.
811 Guo, K.K. Phoon, and M. Yang, eds., ASCE, Reston, VA. 189–195.

812 Lamarche L, & Beauchamp B (2007) A new contribution to the finite line-source model for geothermal
813 boreholes. *Energy and Buildings*, 39(2), 188-198.

814 Lamarche, L., Kaji, S. & Beauchamp, B. (2010) A review of methods to evaluate borehole thermal resistance in
815 geothermal heat pump systems, *Geothermics*, 39, 187-200.

816 Lazzari, S., Priarone, A. & Zanchini, E. (2010) Long-term performance of BHE (borehole heat exchanger) fields
817 with negligible groundwater movement. *Energy*, 35, pp. 4966-4974.

818 Lee, C., Park, S., Choi, H.-J., Lee, I.-M. & Choi, H. (2016) Development of energy textile to use geothermal
819 energy in tunnels. *Tunnelling and Underground Space Technology* 59, 105-113.

820 Lee, C., Park, S., Won, J., Jeoung, J., Sohn, B. & Choi, H. (2012) Evaluation of thermal performance of energy
821 textile installed in tunnel, *Renewable Energy*, 42, 11-22.

822 Li, M. & Lai, A.C.K. (2012) New temperature response functions (g-functions) for pile and borehole ground
823 heat exchangers based on composite-medium-line-source theory. *Energy*, 38(Feb), 255-263

824 Loveridge, F. & Cecinato, F. (2016) Thermal performance of thermo-active CFA piles, *Proceedings of the
825 Institution of Civil Engineers, Environmental Geotechnics*, 3(4), 265-279.

826 Loveridge, F. & Powrie, W. (2014) On the thermal resistance of pile heat exchangers, *Geothermics*. 50, 122 –
827 135.

828 Loveridge, F. & Powrie, W. (2013a) Pile heat exchangers: thermal behaviour and interactions, *Proceedings of
829 the Institution of Civil Engineers Geotechnical Engineering*, 166 (2), 178 - 196.

830 Loveridge, F., Powrie, W. and Nicholson, D. (2014b) Comparison of two different models for pile thermal
831 response test interpretation, *Acta Geotechnica*, 9 (3), 367-384

832 Loveridge, F. & Powrie, W. (2013b) Temperature response functions (G-functions) for single pile heat
833 exchangers, *Energy*, 57, 554 – 564.

834 Loveridge, F., Brettmann, T., Olgun, G. & Powrie, W. (2014a) Assessing the applicability of thermal response
835 testing to energy piles, *DFI-EFFC International Conference on Piling and Deep Foundations*, Stockholm,
836 Sweden, 20-21 May 2014.

837 Loveridge, F., Olgun, C.G., Brettmann, T. & Powrie, W. (2015) The thermal behaviour of three different auger
838 pressure grouted piles used as heat exchangers, *Geotechnical and Geological Engineering*, 33 (2), 273 – 289.

839 Loveridge F. A., Amis T & Powrie W (2012) Energy Pile Performance and Preventing Ground Freezing,
840 *Proceedings of the 2012 International Conference on Geomechanics and Engineering (ICGE'12)*, Seoul, August,
841 2012.

842 Low, J., Loveridge, F., Nicholson, D. & Powrie, W. (2015) A comparison of laboratory and in situ methods to
843 determine soil thermal conductivity for energy foundations applications, *Acta Geotechnica*, 10, 209-218.

844 Maddocks, D.F. & Savvidou, C. (1984) The effects of heat transfer from a hot penetrometer installed in the
845 ocean bed. *Application of Centrifuge Modeling to Geotechnical Design*. W.H. Craig, ed. Balkema, Rotterdam.
846 337-356.

847 Lu, Q. & Narsilio, G.A. (2019) Economic analysis of utilising energy piles for residential buildings. *Renewable*
848 *Energy*; under review.

849 Makasis, N., Narsilio G., Bidarmaghz, A. and Johnston, I.W., (2018a). "Ground-source heat pump systems: The
850 effect of variable pipe separation in ground heat exchangers", *Computers and Geotechnics*, 100 (August), 97-
851 109.

852 Makasis, N., Narsilio G., Bidarmaghz, A. and Johnston, I.W., (2018b). "Carrier fluid temperature data in vertical
853 ground heat exchangers with a varying pipe separation", *Data in Brief*, 18 (June), 1466-1470.

854 Makasis, N., Narsilio G., and Bidarmaghz, A. (2018c). "A robust prediction model approach to energy geo-
855 structure design", *Computers and Geotechnics*, 104 (December), 140-151.

856 Makasis, N., Narsilio G., and Bidarmaghz, A. (2018d) A machine learning approach to energy pile design,
857 *Computers and Geotechnics*, 97 (May), 189-203.

858 Man, Y., Yang, H., Diao, N., Cui, P., Lu L. & Fang, Z. (2011) Development of a spiral heat source model for novel
859 pile ground heat exchangers, *HVAC&R Research*, 17 (6), 1075-1088.

860 Man Y, Yang H, Diao N, Liu J and Fang Z (2010) A new model and analytical solutions for borehole and pile
861 ground heat exchangers. *Intl. J. of Heat and Mass Transfer*, 53(13-14), 253-2601

862 Maragna C; Loveridge F (2019) A resistive-capacitive model of pile heat exchangers with an application to
863 thermal response tests interpretation. *Renewable Energy*, **138**, pp. 891-910

864 Marcotte, D. & Pasquier, P. (2008) On the estimation of thermal resistance in borehole thermal conductivity
865 test. *Renewable Energy*, 33, pp. 2407-2415.

866 Marcotte, D., Pasquier, P., Sheriff, F. & Bernier, M. (2010) The importance of axial effects for borehole design
867 of geothermal heat-pump systems. *Renewable Energy*, 35, pp. 763-770.

868 Marto, A. & Amaludin, A. (2015) Response of shallow geothermal energy pile from laboratory model tests.
869 *International Symposium on Geohazards and Geomechanics (ISGG2015)*. 1-9.

870 McCartney, J.S. (2015) Structural performance of thermo-active foundations. In: *Advances in Thermo-Active*
871 *Foundations*. M. Krarti, ed. ASME Press. New York. pp. 1-44. ISBN: 9780791861059.

872 McCartney, J.S., and Murphy, K.D. (2012) Strain distributions in full scale energy foundations. *J. Deep Found.*
873 *Inst.*, 6(2), 28–36.

874 McCartney, J. S., Sánchez, M., & Tomac, I. (2016) Energy geotechnics: Advances in subsurface energy recovery,
875 storage, exchange, and waste management, *Computers and Geotechnics*, 75, 244-256.

876 McCartney, J.S. (2013) Centrifuge modeling of energy foundations. *Energy Geotechnics: Innovation in*
877 *Underground Engineering*, L. Laloui & A. Di Donna, eds., Wiley-ISTE, London, 99-115.

878 McCartney, J.S., Rosenberg, J.E., & Sultanova, A. (2010) Engineering performance of thermo-active foundation
879 systems. *GeoTrends: The Progress of Geological and Geotechnical Engineering in Colorado at the Cusp of a*
880 *New Decade (GPP 6)*. C.M. Goss, J.B. Kerrigan, J. Malamo, M.O. McCarron, M.O. & R.L. Wiltshire, eds. 27-42.

881 McCartney, J.S. & Rosenberg, J.E. (2011) Impact of heat exchange on side shear in thermo-active foundations.
882 *GeoFrontiers 2011 (GSP 211)*. J. Han & D.E. Alzamora, eds. ASCE, Reston VA. 488-498.

883 McCartney, J.S. & Murphy, K.D. (2017) Investigation of potential dragdown/uplift effects on energy piles.
884 *Geomechanics for Energy and the Environment*. 10(June), 21-28. DOI: 10.1016/j.gete.2017.03.001.

885 Menezes, C., Cripps, A., Bouchlaghem, D. & Russel, R., (2012) Predicted vs actual energy performance on non-
886 domestic buildings: using post occupancy evaluation data to reduce the performance gap, *Applied Energy*, 97,
887 355-364.

888 Mikhaylova, O., Johnston, I.W., and Narsilio, G.A. (2016a) Uncertainties in the Design of Ground Heat
889 Exchangers, *Environmental Geotechnics*, Themed issue on energy geostructures, *Proceedings of the*
890 *Institution of Civil Engineers ICE (UK)*, 3 (4), August 2016, 253-264. DOI: 10.1680/jenge.15.00033.

891 Mikhaylova O., Soga K., Choudhary R., Johnston I. (2016b) Utilisation of Urban Open Spaces for Sustainable
892 Heating and Cooling: A City-Scale Perspective. in Wuttke, F., Bauer, S. & Sanchez, M. (eds.). *Energy*
893 *Geotechnics: Proceedings of the 1st International Conference on Energy Geotechnics, ICEGT 2016*. CRC
894 Press/Balkema, p. 37-44 8 p. Kiel, Germany, 29-31 August 2016

895 Mikhaylova, O., Johnston I.W., & Narsilio, G.A. (2016c) Ground thermal response to borehole ground heat
896 exchangers, In: *Energy Geotechnics: Proceedings of the 1st International Conference on Energy Geotechnics*,
897 F. Wuttke, S. Bauer, M. Sanchez, eds. ICEGT 2016, Kiel, Germany, 29-31 August 2016.

898 Minto, A., Leung, A. K., Vitali, D. & Knappett, J. A. (2016) Thermomechanical properties of a new small-scale
899 reinforced concrete thermo-active pile for centrifuge testing in Wuttke, F., Bauer, S. & Sanchez, M.
900 (eds.). *Energy Geotechnics: Proceedings of the 1st International Conference on Energy Geotechnics, ICEGT*
901 *2016*. CRC Press/ Balkema, p. 37-44 8 p.

902 Mimouni, T. & Laloui, L. (2014) Towards a secure basis for the design of geothermal piles, *Acta Geotechnica*,
903 9 (3), 355-366.

904 Mimouni, T., Dupray, F. & Laloui, L. (2014) Estimating the geothermal potential of heat-exchanger anchors on
905 a cut-and-cover tunnel, *Geothermics*, 51, 380-387.

906 Mimouni, T., & Laloui, L. (2015) Behaviour of a group of energy piles. *Canadian Geotechnical Journal*. 52, 1913-
907 1929.

908 Mogensen P. (1983) Fluid to duct wall heat transfer in duct system heat storages. In: *International conference*
909 *on subsurface heat storage in theory and practice*, Stockholm, Sweden: Swedish Council for Building Research,
910 p. 652–57.

911 Morino, K. & Oka, T. (1994) Study on heat exchanged in soil by circulating water in a steel pile, *Energy Build.*,
912 21 (1), 65–78.

913 Mortada, A., Choudhary, R. & Soga, K. (2018) Multi-dimensional simulation of underground subway spaces
914 coupled with geoenery systems. *Journal of Building Performance Simulation* 11(5), 517-537.

915 Muraya, N.K., O'Neal, D.L. & Heffington, W.M. (1996) Thermal interference of adjacent legs in a vertical U-
916 tube heat exchanger for a ground-coupled heat pump. *ASHRAE Transactions*, 102, pp. 12-21.

- 917 Murphy, K.D., Henry, K.S., & McCartney, J.S. (2014) Impact of horizontal run-out length on the thermal
918 response of full-scale energy foundations. Proceedings of GeoCongress 2014 (GSP 234), M. Abu-Farsakh and
919 L Hoyos, eds. ASCE. pp. 2715-2714.
- 920 Murphy, K.D. & McCartney, J.S. (2014) Thermal borehole shear device. ASTM Geotechnical Testing Journal.
921 37(6), 1040-1055.
- 922 Murphy, K.D., and McCartney, J.S. (2015) Seasonal response of energy foundations during building operation.
923 Geotech. Geol. Eng., 33(2), 343–356.
- 924 Murphy, K.D., McCartney, J.S., and Henry, K.S. (2015) Evaluation of thermo-mechanical and thermal behaviour
925 of full-scale energy foundations. Acta Geotechnica, 10(2), 179–195.
- 926 Nagano, K., Katsura, T., Takeda, S., Saeki, E., Nakamura, Y., Okamoto, A. & Narita, S. (2005) Thermal
927 characteristics of steel foundation piles as ground heat exchangers, Proc. 8th IEA Heat Pump Conference 2005,
928 Las Vegas, P6-12.1-9.
- 929 Nam, Y. & Chae, H-B. (2014) Numerical simulation for optimum design of ground source heat pump system
930 using building foundation as horizontal heat exchanger, Energy, 73, 933 – 942.
- 931 Narsilio G. A., Johnston, I. W., Colls, S., Bidarmaghz, A., Valizadeh-kivi, A., and Neshastehriz, S. (2012) Direct
932 geothermal energy research and demonstration projects for Victoria, Australia. In Choi, Chang-Koon (ed.),
933 Proceedings of the 2012 World Congress on Advances in Civil, Environmental, and Materials Research
934 (ACEM'12). ISBN 978-89-89693-34-5 98530. Seoul, Korea, July 26-29, 2433-2446.
- 935 Narsilio, G. A., Johnston, I. W., Bidarmaghz, A., Colls, S., O. Mikhaylova, O., Kivi, A. and Aditya, R. (2014)
936 Geothermal energy: Introducing an emerging technology. In: Horpibulsuk, S., Chinkulkijniwat, A., and
937 Suksiripattanapong, C., eds. *Proceedings of the International Conference on Advances in Civil Engineering for
938 Sustainable Development (ACESD 2014)*, Suranaree University of Technology, Nakhon Ratchasima, Thailand,
939 27-29 August. Volume 1 of 2, pp. 141-154.
- 940 Narsilio, G.A., Bidarmaghz, A., Johnston, I.W., and Colls, S. (2018) Detailed numerical modelling of ground heat
941 exchangers based on first principles. Computers and Geotechnics, (accepted).
- 942 Narsilio, G., Bidarmaghz, A., Disfani, M., Johnston, I. and Makasis, N. (2016a) Geo-exchange feasibility study –
943 Phase 1: Parkville and Domain metro stations, Melbourne (Vic), Australia. MMRA (Part of Report MM R-AJM-
944 PWAA-RP-MM- 002505.P3.IFR and MM R-AJM-PWAA-RP-MM-003122.P2.IFR). 66 pages.
- 945 Narsilio, G., Makasis, N., Bidarmaghz, A., Disfani, M., (2016b) Geo-exchange feasibility study – Phase 2:
946 Parkville metro station, Melbourne (Vic), Australia. MMRA. 65 pages.
- 947 Nicholson, D., Chen, Q., de Silva, M., Winter, A. & Winterling, R. (2014a) The design of thermal tunnel energy
948 segments for Crossrail, UK, Proc ICE Sustainability, 167 (3), 118-134.
- 949 Nicholson, D., Smith, P., Bowers, G. A., Cuceoglu, F., Olgun, C. G., McCartney, J. S., Henry, K., Meyer, L. L. &
950 Loveridge, F. A. (2014b) Environmental impact calculations, life cycle cost analysis, DFI Journal, 8 (2), 130-146.
- 951 Nicholson, DP, Chen, Q, Pillai, A, Chendorain, M. (2013), Developments in thermal pile and thermal tunnel
952 linings for city scale GSHP systems. In: Thirty-eighth workshop on geothermal reservoir engineering, Stanford
953 University, Stanford, California SGPTR-198; February 11-13, 2013. p. 8.
- 954 Ng, C.W.W., Shi, C., Gunawan, A., Laloui, L., & Liu, H.L. (2015) Centrifuge modelling of heating effects on energy
955 pile performance in saturated sand. Canadian Geotechnical Journal. 52(8): 1–13.

956 Ng, C.W.W., Shi, C., Gunawan, A., & Laloui, L. (2014) Centrifuge modelling of energy piles subjected to heating
957 and cooling cycles in clay. *Géotechnique Letters* 4: 310–316.

958 Olgun, C. G., Ozudogru, T. Y., Abdelaziz, S. L., and Senol, A. (2014) Long-term performance of heat exchanger
959 pile groups. *Acta Geotechnica*. 10(5), 553–569.

960 Olgun, C.G. and McCartney, J.S. (2014) Outcomes from the International Workshop on Thermoactive
961 Geotechnical Systems for Near-Surface Geothermal Energy: From Research to Practice. *The Journal of the
962 Deep Foundations Institute*. 8(2), 58-72.

963 Olgun, C. G. and Bowers, G. A. (2013) Numerical modeling of ground source bridge deck deicing. *International
964 Workshop on Geomechanics and Energy–The Ground as Energy Source and Storage, Lausanne, Switzerland,
965 26-28*

966 Ooka, R., Sekine, K., Mutsumi, Y., Yoshiro, S. & SuckHo, H. (2007) Development of a ground source heat pump
967 system with ground heat exchanger utilizing the cast-in place concrete pile foundations of a building. *EcoStock
968 2007*. 1-8.

969 Oschner, K. (2008) *Geothermal Heat Pumps, A Guide for Planning and Installation*. Earthscan, London, UK.

970 Ouyang, Y., Soga, S., and Leung, Y.F. (2011) Numerical back-analysis of energy pile test at Lambeth College,
971 London. *GeoFrontiers 2011 (GSP 211)*. J. Han & D.E. Alzamora, eds. ASCE, Reston VA. 440-449.

972 Ozudogru, T., Olgun, C.G., & Arson, C. (2015) Analysis of friction induced thermo-mechanical stresses on a heat
973 exchanger pile in isothermal soil. *Geotechnical and Geological Engineering*. 33, 357-371.

974 Pahud, D. (2007) *PILESM2, Simulation Tool for Heating/Cooling Systems with Heat Exchanger Piles or Borehole
975 Heat Exchangers*, User Manual, Scuola Universitaria Professionale della Svizzera Italiana, Lugano, Switzerland.

976 Pahud, D. & Hubbach, M. (2007) Measured Thermal Performances of the Energy Pile System of the Dock
977 Midfield at Zürich Airport, *Proceedings European Geothermal Congress 2007, Unterhaching, Germany, 30
978 May-1 June 2007*.

979 Park, H., Lee, S.R., Yoon, S. & Choi, J.C. (2013) Evaluation of thermal response and performance of PHC energy
980 pile: field experiments and numerical simulation, *Appl. Energy*, 103 (3), 12–24.

981 Park S, Sung C, Jung K, Sohn B, Chauchois A, & Choi H (2015) Constructability and heat exchange efficiency of
982 large diameter cast-in-place energy piles with various configurations of heat exchange pipe. *Applied Thermal
983 Engineering*. 90:1061-1071.

984 Pasten, C., and Santamarina, J. (2014) Thermally induced long-term displacement of thermoactive piles. *J.
985 Geotech. Geoenviron. Eng.*, 10.1061/(ASCE)GT.1943-5606.0001092, 06014003.

986 Paul, N.D. (1996). *The effect of grout thermal conductivity on vertical geothermal heat exchanger design and
987 performance*. Mechanical Engineering Dept., South Dakota State University.

988 Piemontese, M. (2018) *Sensitivity Analysis on the Geothermal Potential of Energy Walls*. Master's Thesis.
989 Politecnico di Torino.

990 Rammal, D., Mroueh, H., & Burlon, S. (2018) Thermal behaviour of geothermal diaphragm walls: Evaluation of
991 exchanged thermal power. *Renewable Energy*. <https://doi.org/10.1016/j.renene.2018.11.068>.

992 Raymond, J., Therrien, R. and Gosselin, L. (2011). Borehole temperature evolution during thermal response
993 tests, *Geothermics*, 40, (2011), pp. 69–78

- 994 Rees, S.J. & Fan, D. (2013) A numerical implementation of the Dynamic Thermal Network method for long time
 995 series simulation of conduction in multi-dimensional non-homogeneous solids. *International Journal of Heat*
 996 *and Mass Transfer*, 61. pp. 475-489.
- 997 Rees, S.J. & He, M. (2013) A three-dimensional numerical model of borehole heat exchanger heat transfer and
 998 fluid flow. *Geothermics*. 46, 1-13.
- 999 Rocha, M. (1957) The possibility of solving soil mechanics problems by the use of models. Proc. 4th
 1000 international Conference on Soil Mechanics and Foundation Engineering. Taylor and Francis. London. Vol. 1.
 1001 183-188.
- 1002 Rosenberg, J.E. (2010) Centrifuge Modeling of Soil Structure Interaction in Thermo-Active Foundations. M.S.
 1003 Thesis. University of Colorado at Boulder.
- 1004 Rotta Loria, A. F., Gunawan, A., Shi, C., Laloui, L., and Ng, C. W. W. (2015a) Numerical modelling of energy piles
 1005 in saturated sand subjected to thermo-mechanical loads. *Geomech. Energy Environ.*, 1, 1–15.
- 1006 Rotta Loria, A.F., Di Donna, A., & Laloui, L. (2015b) Numerical study on the suitability of centrifuge testing for
 1007 capturing the thermal-induced mechanical behaviour of energy piles. *ASCE Journal of Geotechnical and*
 1008 *Geoenvironmental Engineering*. 141 (10), 04015042-1-10.
- 1009 Rotta Lora, A. & Laloui, L. (2016a) The interaction factor method for energy pile groups, *Computers and*
 1010 *Geotechnics*, 80, 121-137.
- 1011 Rotta Loria, A.F. & Laloui, L. (2016b) Thermally induced group effects among energy piles. *Géotechnique*.
 1012 <http://dx.doi.org/10.1680/jgeot.16.P.039>.
- 1013 Rotta Loria, A.F. & Laloui, L. (2017a) The equivalent pier method for energy pile groups. *Geotechnique*
 1014 67(8):691-702.
- 1015 Rotta Loria, A.F. & Laloui, L. (2017b) Group action effects caused by various operating energy piles.
 1016 *Geotechnique*: 10.1680/jgeot.17.P.213.
- 1017 Rotta Loria, A.F. & Laloui, L. (2017c) Thermally induced group effects among energy piles. *Geotechnique*
 1018 67(5):374-393
- 1019 Rui, Y. & Yin, M. (2018) Thermo-hydro-mechanical coupling analysis of a thermo-active diaphragm wall. *Can.*
 1020 *Geotech. J.*, 55, 720-735.
- 1021 Rzyżyński, G. & Bogusz, W. (2016) City-scale perspective for thermoactive structures in Warsaw. *Environmental*
 1022 *Geotechnics* 3(4), 280-290. <https://doi.org/10.1680/jenge.15.00031>
- 1023 Saggi, R. & Chakraborty, T. (2015) Cyclic thermo-mechanical analysis of energy piles in sand. *Geotechnical and*
 1024 *Geological Engineering*. 33, 321-342.
- 1025 Sailer E, Taborda DMG, Zdravkovic L, 2018a, A new approach to estimating temperature fields around a group
 1026 of vertical ground heat exchangers in two-dimensional analyses, *Renewable Energy*, 118, 579-590.
- 1027 Sailer E, Taborda DMG, Zdravkovic L, Potts DM, 2018b, Factors affecting the thermo-mechanical response of
 1028 a retaining wall under non-isothermal conditions, London, 9th European Conference on Numerical Methods
 1029 in Geotechnical Engineering, Publisher: Taylor Francis Group, Pages: 741-749
- 1030 Samarakoon, R., Ghaaowd, I. & McCartney, J.S. (2018) Impact of drained heating and cooling on undrained
 1031 shear strength of normally consolidated clay. *Energy Geotechnics: SEG-2018. Proceedings of the 2nd*

- 1032 International Symposium on Energy Geotechnics. Lausanne, Switzerland. Sep. 26-28. A. Ferrari, L. Laloui, eds.
1033 Springer, Vienna. 243-249.
- 1034 Sanchez, M., Falcão, F., Mack, M., Pereira, J.M., Narsilio, G., and Guimarães, L (2017) Salient Comments from
1035 an Expert Panel on Energy Geotechnics. *Environmental Geotechnics*, 4 (EG2): 135–142
- 1036 Sanner, B., Hellstrom, G., Spitler, J. & Gehlin S.E.A. (2005) Thermal Response Test – Current Status and World-
1037 Wide Application, In: *Proceedings World Geothermal Congress, 24-29th April 2005 Antalya, Turkey*.
1038 International Geothermal Association.
- 1039 Savvidou, C. (1988) Centrifuge modelling of heat transfer in soil. *Proc., Centrifuge 88*, J.-P. Corté, ed., Balkema,
1040 Rotterdam. 583–591.
- 1041 Schneider, M. & Moormann, C. (2010) GeoTU6 – a geothermal research project for tunnels. *Tunnel*. 2/2010,
1042 14-21.
- 1043 Sekine, K., Ooka, R., Yokoi, M., Shiba, Y. & Hwang, S. (2007) Development of a ground-source heat pump
1044 system with ground heat exchanger utilizing the cast-in-place concrete pile foundations of buildings, *ASHRAE*
1045 *Trans*, January 2007, 558-566.
- 1046 Shafagh, I. & Rees, S. (2018) A foundation wall heat exchanger model and validation study. *Proc. IGSHPA*
1047 *Research Conf.*, Stockholm, 336-344.
- 1048 Shafagh, I. & Rees, S. (In Review) Conduction shape factors in rectangular sections with circular eccentric inner
1049 boundaries. *International Journal of Thermal Sciences*. In Review.
- 1050 Sharqawy, M.H., Mokheimer, E.M. & Badr, H.M. (2009) Effective pipe-to-borehole thermal resistance for
1051 vertical ground heat exchangers. *Geothermics* 38, 271-277.
- 1052 Shonder, J.A. & Beck, J.V. (1999) Determining effective soil formation thermal properties from field data using
1053 a parameter estimation technique. *ASHRAE Trans*. 105, pp. 458-466.
- 1054 Shonder, J.A., & Beck, J.V. (2000) Field test of a new method for determining soil formation thermal
1055 conductivity and borehole resistance. *ASHRAE Trans*. 106, 843-850.
- 1056 SIA-D0190 (2005) *Utilisation de la chaleur du sol par des ouvrages de fondation et de soutènement en béton*,
1057 D 0190, Swiss Society of Engineers and Architects, Zurich, Switzerland.
- 1058 Signorelli, S., Bassetti, S., Pahud, D. & Kohl, T. (2007) Numerical evaluation of thermal response tests,
1059 *Geothermics*, 36, 141-166.
- 1060 Singh, R., Bouazza, A., and Wang, B. (2015). Near-field ground thermal response to heating of a
1061 geothermal energy pile: observations from a field test. *Soils and Foundations*
- 1062 Soga, K. & Rui. (2016) *Energy geostructures*. A chapter in *Advances in ground-source heat pump systems* (ed.
1063 S.J. Rees). Elsevier.
- 1064 Soga, K, Yi, R., & Nicholson, D. (2015), Behaviour of a thermal wall installed in the Tottenham Court Road
1065 station box. *Proc. Crossrail Conf.*, Crossrail Ltd & Federation of Piling Specialists, City Hall, London, 112–119
- 1066 Soga, K., Qi, H., Rui, Y. & Nicholson, D. (2014) Some considerations for designing GSHP coupled geotechnical
1067 structures based on a case study. 7th International Congress on Environmental Geotechnics (7ICEG2014),
1068 Melbourne, 10-14th November, 2014.

1069 Spitler, J.D. & Gehlin, S.E.A. (2015) Thermal response testing for ground source heat pump systems – An
1070 historical review, *Renewable and Sustainable Energy Reviews*, 50, 1125-1137.

1071 Spitler, J.D., Fisher, D.E., Cullin, J. R., Xing, L. Lee, E., Rees, S.J. & Fan, D. (2011) Foundation heat exchanger
1072 model and design tool development and validation, final report to Oak Ridge National Laboratory. Available
1073 online http://temp-hvac.okstate.edu/sites/default/files/pubs/reports/01-FHX_2013.pdf.

1074 Stephen, P. <https://www.railmagazine.com/infrastructure/stations/cooling-thetube>. Rail Magazine
1075 (February), 2016.

1076 Serpi, D., Coletto, A., & Mauri, L (2017), Investigation on the behaviour of a thermo-active diaphragm wall by
1077 thermo-mechanical analyses. *Geomech. for Energy and Environ.*, 9, 1-20.

1078 Serpi, D., Tomaselli, G., Angelotti, A. (2018) Energy performance of ground heat exchangers embedded in
1079 diaphragm walls: Field observations and optimization by numerical modelling. *Renewable Energy*.
1080 <https://doi.org/10.1016/j.renene.2018.11.102>

1081 Stewart, M.A. & McCartney, J.S. (2012). Strain distributions in centrifuge model energy foundations.” *Proc.,*
1082 *GeoCongress 2012 (GSP 225)*, R.D. Hryciw, A. Athanasopoulos-Zekkos, & N. Yesiller, eds., ASCE, Reston, VA,
1083 4376–4385.

1084 Stewart, M.A. & McCartney, J.S. (2014) Centrifuge modeling of soil-structure interaction in energy
1085 foundations. *ASCE Journal of Geotechnical and Geoenvironmental Engineering*. 140 (4), 04013044-1-11.

1086 Sun, M., Xia, C. & Zhang, G. (2013) Heat transfer model and design method for geothermal heat exchange
1087 tubes in diaphragm walls, *Energy and Buildings*, 61, 250 – 259.

1088 Suryatriyastuti, M.E., Mroueh, H., & Burlon, S. (2014) A load transfer approach for studying the cyclic
1089 behaviour of thermo-active piles. *Computers and Geotechnics*. 55, 378-391.

1090 Suryatriyastuti, M.E., Mroueh, H., & Burlon, S. (2012) Understanding the temperature-induced mechanical
1091 behaviour of energy pile foundations. *Renewable and Sustainable Energy Reviews*. 16, 3344-3354.

1092 Suryatriyastuti, M.E., Burlon, S. & Mroueh, H., (2016) On the understanding of cyclic interaction mechanisms
1093 in an energy pile group. *Int. J. Numer. Anal. Meth. Geomech.* 40(1), 3-24.

1094 Sutman, M., Brettmann, T., and Olgun, C. G. (2014) Thermo-mechanical behaviour of energy piles: Full-scale
1095 field test verification. *DFI 39th Annual Conf. on Deep Foundations*, Deep Foundations Institute. 1-10.

1096 Tang, A.M., Kalantidou, A., Pereira, A., Hassen, G., & Yavari, N. (2014). Mechanical behaviour of energy piles
1097 in dry sand. *Geotechnical Engineering Journal of the SEAGS & AGSSEA*. 4 (3), 86-89.

1098 Tinti, F., Boldini, D., Ferrari, M., Lanconelli, M., Kasmaee, S., Bruno, R., Egger, H., Voza, A. & Zurlo, R. (2017)
1099 Exploitation of geothermal energy using tunnel lining technology in a mountain environment. A feasibility
1100 study for the Brenner Base tunnel – BBT. *Tunnelling and Underground Space Technology* 70, 182-203. Doi:
1101 10.1016/j.tust.2017.07.011

1102 TRNSYS. (2018) Available on the web at: <http://sel.me.wisc.edu/trnsys/index.html>.

1103 Wang, B., Bouazza, A., & Haberfield, C. (2011) Preliminary observations from laboratory scale model
1104 geothermal pile subjected to thermal-mechanical loading. *Geo-Frontiers 2011 (GSP 211)*. J. Han & D.E.
1105 Alzamora, eds. ASCE, Reston VA. 430-439.

1106 Wang, B., Bouazza, A., Barry-Macaulay, D., Singh, M.R., Webster, M., Haberfield, C., & Chapman, G. (2012a)
1107 Field and laboratory investigation of heat exchanger pile. *GeoCongress 2012*. Oakland, CA. 4396-4405.

1108 Wang, W., Regueiro, R., Stewart, M.A., & McCartney, J.S. (2012b) Coupled thermo-poro-mechanical finite
1109 element analysis of a heated single pile centrifuge experiment in saturated silt. Proc., GeoCongress 2012 (GSP
1110 225), R. D. Hryciw, A. Athanasopoulos-Zekkos, & N. Yesiller, eds., ASCE, Reston, VA. 4406-4415.

1111 Wang, W., Regueiro, R. & McCartney, J.S. (2015a) Coupled axisymmetric thermo-poro-elasto-plastic finite
1112 element analysis of energy foundation centrifuge experiments in partially saturated silt. *Geotechnical and
1113 Geological Engineering*. 33 (2), 373-388.

1114 Wang, B., Bouazza, A., Singh, R., Haberfield, C., Barry-Macaulay, D. & Baycan, S. (2015b). Posttemperature
1115 effects on shaft capacity of a full-scale geothermal energy pile. *J. Geotech. Geoenviron. Eng.* 141 (4): 04014125.
1116 [https://doi.org/10.1061/\(ASCE\)GT.1943-5606.0001266](https://doi.org/10.1061/(ASCE)GT.1943-5606.0001266).

1117 Wagner, V., Bayer, P., Kübert, M., Blum, P. (2012) Numerical sensitivity study of thermal response tests,
1118 *Renewable Energy*, 41(0), pp. 245-253, doi: 10.1016/j.renene. 2011.11.001.

1119 Witte, H.J.L., van Gelder, G.J. & Spitler, J.D. (2002) In situ measurement of ground thermal conductivity: a
1120 Dutch perspective. *ASHRAE Transactions*, 108 (1), 263 – 272.

1121 Wood, C.J., Liu, H. & Riffat, S.B. (2010a) Comparison of a modelled and field tested piled ground heat
1122 exchanger system for a residential building and the simulated effect of assisted ground heat recharge. *Intl. J.
1123 Low Carbon Technologies*, 5(3), 137-143

1124 Wood, C.J., Liu, H. & Riffat, S.B. (2010b) An investigation of the heat pump performance and ground
1125 temperature of a pile foundation heat exchanger system for a residential building, *Energy*, 35, 3932-4940.

1126 Viera A; Alberdi-Paolga M; Christodoulides P; Javed S; Loveridge F; Nguyen F; Cecinato F; Maranha J; Florides
1127 G; Prodan I (2017) Characterisation of ground thermal and thermo-mechanical behaviour for shallow
1128 geothermal energy applications. *Energies*, 10 (12), 2044.

1129 Xia, C., Sun, M., Zhang, G., Xiao, S. & Zou, Y. (2012) Experimental study on geothermal heat exchangers buried
1130 in diaphragm walls, *Energy and Buildings*, 5, 50 – 55.

1131 Xing, L., Cullin, J. R., Spitler, J. D., Im, P. & Fisher, D. E. (2012) Foundation heat exchangers for residential ground
1132 source heat pump systems – numerical modelling and experimental validation, *HVAC&R Research*, 17 (6),
1133 1059-1072.

1134 Yavari, N., Tang, A. M., Pereira, J.-M. & Hassen, G. (2014a) Experimental study on the mechanical behaviour
1135 of a heat exchanger pile using physical modelling. *Acta Geotechnica*. 9 (3), 385-398.

1136 Yavari, N., Tang, A. M., Pereira, J.-M. & Hassen, G. (2014b) A simple method for numerical modelling of energy
1137 pile's mechanical behaviour. *Géotechnique Letters*. 4, 119–124.

1138 Yavuzturk, C., Spitler, J. D. & Rees, S. J. (1999) A Transient Two-Dimensional Finite Volume Model for the
1139 Simulation of Vertical U-Tube Ground Heat Exchangers. *ASHRAE Transactions*, 105(2), pp. 465-474.

1140 Yoon, S., Lee, S.-R., Xue, J., Zosseder, K., Go, G.-H. & Park, H. (2015) Evaluation of the thermal efficiency and a
1141 cost analysis of different types of ground heat exchangers in energy piles, *Energy Conservation and
1142 Management*, 105, 393-402.

1143 Yu X., Zhang, N., Pradhan, A. & Puppala, A. (2016) Geothermal energy for bridge deck and pavement deicing—
1144 A brief review. *Geo-Chicago 2016*. ASCE. <https://doi.org/10.1061/9780784480137.057>

1145 Zarrella, A. & De Carli, M. (2013) Heat transfer analysis of short helical borehole heat exchangers, *Applied
1146 Energy*, 102, 1477-1491.

1147 Zarrella, A., De Carli, M. & Galgaro, A. (2013) Thermal performance of two types of energy foundation pile:
1148 helical pipe and triple U-tube, *Applied Thermal Engineering*, 61, 301-310.

1149 Zeng, H.Y., Diao, N.R. & Fang, Z. (2002) A finite line-source model for boreholes in geothermal heat exchangers.
1150 *Heat Transfer - Asian Research*, 31(7), 558-567

1151 Zhang, G. Xia, C., Xhao, X. & Zhou, S. (2016a) Effect of ventilation on the thermal performance of tunnel lining
1152 GHEs, *Applied Thermal Engineering*, 93, 416 – 424.

1153 Zhang, G., Guo, Y., Zhou, Y., Ye, M., Chen, R., Zhang, H., Yang, J., Chen, J., Zhang, M., Lian, Y. & Liu, C. (2016b)
1154 Experimental study on the thermal performance of tunnel lining GHE under groundwater flow, *Applied
1155 Thermal Engineering*, 106, 784 – 795.

1156 Zhang, G., Liu, S., Zhao, X., Ye, M., Chen, R., Zhang, H., Yang, J. & Chen, J. (2017) The coupling effect of
1157 ventilation and groundwater flow on the thermal performance of tunnel lining GHEs. *Applied Thermal
1158 Engineering* 112, 595-605.

1159 Zhang, G., Xia, C., Yang, Y., Sun, M. & Zou, Y (2014) Experimental study on the thermal performance of tunnel
1160 lining ground heat exchangers, *Energy and Buildings*, 77, 149-157.

1161 Zhang, G., Xia, C., Sun, M., Zou, Y. & Xiao, S. (2013) A new model and analytical solution for the heat conduction
1162 of tunnel lining ground heat exchangers, *Cold Regions Science and Technology*, 88, 59-66.

1163

1164

1165	List of Tables	
1166	Table 1 Main types of G-function for use with piles.....	11
1167	Table 2 Methods for calculating ground heat exchanger steady state thermal resistance.....	12
1168	Table 3 Summary of pile thermal performance tests.....	28
1169	Table 4 Summary of operational pile performance.....	30
1170	Table 5 Summary of pile thermal response tests.....	32
1171	Table 6 Summary of wall thermal performance.....	37
1172	Table 7 Summary of tunnel thermal performance.....	41
1173	Table 8 Summary of laboratory-scale tests on energy piles.....	46
1174	Table 9 Summary of centrifuge-scale tests on energy piles.....	51
1175		
1176		

1177	List of Figures	
1178	Figure 1 Typical arrangement of an energy pile.....	8
1179	Figure 2 Schematic of the classical G-function models: (a) infinite line source (ILS), (b) infinite cylindrical source	
1180	(ICS), (c) finite line source (FLS). T_{∞} =far field temperature; H=heat exchanger length; h=depth below ground	
1181	surface. Adapted from Bidarmaghz 2015.	9
1182	Figure 3 Example G-functions showing development of long-term steady state conditions for heat exchangers	
1183	of finite length. Aspect ratio = pile length / pile diameter	10
1184	Figure 4 Different G-functions displayed at short time scales. Pile upper and lower bound G-functions after	
1185	Loveridge & Powrie (2013b).....	10
1186	Figure 5 Example G-functions for different arrangements of boreholes (Bourne-Webb et al. 2016). t^* is the	
1187	ratio of the elapsed time and time to steady state; r^* is the non-dimensional radial coordinate.	14
1188	Figure 6 Effect of pipe arrangements and temperature difference between fluid and the ground on the heat	
1189	transfer rate obtained from energy walls. (U = single U tube; UU = two U-tubes connected in parallel; W1 or	
1190	W2 = two U-tubes connecting in series; parametric study includes both U and UU arrangements).	20
1191	Figure 7 Schematic view of a energy tunnel. Absorber pipes are embedded into the tunnel lining (adapted from	
1192	Zhang et al. 2013, reproduced with permission, Licence Number 4585510080214)	21
1193	Figure 8 Typical layout of absorber pipes in energy tunnels: (a) longitudinal meandering pipe, (b) transverse,	
1194	and (c) slinky (only found in energy textiles to date).	23
1195	Figure 9 Unit heat exchange rates from short term performance tests of piles. Data taken from the sources	
1196	listed in Table 3.....	29
1197	Figure 10 Comparison of Thermal Conductivity derived from Laboratory Testing and Thermal Response Testing	
1198	(TRT) on Energy Piles. Laboratory values from the needle probe, using a weighted average where different soil	
1199	units are present. TRT results from line source interpretations, average where there are multiple tests or	
1200	injection and recovery values.....	34
1201		